Bayerische Julius-Maximilians Universität Würzburg

Fakultät für Biologie

Use of Tumor Vasculature for Successful Treatment of Carcinomas by Oncolytic Vaccinia Virus

Doctoral Thesis

For a doctoral degree at Julius-Maximilians-Universität Würzburg

submitted by

Prisca Gnamlin

from

France

Würzburg, 2015

Dissertation Examination Committee:

Chairman: Prof. Dr. Markus Engstler

Primary Supervisor: Prof. Dr. A. A. Szalay

Secondary Supervisor: Prof. Dr. G. Krohne

Date of Public Defense: _____

Date of Receipt of Certificates: _____

Le médisant et le lâche ne dénigrent que ceux qui réalisent et s'accomplissent.

Le temps m'a appris à les pardonner.

A ceux que j'aime et qui me soutiennent ainsi qu'à ceux qui n'ont jamais cru en moi, car c'est aussi grâce à vous….

Table of contents

Summary ..... *I*

Zusammenfassung ..... *IV*

1 Introduction *1*

1.1 Cancer **1**
1.1.1 Cancer definition and epidemiology 1
1.1.2 Characteristics of tumorigenesis 2
1.1.3 Tumor induced angiogenesis 5
1.1.3.1 The angiogenic switch 5
1.1.3.2 Vascular Endothelial Growth Factor 6
1.1.3.3 Angiopoetin-2 7
1.1.3.4 Placental Growth Factor 8
1.1.4 Angiogenic factors and endothelial junctions regulation 10
1.1.5 Angiogenic factors and endothelial cell immune profile 10
1.1.6 Current treatments and resistance 10

1.2 Vaccinia Virus **12**
1.2.1 Vaccinia virus historical use 12
1.2.2 Virology 13
1.2.3 Vaccinia virus and oncolytic virotherapy 14

2 Aim of my thesis *16*

2.1 Part 1: The roles of angiogenic factors in tumor-induced angiogenesis and beyond **16**

2.2 Part 2: Effect of VEGF blockade on VACV treatment **16**

2.3 Part 3: Evaluate different strategies to circumvent anti-VEGF resistance **16**

3 Material and Methods *18*

3.1 Material **18**
3.1.1 Cell lines and culture media 18
3.1.2 Chemical and enzymes 22
3.1.3 Buffers and solutions 27
3.1.4 Antibodies 29
3.1.5 Kits 30
3.1.6 Synthetic oligonucleotides 31
3.1.7 Laboratory equipment and other material 32
3.1.8 Recombinant vaccinia virus strains 36
3.1.9 Laboratories animals 39

3.2 Methods **39**
3.2.1 *Cell culture* 39
3.2.1.1 Maintenance and passaging of human and murine cells 39
3.2.1.2 Cell quantification 39
3.2.1.3 Angiogenic factors levels modulation 40
3.2.1.4 Tube formation assay 40

3.2.2 Enzyme-Linked Immunosorbent Assays (ELISAs) 41
3.2.2.1 Binding activity assessment by ELISA 41
3.2.2.2 Angiogenic profiles of tumor cells 41
3.2.2.3 In-cell ELISA 42
3.2.3 Protein production and purification 43
3.2.3.1 Purification GLAF-1, anti-PlGF and anti-Ang-2 antibodies from VACV infected cells 43
3.2.3.2 Production and purification of aPlGF antibody 44
3.2.3.2.1 Synthesis of an aPlGF expressing plasmid 44
3.2.3.2.2 Production and purification of aPlGF 44
3.2.4 Virological methods 44
3.2.4.1 Infection of mammalian cells using therapeutic VACV 44
3.2.4.2 Vaccinia virus titration using plaque assay 45
3.2.5 *In vivo* experiments 45
3.2.5.1 Xenograft tumors implantation and monitoring 45
3.2.5.2 Organs and tumors preparation for virus and human cells detection 46
3.2.5.3 Human cell detection 46
3.2.5.4 Histological preparations 47
3.2.5.4.1 Sample preparation and immunostaining of paraffin sections 47
3.2.5.4.2 Sample preparation and immuno-staining of agarose sections 48
3.2.6 Statistical analysis 48

4 Results 49

4.1 Angiogenic factors VEGF, Ang-2 and PlGF are expressed by various tumor cell types. 49

4.2 Therapeutic VACVs lyse efficiently human tumor cells and produce functional anti-PlGF, anti-Ang-2 and anti-VEGF single chain antibodies. 51

4.3 Human angiogenic factors stimulate tube formation by murine endothelial cells *ex vivo* 53

4.4 Angiogenic factors modulate tumor cell adhesion patterns 56

4.5 Specific tumor cell lines form blood vessel-like structures 60

4.6 VACV mediated anti-angiogenesis therapies reduce tumor induced vascular leakage 62

4.7 VACV is able to infect murine tumor endothelial cells. 65

4.8 Anti-VEGF scAb expression increases VACV replication and/or entry. 68

4.9 VACV mediated anti-VEGF and anti-Ang-2 therapies target and lyse PC14PE6-RFP primary tumors and metastases more efficiently than GLV-1h68 73

4.10 Angiogenic factor blockade improved VACV oncolytic therapy in different tumor models 76
4.10.1 Angiopoietin 2 blockade improved oncolytic VACV treatment of Colo205 tumors 76
4.10.2 PlGF blockade improves VACV treatment of MEL1936 tumors 79
4.10.3 Combination therapy to circumvent angiogenesis resistance 81
4.10.3.1 Anti-Ang-2 and Anti-VEGF combined therapy mediated by VACV 81
4.10.3.1.1 Ang-2 combination therapy lead to a faster tumor growth delay 81
4.10.3.1.2 Anti-Ang-2 combination therapy modifies Colo205 tumors vasculature. 83

4.10.3.2 Anti-PlGF and Anti-VEGF combined therapy mediated by VACV. 84

5 Discussion 91

5.1 A549 tumor cells can form blood vessel-like structures 91

5.2 PC14PE6-RFP tumor cells binds to the endothelium 92

5.3 A personalized treatment is necessary for a successful anti-angiogenesis cancer treatment. 92

5.4 Fluid mechanics principles guiding the reduction of PC14PE6-RFP and A549 tumor cells dissemination 93

5.5 Effect of -angiogenic factors on endothelial and tumor cells adhesion pattern ... 95

5.6 VEGF blockade increases vaccinia virus infectivity 96

5.7 Therapeutic vaccinia viruses can colonize tumor endothelial cells. 98

6 Conclusions 100

7 References 101

8 Appendix 113

8.1 List of figures 113

8.2 Publications 115

8.3 Eidesttatliche Erklärung. 116

8.4 Acknowledgements 117

Summary

Tumor-induced angiogenesis is of major interest for oncology research. The statement of Judah Folkman in 1971 declaring that tumors cannot grow over 2 mm in diameter without inducing angiogenesis was confirmed by numerous studies over the last decades, and started the quest of tumor-associated vasculature understanding. Therefore we learned that most tumor types exhibit an abnormal expression of pro-angiogenic factors able to stimulate the proliferation, survival and migration of endothelial cells. One particular angiogenic factor was found to be a powerful effector of endothelial cells. Vascular endothelial growth factor (VEGF) is described as the most potent pro-angiogenic factor characterized so far. VEGF blockade has been shown to be sufficient for angiogenesis inhibition and subsequent tumor regression in several preclinical tumor models. Bevacizumab was the first treatment targeting specifically tumor-induced angiogenesis through VEGF blockade to be approved by the Food and Drugs Administration (FDA) for cancer treatment. However, after very promising results in preclinical evaluations, VEGF blockade did not exhibit the expected success in patients. Some tumors were found to develop resistance mechanisms to VEGF blockade. Several factors have been accounted for the relapse of patients, the over-expression of other pro-angiogenic factors, the noxious influence of VEFG blockade on normal tissues, the selection of hypoxia resistant neoplastic cells, the recruitment of hematopoietic progenitor cells and finally the transient nature of angiogenesis inhibition by VEGF blockade. The development of new blocking agents against other angiogenic factors like placental growth factor (PlGF) and Angiopoietin-2 (Ang-2) allows the development of an anti-angiogenesis strategy adapted to the profile of the tumor.

Oncolytic virotherapy uses the natural propensity of viruses to colonize tumors to treat cancer. Vaccinia virus (VACV) belongs to the family of *Poxviridae*. It is already historically known as a stable immunization agent, and now described as an efficient expression vector. The recombinant vaccinia virus GLV-1h68 was shown to infect, colonize and lyse efficiently several tumor types. Its descendant GLV-1h108, expressing an anti-VEGF antibody, was proved in previous studies to inhibit efficiently tumor

induced angiogenesis. Additional VACVs expressing single chain antibodies (scAb) antibodies against PlGF and Ang-2 were designed.

First, GLV-1h343, GLV-1h344, and GLV-1h345 VAVCs were engineered to express the same anti-PlGF scAb under the early, early-late or late synthetic promoter of VACV. Then, GLV-1h492, GLV-1h493 and GLV-1h494 were designed to encode an anti-Ang-2 scAb under the early, early-late or late VACV promoter. Additionally, two virus strains were engineered to target two angiogenic factors at once. GLV-1h471 encodes for an anti-PlGF and an anti-VEGF scAb. The GLV-1h495 strain expresses an antibody targeting VEGF and an antibody targeting Ang-2.

In this study, VACV-mediated anti-angiogenesis treatments have been evaluated in several preclinical tumor models, PC14PE6-RFP (lung adenocarcinoma), Colo205 (colorectal cancer), MEL1936 (melanoma) and A549 (lung adenocarcinoma). The efficiency of PlGF blockade, alone or in combination with VEGF, mediated by VACV has been established in MEL1936 xenografts and confirmed in A549 tumors. GLV-1h343, GLV-1h344 and GLV-1h471 reduced MEL1936 tumor burden 5- and 2-folds more efficiently than GLV-1h68, respectively.

Ang-2 blockade efficiency for cancer treatment gave controversial results when tested in different laboratories. Here we demonstrated that unlike VEGF, the success of Ang-2 blockade is not only correlated to the strength of the blockade. A particular balance between Ang-2, VEGF and Ang-1 needs to be induced by the treatment to see a regression of the tumor and an improved survival. We saw that GLV-1h492, GLV-1h494 and GLV-1h495 treated Colo205 tumors grew on average 3-folds less than the GLV-1h68-treated ones. These same viruses induced statistically significant tumor growth delays at early (3 and 7 days post-treatment) and late time points (31, 35 and 42 days post-treatment). Moreover, this study unveiled the need to establish an angiogenic profile of the tumor to be treated as well as the necessity to better understand the synergic effects of VEGF and Ang-2. In addition to its effect on primary tumors, angiogenesis inhibition by VACV-mediated PlGF and Ang-2 blockade was able to reduce the number of metastases and migrating tumor cells (even more efficiently than VEGF blockade).

VACV colonization of A549 tumor cells, *in vitro,* was shown to be limited by VEGF, when the use of the anti-VEGF VACV GLV-1h108 drastically improved the colonization efficiency up to 2-fold, 72 hours post-infection. These *in vitro* data were confirmed by *in vivo* analysis of PC14PE6-RFP tumors. Fourteen days post-treatment, the anti-VEGF virus GLV-1h108 was colonizing 78.8% of the tumors when GLV-1h68 colonization rate was 49.6%. These data confirmed the synergistic effect of VEGF blockade and VACV replication for tumor regression.

Three of the tumor cell lines used to assess VACV-mediated angiogenesis inhibition were found, in certain conditions, to mimic either endothelial cell or pericyte functions, and participate directly to the vascular structure. The expression by these tumor cells of e-selectin, p-selectin, ICAM-1 and VCAM-1, adhesion proteins normally expressed on activated endothelial cells, corroborates our finding. These adhesion proteins detected by In-cell ELISA in cell culture, play an important role in immune cell recruitment, and were found to vary in presence of VEGF, PlGF and Ang-2, confirming the involvement of pro-angiogenic factors in the immuno-modulatory abilities of tumors.

In this study VACV-mediated angiogenesis blockade proved its potential as a therapeutic agent able to treat different tumor types and prevent the resistance observed during bevacizumab treatment by acting on different factors. First, the possible expression of several antibodies by this delivery agent would prevent another angiogenic factor to take over VEGF and stimulate angiogenesis. Then, the ability of VACV to infect tumor cells would prevent them to form blood vessel-like structures to sustain tumor growth, and the localized delivery of the antibody would decrease the risk of adverse effects. Next, the blockade of pro-angiogenic factors would improve VACV replication and decrease the immune-modulatory effect of tumors. Finally the fact that angiogenesis blockade lasts until total regression of the tumor would prevent the recovery of the tumor-associated vasculature and the relapse of patients.

Zusammenfassung

Ein Hauptinteresse der onkologischen Forschung liegt auf dem Verständnis der Tumor-induzierten Angiogenese. Judah Folkman postulierte 1971, dass Tumore ohne Angiogenese zu induzieren nicht größer als 2 mm im Durchmesser wachsen können. Diese Aussage wurde in den folgenden Jahrzehnten in unterschiedlichen Studien bestätigt und etablierte die Forschung über die Tumor-assoziierte Vaskularisation. Im Zuge dieser Forschung konnte bereits festgestellt werden, dass die meisten Tumortypen eine abnorme Expression angiogener Faktoren zeigen, welche in der Lage sind die Proliferation von Endothelzellen zu stimulieren, das Überleben dieser zu sichern und deren Migration zu fordern. Im Besonderen wurde der *vascular endothelial growth factor* (VEGF) bis jetzt als der effektivste angiogene Faktor beschrieben. Es konnte gezeigt werden, dass die Hemmung des VEGF zur Inhibition der Angiogenese führt, das wiederum zu Tumorregression in vorklinisch untersuchten Tumormodellen führte. Bevacizumab ist das erste FDA (*Food and Drugs Administration*) zugelassene Krebs-Therapeutikum, welches spezifisch auf die Tumor-induzierte Angiogenese durch VEGF-Inhibition abzielt. Nach erfolgversprechenden Ergebnissen in vorklinischen Untersuchungen, konnte jedoch der erwartete Erfolg durch VEGF-Hemmung im Patienten nicht erzielt werden. Es schien, dass einige Tumore Resistenzmechanismen gegen die VEGF-Hemmung entwickelten. Hierfür könnten verschiedene Faktoren ursächlich sein, wie die Überexpression anderer angiogener Faktoren, der schädliche Einfluss der VEGF-Hemmung auf nicht entartetes Gewebe, der Selektionsdruck auf hypoxisch resistente bzw. resistentere neoplastische Zellen, die Rekrutierung hematopoietischer Vorläuferzellen und letztendlich die transiente Natur der Angiogenese-Inhibition bedingt durch VEGF-Hemmung. Die Entwicklung von neuen Angiogenese hemmenden Stoffen gegen angiogene Faktoren, wie den *placental growth factor* (PIGF) oder Angiopoietin-2 (Ang-2), ermöglichen eine an das jeweilige Tumor-Profil angepasste anti-angiogene Strategie.

Die onkolytische Virustherapie nutzt zur Tumorbehandlung die natürliche Eigenschaft der Viren Tumore zu kolonisieren. Das Vaccinia-Virus (VACV) gehört zur Familie der Poxviridae und wurde bereits lange Zeit als Vakzin zur Immunisierung gegen Pocken eingesetzt. Weiterhin ist es als effizienter Expressionsvektor beschrieben. Es konnte

gezeigt werden, dass das von Genelux entwickelte rekombinante VACV GLV-1h68 effizient verschiedene Tumortypen infiziert, kolonisiert und letztendlich lysiert. Das VACV GLV-1h108, welches auf der Basis des GLV-1h68 generiert wurde, kodiert einen anti-VEGF Antikörper. Es konnte gezeigt werden, dass dieses Virus in der Lage ist die Tumor-induzierte Angiogenese effizient zu inhibieren. Zusätzlich zu diesem VACV wurden weitere Konstrukte kloniert, welche für Antikörper gegen PIGF und Ang-2 kodieren.

GLV-1h343, GLV-1h344 und GLV-1h345 VACV kodieren denselben anti-PIGF Antikörper (Ak) unter der Kontrollen von drei verschiedenen Promotoren. GLV-1h492, GLV-1h493 und GLV-1h49 kodieren einen anti-Ang-2 Ak unter der Kontrollen von drei synthetischen VACV Promotoren. Zusätzlich wurden zwei Virusstämme konstruiert, die gleichzeitig zwei Angiogenesefaktoren anzielen. GLV-1h471 kodiert für einen anti-VEGF Ak. Der GLV-1h495 Stamm exprimiert einen Antikörper, der gegen VEGF gerichtet ist, und einen Antikörper, der gegen Ang-2 gerichtet ist.

In dieser Arbeit wurden verschiedene VACV-vermittelte anti-Angiogenese Therapien in vorklinischen Tumormodellen PC14PE6-RFP (Lungenadenokarzinome), Colo205 (KolonKarzinom), MEL1936 (Melanom) und A549 (Lungenadenokarzinome) evaluiert. Die Effizienz der VACV-vermittelten Hemmung von PIGF und Ang-2, singulär oder in Kombination mit VEGF Hemmung, wurde mit Tumor-Xenotransplantaten ermittelt und wurde in A549 Tumoren bestätigt. GLV-1h343, GLV-1h344 und GLV-1h471 reduzierten die Belastung für MEL1936 Tumoren fünf, beziehungsweise zwei mal effizienter als GLV-1h68.

Verschiedene Wissenschaftler kamen zu kontroversen Ergebnissen in Bezug auf die Potenz einer Krebsbehandlung mittels Ang-2 Hemmung. In dieser Studie konnte gezeigt werden, dass anders als VEGF, der Erfolg der Ang-2 Hemmung nicht nur mit der Stärke der Hemmung korreliert. Um Tumorregression sowie eine verbesserte Überlebensrate zu verursachen muss eine Behandlung eine bestimmte Balance zwischen Ang-2, VEGF und Ang-1 induzieren. Hier konnte man sehen, dass die GLV-1h68 behandelten Tumoren drei mal größer als GLV-1h492, GLV-1h494 und GLV-1h495 behandelten Colo205 Tumoren geworden sind. Dieselben Virus Stämme verursachten eine

erhebliche Verspätung der Wachstum der MEL1936 Tumoren während die frühen (3 und 7 Tage nach Behandlng) und der später Zeitpunkte (31, 35 und 42 Tage nach Behandlung). Ausserdem hat diese Arbeit die Notwendigkeit enthüllt, ein angiogenes Profil des zu behandelnden Tumors zu etablieren sowie den Bedarf die synergistischen Effekte von VEGF und Ang-2 besser zu verstehen. Des weiteren konnte durch Inhibition der Angiogenese durch VACV-verursachte PIGF und Ang-2 Hemmung die Anzahl der Metastasen und der migrierenden Tumorzellen reduziert werden (sogar effizienter als durch VEGF-Hemmung). Es konnte gezeigt werden, dass VEGF die VACV-Kolonisierung von A549-Tumorzellen limitiert, da der Einsatz eines anti-VEGF VACV GLV-1h108 zu einer drastischen Verbesserung der Effizienz der Kolonisierung führt, mit einer zweifachen Kolonisierung 72 Stunden nach der Infektion. In vivo Analyse der PC14PE6 Tumoren bestätigten dieser in vitro Daten. Vierzehn Tage nach der Behandlung kolonisierte das anti-VEGF Virus GLV-1h108 78,85% der Tumoren während die Kolonizationsquote des GLV-1h68 49,64 % war. Diese in Zellkultur erhobenen Daten bezüglich des synergistischen Effekts der VEGF-Hemmung und der VACV-Replikation resultierend in Tumorregression, konnten *in vivo* in einer PC14PE6-RFP verifiziert werden.

Drei der getesteten Tumorzelllinien, in welchen die VACV-vermittelte Angiogenese-Inhibition untersucht wurde, waren unter bestimmten Bedingungen in der Lage Endothelzellen oder Pericyten nachzuahmen und als Teil der Vaskulatur zu fungieren. Die Expression von Adhäsionsproteinen typisch für Endothelzellen wie e-Selektin, p-Selektin, ICAM-1 und VCAM-1 in diesen Tumorzellen untermauert unsere Ergebnisse. Diese Adhäsionsmoleküle, die durch In-cell ELISA detektiert wurden, spielen eine wichtige Rolle bei der Immunzell-Rekrutierung. Weiterhin konnte ein unterschiedliches Expressionsmuster in Anwesenheit von VEGF, PIGF und Ang-2 festgestellt werden, wodurch die Beteiligung angiogener Faktoren bei den immunmodulatorischen Eigenschaften von Tumoren gezeigt werden konnte.

In dieser Arbeit konnte gezeigt werden, dass eine VACV-vermittelte anti-angiogene Behandlung für verschiedene Tumorvarianten erfolgsversprechend ist und außerdem keine Resistenzbildung wie im Falle einer Bevacizumab-Behandlung nach sich zieht. Die Möglichkeit verschiedene Antikörper gegen unterschiedliche angiogene Faktoren zu

exprimieren würde verhindern, dass diese die die Angiogenese stimulierende Wirkung des VEGF übernehmen. Die Eigenschaft des VACV Tumorzellen zu infizieren verhindert, dass diese Blutgefäß-ähnliche Strukturen bilden würden, welche das Tumorwachstum gewährleisten. Weiterhin würde die lokal begrenzte Antikörper-Freisetzung das Risiko von Nebenwirkungen senken. Die Inhibition angiogener Faktoren würde die VACV Replikationsrate steigern und den immunmodulatorischen Effekt der Tumore abschwächen. Letztlich würde die Hemmung der Angiogenese bis zur völligen Regression des Tumors aufrechterhalten, die Neubildung Tumor-assoziierter Vaskulatur verhindern und somit den Rückfall des Patienten.

1 Introduction

1.1 Cancer

1.1.1 Cancer definition and epidemiology

Cancer is defined as a group of diseases involving the evolution of normal cells to a neoplastic and proliferative state. These insular masses of abnormal cells are able to invade normal tissues and organs by dividing themselves and growing beyond their allocated limits. This group of diseases was responsible for 8.2 million death worldwide in 2012 and 1600 death per day (estimated) in 2014 in United States only (Figure 1). These numbers are expected to increase by 70% over the next two decades (1) [1].

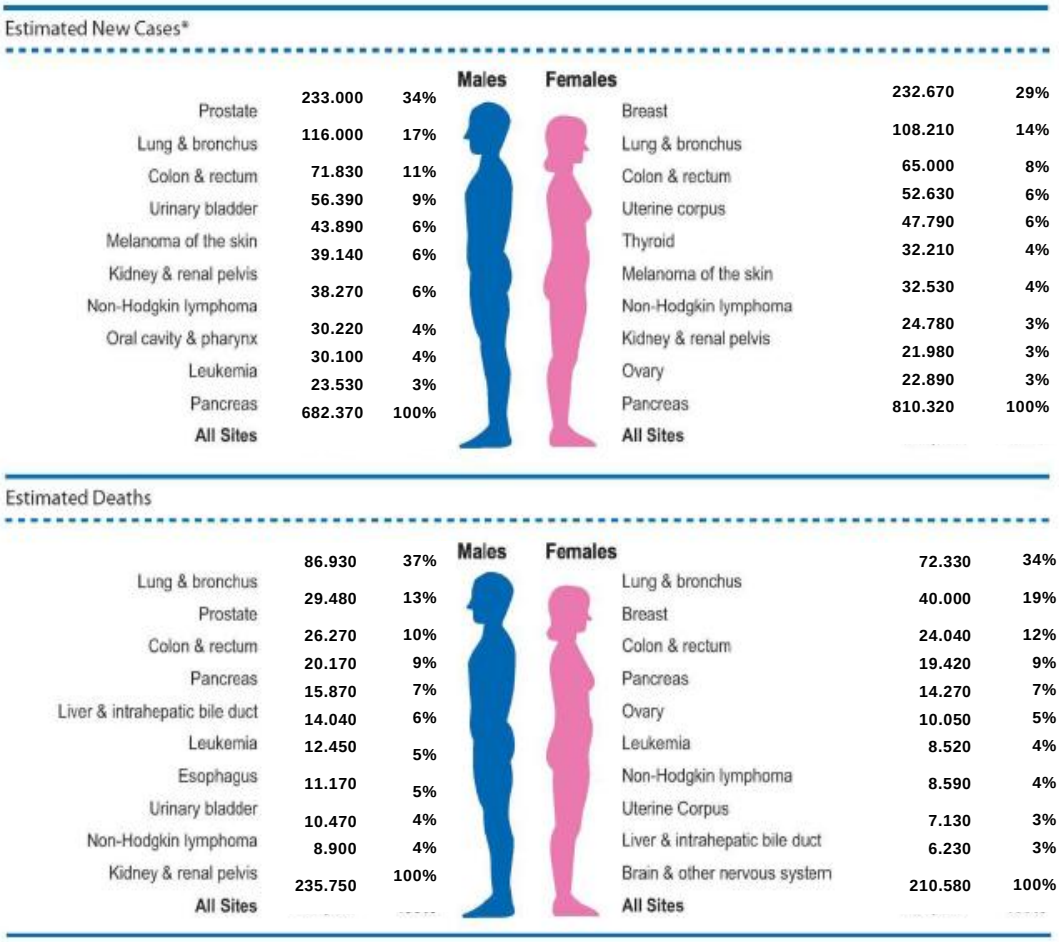

Figure 1: Cancer new cases and deaths in 2014 in United States (estimated numbers, from American Society of Cancer, Fact and Figures 2014 [1]). Adapted from Cancer Facts and figures 2012.

Despite numerous research programs and a continuous effort in medical technics, the extreme diversity of the profiles, metabolisms and progression strategies of the

different tumor types complicate the elaboration of a cure. Breast and lung cancer are the most frequent cancer types occurring among female and male individuals, respectively. Within these two tumor types, different subtypes have been described and characterized according to the physiology of the tumor for instance, breast tumors are categorized by their Her2 expression (Her2 positive and Her2 negative) while lung carcinomas are differentiated according to their phenotype (small cell and non-small cell lung carcinomas). Several factors are responsible for tumor pathogenesis. The genetic profile of an individual, its environment, pathogens encountered during his life, and his lifestyle (from alimentation to sport practice) altogether influence the probability of this individual to develop a tumor. This combination of factors making the categorization of cancer and thus the development of an appropriate treatment for each of these subtypes even more laborious. Nevertheless, the scientific understanding of the mechanisms defining and regulating carcinogenesis took a turn when Hanahan and Weinberg, 2000 [2] provided a logical framework embracing the diversity of this phenomenon along with its multifactorial features.

1.1.2 Characteristics of tumorigenesis

Six hallmarks of cancer have been described, the first and maybe the most fundamental trait of cancer cells is their ability to sustain chronic proliferation (Figure 2). In normal tissues, the cell-cycle and thus cells proliferation is tightly regulated by a controlled production and release of growth-promoting factors responsible for the entry and progression through the cell division cycle. These regulated divisions allow the tissue to control its physical limits and answer its physiological needs by adjusting the cell proliferation rate. For instance in case of injury, the production and release of growth-promoting signals shall increase to push a more important number of cells through the cell-growth and –division cycle, and allow the repair of the wound.

The second hallmark described is the evasion from growth suppressors. Logically, if we consider that the tumor's ultimate goal is, more than survive, live and proliferate, the over-expression of growth-promoting signals only is not sufficient for sustained proliferation, programs that negatively regulate cell proliferation must also be down-regulated. Factors intervening in these regulatory programs often depend on tumor suppressor gene expression. However several of these genes were found to exhibit an

impaired expression in cancer cells. The down-regulation of these genes, but also the modification of the signaling pathways regulating their targets, disable the control of the entry and progression of cells in the cell cycle. Evading growth suppressor effects also prepares tumor cells for an effective proliferation and evasion of their allocated compartment. In healthy cells propagated in two-dimensional culture, further proliferation is suppressed by cell contact. In other words, in a healthy tissue, an important cell population triggering cell-to-cell contact suppresses cell proliferation to contain them is a specific location. Therefore the suppression of this mechanism in tumor cells allow them to grow beyond these boundaries.

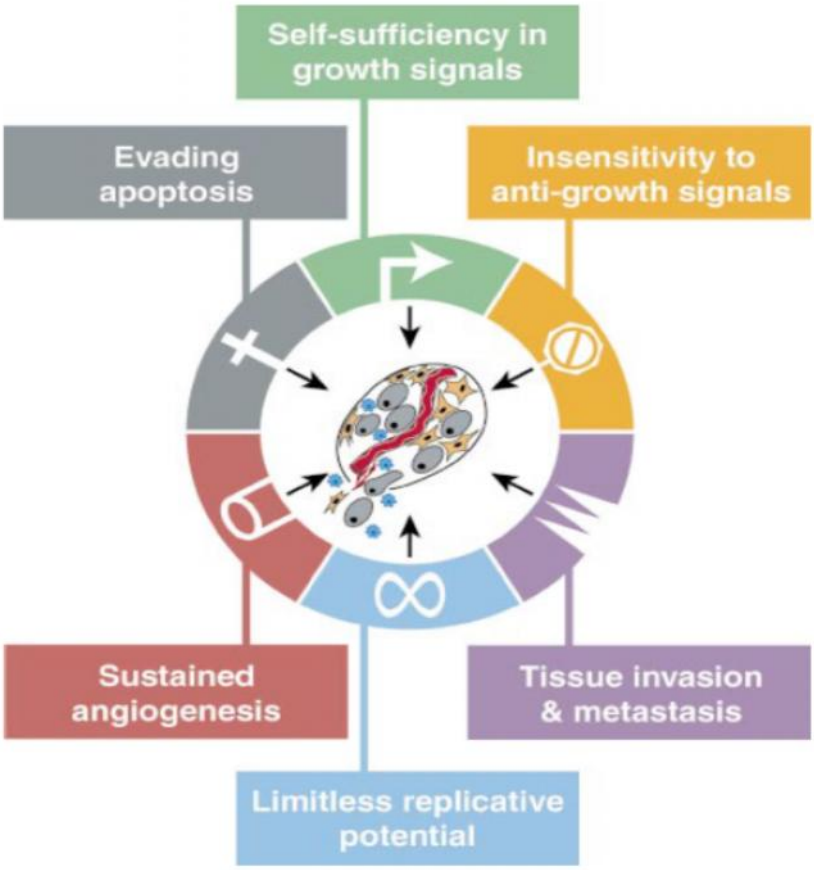

Figure2: Hallmarks of cancer (from [2]).

Another crucial characteristic of tumor cells described by Hanahan and Weinberg, 2000 [2] is their ability to resist cell death. Apoptosis is a naturally occurring process leading to a physiologically organized cell death. The dying cell is progressively disassembled in

apoptotic bodies containing the cell content. These bodies are cleaned by phagocytic cells before damaging the surrounding tissue. Several factors playing an active role in the apoptosis process, sensors, signaling pathways, and receptors, are impaired in tumor cells, thus the apoptosis process is inhibited.

In addition to resisting to cell death signals, tumor cells are able to replicate indefinitely. This unlimited replicative potential favors the rapid development of a macroscopic tumor. DNA modifications in the telomere region was shown to be accountable for the replicative immortality of tumor cells. Telomerase, the enzyme responsible for the polymerization and elongation of the telomere region of human chromosomes, is significantly over-expressed in immortalized cells while almost undetected in healthy ones. The elongation of the telomere region inhibits the induction of apoptosis and senescence (permanent-cycle arrest).

Tumors also possess a metastatic potential. As described previously tumors differ physiologically, genetically and molecularly but they also have variable strategies to form metastases. Because of the variability of this neoplastic disease, the modifications and strategies used to reach, invade and metastasize in other organs are broad. Nevertheless, every tumor has the potential to initiate a secondary tumor epicenter and metastasize. The development of metastases is always correlated with poor prognosis. Understanding and limiting this phenomenon is of first importance for the success of any cancer treatment. Before reaching a metastatic niche, tumor cells have to escape the primary tumor site and travel through the organism to find a suitable nest. Despite its variable pattern, general mechanisms allowing tumor cell circulation within the patient were identified. Two major metastatic routes have been described, the lymphatic and the vascular route. The lymphatic system accounts for the most important part of tumor cell circulation. This system allows cancer cells to travel between the organs and use lymph nodes as relay points. Nevertheless the vasculature system also plays a key role in this process. The cancer circulating cells will stop in a region favorable for tumor implantation described as metastatic niche. The detection and quantification of circulating cells was also shown to be an excellent monitor of the tumor stage and prognosis. An important amount of circulating tumor cells is often correlated with an important risk of metastasis and a poor prognosis. The prevention of tumor cells'

escape from the primary tumor site into the lymphatic and vascular systems would limit considerably the metastatic potential of tumors and help improving the life expectancy of patients.

The last hallmark of cancer described is the capacity of tumors to induce angiogenesis. Like all human tissues, tumors need nutrients and oxygen to stay alive, develop and invade other tissues. The development of a new vasculature associated to the tumor is the result of a process called angiogenesis. This neo-vasculature is responsible for the sustenance of tumors and the evacuation of metabolic wastes. However, as mentioned previously, this newly formed vasculature also serves as a route for circulating cells to escape the primary tumor site and form metastases. The particularities of tumor-induced vasculatures were investigated in this study.

1.1.3 Tumor induced angiogenesis

The development of any tissue or organ has to be sustained by an adapted vasculature. Tumor-associated vasculatures are described as leaky and tortuous structures [3]. The understanding of their role in tumor progression is an important subject of research in the oncology field.

1.1.3.1 The angiogenic switch

The tumor-associated vasculature, generated by angiogenesis provides nutrients and oxygen to the tumor. Judah Folkman documented in 1971 [4] the absolute necessity for tumors to induce the formation of a vasculature to grow beyond 2 mm^3. This scientific finding generated decades of active research on tumor-induced angiogenesis, angiogenic factors and their incidence on tumor progression. These studies largely confirmed this observation by both traditional transplant tumor models and genetically engineered mouse models depraved of certain angiogenic factors [2, 5-11]. Tumor progression was shown to be tightly related if not dependent on the development of an adapted vasculature. The notion of angiogenic-switch introduced by Hanahan and Folkman, 1996 [9] describes the modification of the angiogenic profile of the tumor, that starts over-expressing angiogenic factors to induce its vascularization.

1.1.3.2 Vascular Endothelial Growth Factor

Among the broad number of angiogenic factors abnormally expressed by tumor cells, the vascular endothelial growth factor (VEGF) is described as the most potent [12-15]. In addition to driving angiogenesis, this angiogenic factor also stimulates endothelial cell survival. VEGF was first described as a protein able to induce vascular leakage in the skin and named tumor vascular permeability factor (VPF) in 1983 [16, 17]. VEGF actually belongs to a family of angiogenic factors also comprising VEGF- B, -C, -D, -E and placental growth factor, and activating VEGFR1, 2, 3 and neuropilins. It is the activation of these tyrosine kinase receptors, expressed on endothelial cells, monocytes, macrophages and hematopoietic stem cells, which is responsible for the effects of the VEGF family in the angiogenic process (Figure 3) [19].

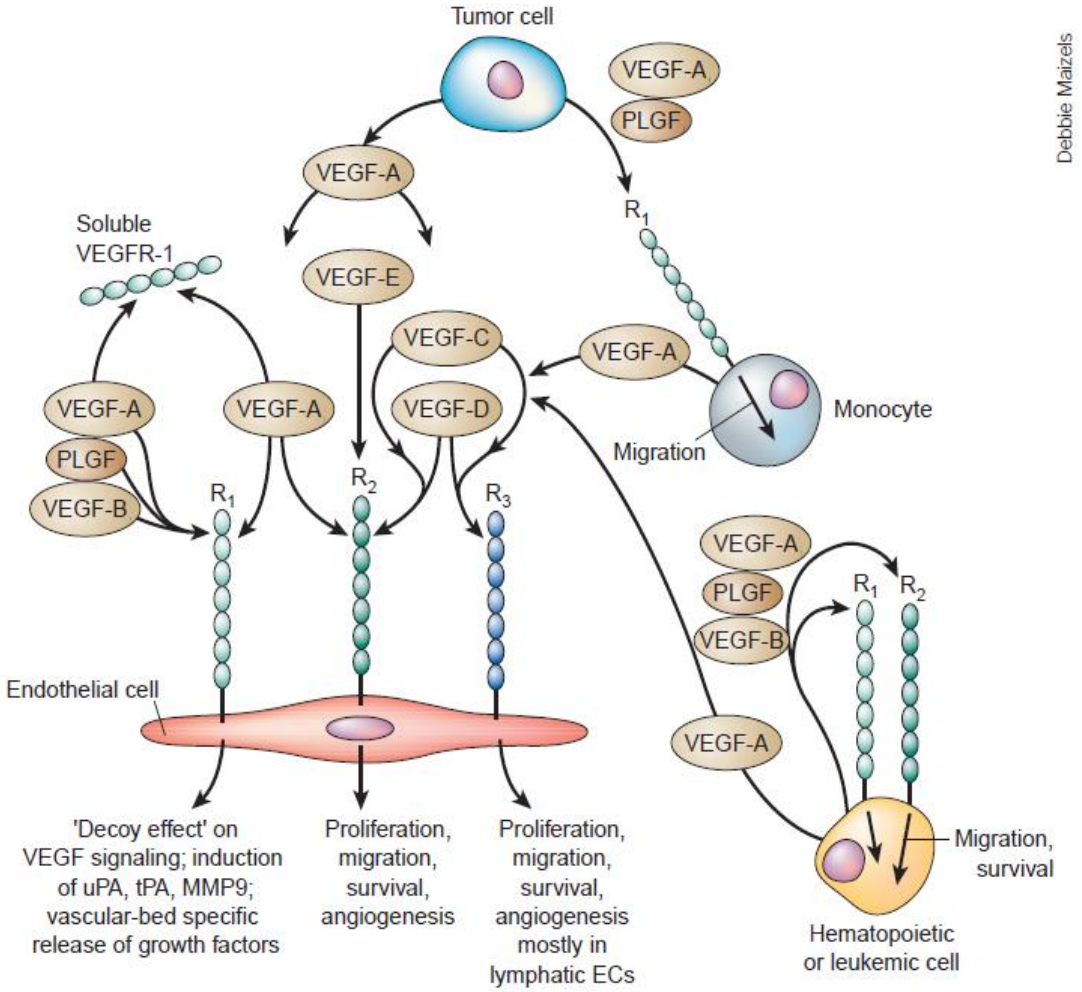

Figure 3: The VEGF family and its receptors (from [18]). Schematic representation of tumor-expressed VEGF factors on endothelial and hematopoietic cells.

These different isoforms may play distinct roles in angiogenesis during development. VEGF and the VEGF family are said to be normally expressed during embryogenesis, development, and in a lesser extent, during the wound healing process. Even though VEGF binding affinity for VEGFR1 is ten times higher than for VEGFR2, the latest is mainly responsible for VEGF signaling in endothelial cells [18]. Despite the redundancy of angiogenic factors, the blockade of VEGF pathway alone has been shown to significantly reduce, if not suppress angiogenesis in many solid tumor models. This reduction of tumor-associated vasculature was followed by the regression of orthotopic xenograft tumors in pre-clinical models.

1.1.3.3 Angiopoetin-2

Angiopoietins 1 and 2 are particular angiogenic factors implicated in vascular remodeling [19]. Their effect on the vasculature is mediated through the Tie-2 receptor, able to capture two of the four members of the angiopoietin family, angiopoietin-1 (Ang-1) and angiopoietin-2 (Ang-2). These two factors compete to access their receptor on endothelial cells. Angiopoietins are particular angiogenic factors because of their singular mode of action. Ang-1 binding to the Tie-2 receptor induces the recruitment and binding of pericytes, forming a supportive coat around the endothelium [20].

Ang-1 helps covering endothelial cells and thus structuring blood vessels, rending the extravasation of liquid and molecules into the interstitium more difficult. Ang-2 induces the opposite effect. When Tie-2 is activated by this effector, it facilitates the detachment of pericytes from endothelial cells, increasing drastically the permeability of blood vessels and the availability of the endothelium to other angiogenic factors (Figure 4).

Ang-2 over-expression in tumors has been established in several tumor types, however the actual interest of Ang-2 blockade for angiogenesis reduction in tumors stays controversial. Angiopoietins work in team with angiogenic factors directly stimulating endothelial cells, like VEGF. Ang-2 allows a fast modulation of the vasculature structure and the development of new blood vessels, while Ang-1 limits the access of angiogenic factors like VEGF and decreases blood vessels permeability. In the context of leaky blood vessels, like tumor-associated blood vessels, the blockade of Ang-2 is said to promote the formation of a more stable and less fenestrated vasculature [21]. The balance between Ang-1, Ang-2 and angiogenic factors like VEGF is the key for understanding and foreseeing Ang-2 blockade outcome.

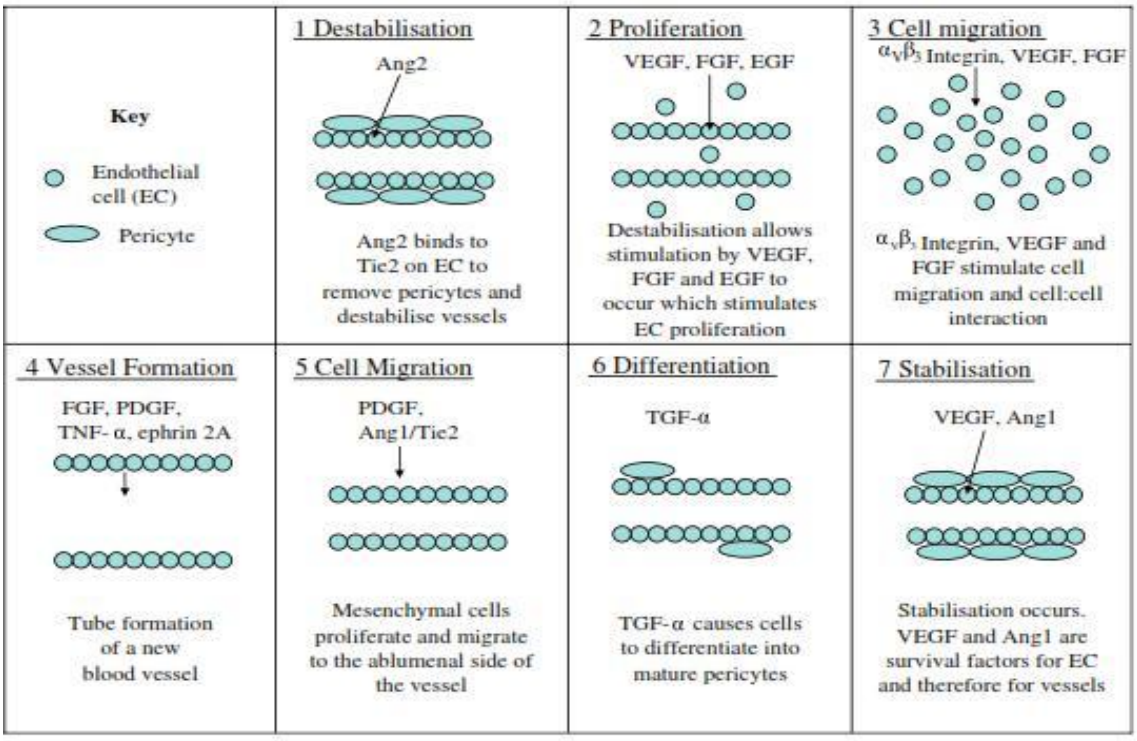

Figure 4: Role of angiopoietins in angiogenesis (from [20]).

1.1.3.4 Placental Growth Factor

Placental growth factor (PlGF) is a member of the VEGF family and activates the VEGFR1 receptor. This activation increases the proliferation, migration and survival of endothelial cells and thus stimulates angiogenesis [22]. However it has been demonstrated that PlGF binding leads to the phosphorylation of different tyrosine residues of VEGFR1 than VEGF binding, consequently, they might act through different pathways. In normal tissues, PlGF is present at low levels to contribute to the

angiogenesis activation during pregnancy, and stimulate the wound healing process. This angiogenic factor is expressed by several cell types including endothelial cells, vascular smooth muscle cells, immune cells implicated in the inflammation process, fibroblasts, but also several types of tumor cells. More specifically, PlGF was shown to be over-expressed in human gastric, breast, renal, and lung cancers and to display a prognostic interest with a PlGF expression in tumor tissues and sera correlating with tumor stage, vascularity, metastasis and survival.

This angiogenic factor has been revealed as a potential target for cancer therapy not only because of its effect on endothelial cells but also for its ability to attract and activate macrophages and myeloid progenitors, cells known to, in particular cases, produce angiogenic and lymphangiogenic factors (Figure 5)|23].

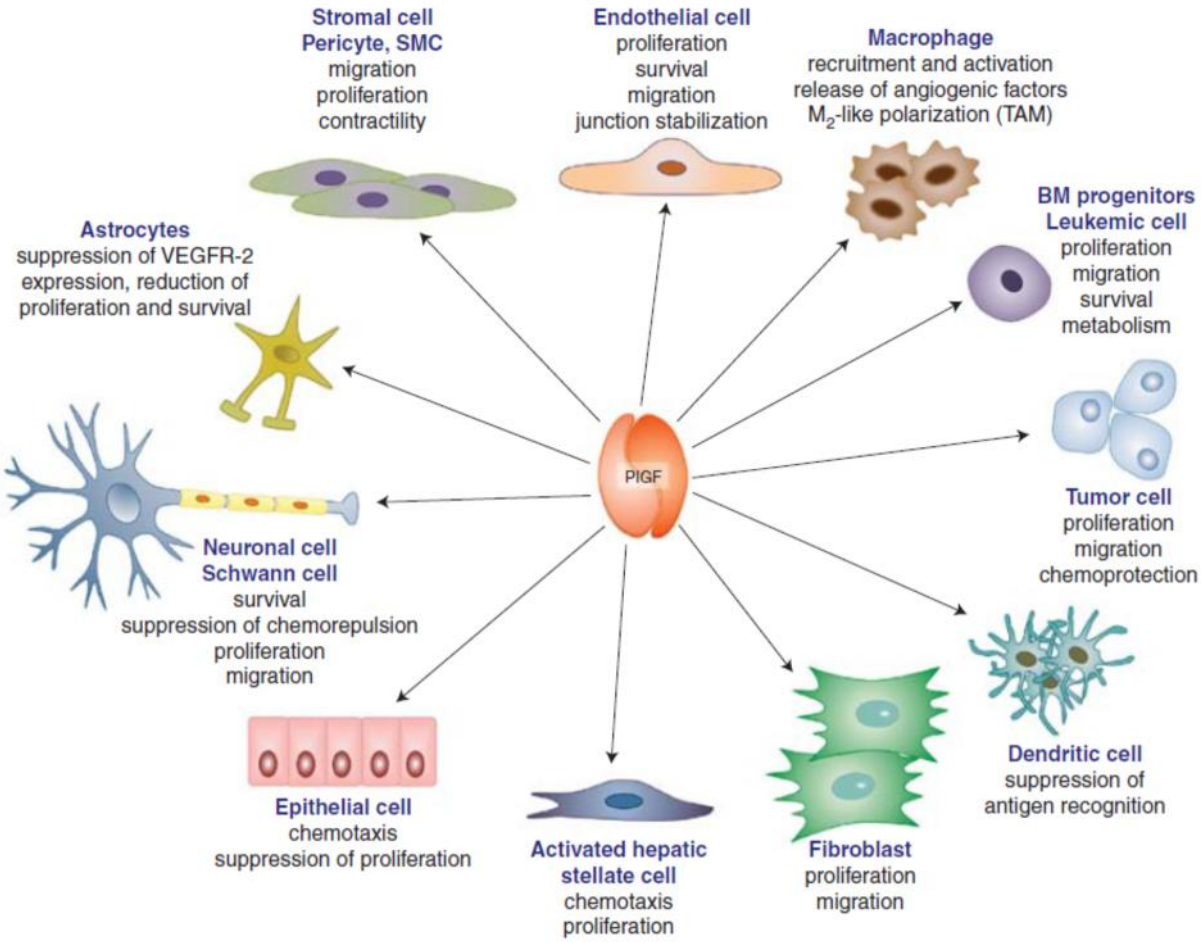

Figure 5: PlGF pleiotropic effect (from |23]). Schematic representation of PlGF effects in a pathologic context.

1.1.4 Angiogenic factors and endothelial junctions regulation

As mentioned previously VEGF holds an important role in angiogenesis. This angiogenic factor operates on endothelial cells through its VEGFR2 receptor, stimulating the proliferation, migration and survival of endothelial cells [18]. As a result, VEGF is able to increase the permeability of the endothelium. VEGF is a key effector of this system but also interacts with other signaling pathways. The effect of VEGF and the response of the endothelium is therefore also dependent of other factors (e.g. immunologic). VE-cadherin is a junctional protein involved in the maintenance of the endothelial barrier integrity. VEGF is thought to induce the phosphorylation of VE-cadherin and the loosening intercellular junctions [24]. VE-cadherin was also shown to contribute to neo-vascularization processes independently of angiogenic factor stimulation, showing the importance of the adhesion protein expression profile of endothelial cells in cancer progression [25-27]. VE-cadherin is one example of the implication of adhesive junctions in angiogenesis and tumor evolution.

1.1.5 Angiogenic factors and endothelial cell immune profile

The influence of angiogenic factors expressed by tumor cells on the ability of the endothelium to bind leukocytes, has been assessed in different studies. Endothelial cells isolated from human tumors expressed significantly lower levels of adhesion molecules involved in leukocyte-binding [28-33]. ICAM-1 is the most important adhesion molecule involved in the docking and extravasation of immune cells into the inflamed tissue [34]. The effect of different angiogenic factors on ICAM-1 expression has been evaluated on human umbilical vein endothelial cells (HUVEC). ICAM-1 was shown to be down-regulated in these cells, in presence of angiogenic factors. Nevertheless, the inhibition was limited. Contradictory results were found in other studies, claiming that VEGF increases ICAM-1 expression [30]. Even though researchers do not seem to agree on a general mechanism, endothelial cell response to angiogenic factors has been shown to be more diversified and important than initially thought (stimulate blood vessel formation), adding an immunologic component to endothelial cell response.

1.1.6 Current treatments and resistance

Angiogenic factor over-expression has been shown to promote abnormal vascular development in tumors. Angiogenesis is a vital process for the tumor. The perspective of

a simple way to block tumor progression by inhibiting the formation of tumor-associated blood vessels led to the development of several treatments. Two types of molecules were developed to target tumor-induced angiogenesis, receptor tyrosine kinase (RTK) inhibitors and antibodies [35 36].

RTKs mediate the transmission of extracellular signals, including growth factors, into the cytoplasm. The binding of a growth factor ligand to RTKs induce the auto-phosphorylation of the receptor. This phosphorylation leads to the transduction of the signal and the activation of endothelial cells proliferation in case of angiogenic factors. Many of these factors, shown to be expressed in different tumor types, bind to RTKs. We can cite VEGF, platelet derived growth factor (PDGF), angiopoietins and epidermal growth factor as a non-exhaustive list. RTKs have a central function in angiogenesis regulation but also in other aspects of cell metabolism. Several inhibitors of activated RTKs have been developed including Sunitinib and Sorafenib. These small proteins are taken orally and target activated RTKs, influencing tumor-associated angiogenesis, tumor cell proliferation and metastases. Despite an interesting broad range of action on the tumor progression, this strategy also exhibits several side effects [36].

The second type of molecules targeting angiogenesis are the antibodies. This type of treatment is more specific to angiogenesis. Bevacizumab, the first specific anti-angiogenesis treatment approved by the FDA targets VEGF. Despite very promising results in preclinical evaluations, bevacizumab did not meet expectations in cancer patients. In addition to the side effects experienced by patients, most likely due to the fact that bevacizumab administration is intravenous, and thus not restricted to the tumor site, tumors also developed ways to circumvent the treatment. First of all, the redundant profile of angiogenic factors in tumors allow them to adapt to the treatment. Angiogenic factors can substitute for one another to keep on stimulating the development of new blood vessels. Furthermore, as mentioned previously, some angiogenic factors are also able to attract hematopoietic progenitors and certain types of immune cells, both able to produce angiogenic factors. The attracted cells thus help counterbalance the VEGF blockade and maintain a level of angiogenic factors sufficient to stimulate angiogenesis [37, 38]. Finally, another way to circumvent VEGF blockade is the selection of tumor cells resistant to hypoxia. The lack of oxygen, hypoxia, activates a

downstream pathway through HIF (Hypoxia inducible factor), that leads to the activation of angiogenic factors production. In other words, in case of hypoxia, the tumor activates angiogenesis by producing more angiogenic factors. However, certain tumor cells are able to maintain a dormant phenotype that requires a very low amount of oxygen and thus allow them to survive in a hypoxic environment without activating angiogenesis. When the bevacizumab treatment is stopped, these cells can then reinitiate the development of the tumor [39-43]. These resistance mechanisms all lead to the results observed in cancer patients, in which VEGF blockade induced a diminution of the tumor size at first, but was then sometimes followed by relapses [36]. For these patients, VEGF blockade improved temporarily the tumor decay, but did not improve their life expectancy.

Nevertheless, blocking angiogenesis still stand as an excellent strategy for cancer treatment, it just appears that it will need further understanding of the resistance mechanisms and a better treatment strategy.

1.2 Vaccinia Virus

1.2.1 Vaccinia virus historical use

The introduction by Edward Jenner of the vaccination against the deadly variola virus using another family member of the Poxviridae led to the complete eradication of smallpox in the late 1970s [44]. Vaccinia virus (VACV) belongs to the Orthopoxvirus genus, one of the eight genera of the Chordopoxvirinae subfamily. Along with VACV, this genus comprised variola virus, the vector of smallpox, and cowpox virus. Cowpox virus is the original vaccination agent used by Edward Jenner in the late 1700s for variola virus immunization [45]. For a still unknown reason, the democratization of immunization against variola virus also led to a change of the agent used. Vaccinia virus replaced cowpox as a vaccination agent, and many different VACV strains were used during the eradication program, including the New York City Board of Health strain (NYCBH), the Paris strain, the Copenhagen strain (Cop) and the Listeria strain, developed at the Lister Institute of the United Kingdom, and considered as the most widely used vaccinia vaccine throughout the world.

1.2.2 Virology

Poxviruses, including VACV, are large genome (130-375 kb) DNA viruses with the singular ability to complete their replication cycle in the cytoplasm of the infected cell, while other DNA viruses need to enter the nucleus and even integrate their genome into the DNA of the host-cell to complete their replication [45,46].

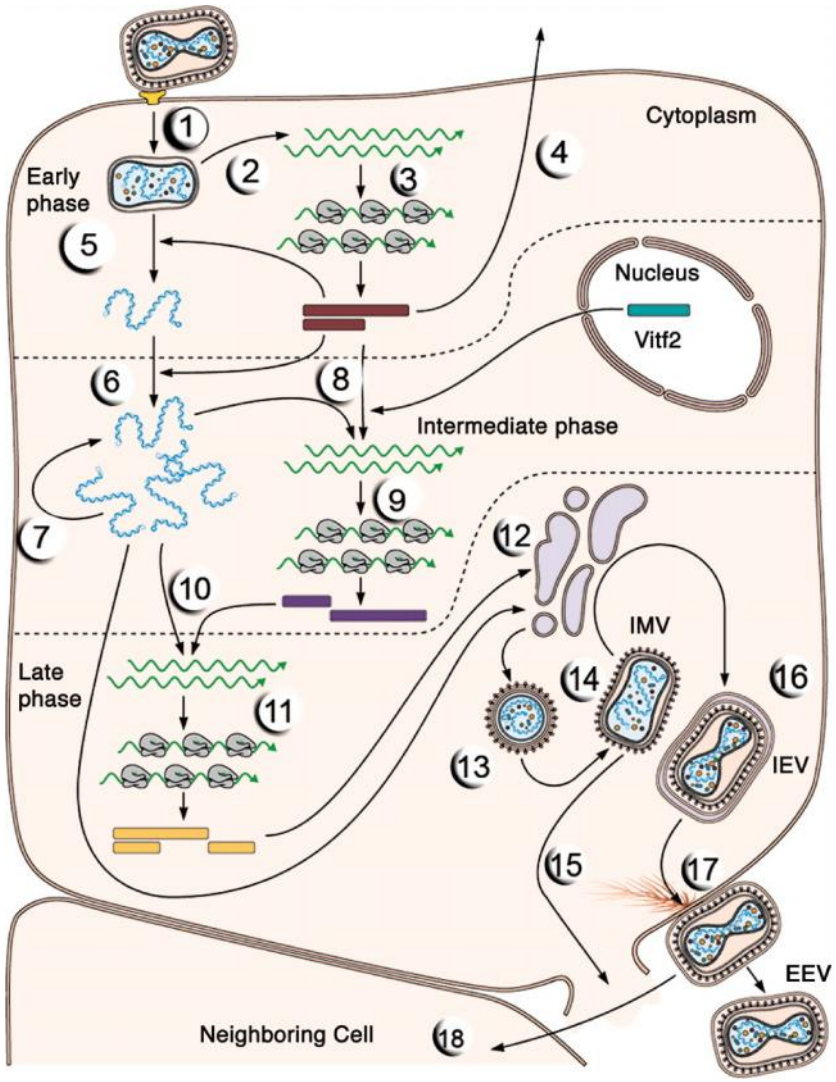

Figure 6: Schematic representation of Vaccinia virus replication cycle (modified from [46]). (1) EEV entry (2-4) early proteins synthesis (5-7) viral DNA replication (8-11) Transcription of early and late genes (12-14) Production of IMVs (15) IMV expulsion via cell lysis. (16), IEVs creation. (17) Transformation of IEVs into CEVs (18) Transformation of bounded CEVs into free EEVs

Vaccinia virus replication cycle produces four different types of virions. The first are the intracellular mature virions (IMV), formed in the cytoplasmic factories of the infected-

cell, using noninfectious precursors, the immature crescent particles. Intracellular mature virions are constituted of a unique membrane and represent, in quantity, the majority of the infectious progeny of the infected cell. These virions stay within the cell until lysis. Some of the IMVs use microtubules to leave the production site and join the trans-Golgi network where they acquire their double lipid membrane to form intracellular enveloped virions (IEV). IEVs are able to reach the cell surface and form two different types of virions, cell-associated enveloped virus (CEV) or extracellular enveloped virus (EEV) (Figure 6). CEV particles are retained on the cell surface. The formation of an actin tail capable of propelling a virion away from a cell can transform a cell-associated enveloped virion into an extracellular enveloped virion, the most important disseminative form of the virus within the infected organism. IMVs particles are physically robust structures that endure freezing, thawing, desiccation and physical pressure, which enable them to survive in the environment. Even though their limited motility doesn't favor a cell-to-cell transmission within the same host, their robust structure is favorable to a host-to-host dissemination [45-50].

Vaccinia virus receptor(s) and mode of entry are still not known. Some studies described possible modes of entry by relating physiological processes occurring after vaccinia virus entry. However these hypothesis need to be confirmed in a broader range of cell types for example [49, 52]. We can then read studies suggesting that VACV entry may occur by fusion with the plasma membrane or during the internalization of extracellular fluid via endosomes and micropinocytosis but these hypotheses also need to be confirmed.

Vaccinia virus replication requires unknown protein interactions to be established between virus and host, and is able to infect human cells very efficiently [53].

1.2.3 Vaccinia virus and oncolytic virotherapy

The propensity of viruses to interfere in tumor progression has been observed decades ago, but it was only in 1991 that the use of an attenuated virus for the treatment of glioblastoma in nude mice was described [55]. Several types of viruses are being modified and developed as therapeutic agents, e.g. adenoviruses and herpes viruses [56]. With the success of smallpox eradication, and the readily established methods for vaccinia virus production as a therapeutic agent, VACV became of interest as a cancer

treatment [57, 58]. One of the advantages of vaccinia virus as an expression vector and as a therapeutic tool is the ability of his genome to integrate foreign genes up to 25kb length and still be able to sustain viral replication. Which allows the insertion of additional therapeutic and/or imaging agents for increased therapeutic impact and better monitoring of the virus. Moreover, since vaccinia virus replication cycle is contained in the cell cytoplasm, the risk of adverse genetic modification of patients DNA and viral genome is limited [46]. Altogether its specificities designate vaccinia virus as a promising tool for cancer treatment.

2 Aim of my thesis

A good understanding of the tumor micro-environment and especially of the formation and function of the tumor vasculature is of major interest to allow the design of a long lasting anti-tumor treatment, able to prevent and circumvent the development of treatment resistance.

2.1 Part 1: The roles of angiogenic factors in tumor-induced angiogenesis and beyond

The development of a tumor vasculature is a crucial step for the survival and evolution of a tumor. This fact has been solidly demonstrated by several studies [5-11] led by the article of Folkman and al., 1971 [4]. The blockade of VEGF, the most potent angiogenic factor described so far, over-expressed by tumor cells, was supposed to be sufficient to impair tumor induced angiogenesis and thus tumor growth. The growing evidence that tumors can circumvent that blockade underline the need to dig deeper in the physiology and molecular biology of tumor-associated vasculature.

2.2 Part 2: Effect of VEGF blockade on VACV treatment

Vaccinia virus is a promising tool for cancer treatment, but combining it with the expression of a foreign protein requires to determine first whether the expression of these proteins alters vaccinia virus replication cycle and then if the effect of these proteins, in this case single chain antibodies, limits VACV oncolytic effect.

2.3 Part 3: Evaluate different strategies to circumvent anti-VEGF resistance

Because of its powerful role as an angiogenic factor and its over-expression in broad tumor types, the effect of VEGF on tumor vasculature development has been extensively studied. However the lack of continuous long term therapeutic effect on patients treated with bevacizumab exposed the need to elaborate a strategy, compatible with VEGF blockade, to anticipate resistance.

PlGF and Ang-2 are two angiogenic factors with different receptors and different mechanisms of action. Despite controversial results, they have been both described as

significant angiogenesis inducers in the tumor-induced angiogenesis process. It was the goal of this thesis to determine whether the blockade of Ang-2 and PlGF improve and complement the anti-VEGF strategy.

3 Material and Methods

3.1 Material

3.1.1 Cell lines and culture media

Cell lines

PC14PE6-RFP	Human lung adenocarcinoma
2H-11	Murine tumor endothelial cells
A549	Lung adenocarcinoma
MEL1936	Human melanoma
Colo205	Human colon adenocarcinoma
HEK293	Human embryonic kidney cells
HeLa	Human cervical adenocarcinoma
CV-1	African green monkey kidney fibroblast
PC-3	Human prostate carcinoma
DBTRG	Human glioblastoma
HT-29	Human colorectal adenocarcinoma
U-138-MG	Human glioglastoma
MCF-7	Human breast adenocarcinoma
GI-101	Human breast carcinoma
MEL888	Human melanoma
PLC	Human liver hepatoma
HT-1080	Human fibrosarcoma
MDA-MB-435	Metastatic human breast carcinoma
MDA-MB-231	Human breast adenocarcinoma
DU-145	Human prostate carcinoma

Cell line	Medium
CV-1, 2H-11, HeLa, MDA-MB-231 and PLC	DMEM High glucose (4,5 g/L) 10% FBS 1% Antibiotic-Antimycotic
CV-1, 2H-11 and HeLa infection media	DMEM High glucose (4,5g/L) 2% FBS 1% Antibiotic-Antimycotic
MEL1936, A549 and Colo205	RPMI 1640 10% FBS 1% Antibiotic-Antimycotic
MEL1936, A549, and Colo205 infection media	RPMI 1640 2% FBS 1% Antibiotic-Antimycotic
PC14PE6-RFP	DMEM High glucose (4,5 g/L) 10% FBS 1% Antibiotic-Antimycotic 1% Glutamax 1% Non essential amino acids
PC14PE6-RFP infection medium	DMEM High glucose (4,5 g/L) 2% FBS 1% Antibiotic-Antimycotic

	1% Glutamax 1% Non essential amino acids
GI-101	RPMI 1640 20% FBS 1% Antibiotic-Antimycotic 1.2% Sodium pyruvate 1.2% HEPES 0.6‰ BE2 (Estradiol/Progesteron)
HT-29	DMEM High glucose (4,5g/L) 10% FBS 1% Antibiotic-Antimycotic 2.2% Sodium pyruvate
HEK293	DMEM High glucose 10% FBS 1% Antibiotic-Antimycotic
HT-1080	EMEM 10% FBS 1% Antibiotic-Antimycotic 2mM Glutamine 1% Non essential Amino acids

MDA-MB-435 and U-138-MG	DMEM High Glucose (4.5 g/L) 10% FBS 1% Antibiotic-Antimycotic 4mM L-gluamine
MCF-7	RPMI 1640 20% FBS 1.2% Glucose 1% HEPES 1% Sodium pyruvate 1% Antibiotic-Antimycotic 0.6‰ BE2 (Estradiol/Progesteron)
DBTRG	RPMI 1640 10% FBS 1% Antibiotic-Antimycotic 2.2% Sodium pyruvate
DU-145	EMEM 10% FBS 1% Antibiotic-Antimycotic 1% Non essential Amino acids 1% Sodium pyruvate

3.1.2 Chemical and enzymes

Chemical	
100 bp DNA Ladder	New England Biolabs
1 kb DNA Ladder	New England Biolabs
3,3',5,5-Tetramethylbenzidine (TMB) liqud	Sigma
45% Glucose solution	Cellgro
Accuprime Pfx supermix	Invitrogen
Acetic acid ($C_2H_4O_2$)	Fisher
Acridine orange	Fisher
Agarose	BioRad
Agarose Low Melt	BioRad
Ampicillin	Sigma
Angiopoietin-2 (recombinant)	R&D systems
Antibiotic-Antimycotic Solution	Cellgro
Basement Membrane matrix (matrigel)	BD Biosciences
Benzonase ® Nuclease	Novagen
Blocker ™ Casein in PBS	Pierce
Bovine serum albumin (BSA)	Sigma
Bovine plasma gamma globuline	BioRad

Bromophenol Blue	Aldrich chemical company
Carboxymethylcellulse (CMC)	MP
Clearslip mounting media	IMEB Inc.
Complete His-Tag Purification Resin	Roche
Coomassie brilliant blue G-20	Sigma
Crystal violet	Sigma
Diaminoethanetetraacetic acid (EDTA)	Sigma
Dulbecco's Modification of Eagle's Medium (DMEM)	Cellgro
Dimethyl sulfoxide (DMSO)	VWR
Deoxycholic acid	Fisher Biotech
Difco ™ Agar	BD
Difco ™ LB Broth	BD
Dulbecco's Phosphate Buffered Saline (DPBS) 1x	Cellgro
EDTA-Trypsin	Cellgro
Eagles Minimum Essential medium (EMEM)	Cellgro
Ethanol	Sigma
Ethidium bromide	Sigma
Fetal Bovine Serum	Cellgro
Formaldehyde	Fisher

Formalin	Fisher
Fugene transfection reagent	Roche
Glycerol	Fisher
Hematoxylin QS	Vector
HEPES buffer	Cellgro
Hoechst	Sigma
HyClone Hypure cell culture water	Fisher
Hydrochloric acid (HCl) 12M	VWR
Hydrogen peroxide (H_2O_2)	Sigma
Hypoxanthine	Sigma
Imidazole	Sigma
Isoflorane	Explora
Isopropyl alcohol	EMD
Kanamycin	Sigma
Laemmli sample buffer 4x	BioRad
Lipofectamine	OzBiosciences
Magnetofectamine	OzBiosciences
Methanol	Sigma
Modified Eagle's medium (MEM)	Cellgro
Monosodium phosphate	Fisher

Mowiol 4-88	Sigma
N-,N-Dimethylformamide ($(CH_3)_2N(O)H$)	Sigma
Non-essential amino acids (NEAA)	Cellgro
Nonidet P-40	Sigma
Nocodazole	Sigma
NuPAGE 10% Bis-Tris Gel	Invitrogen
NuPAGE 12% Bis-Tris Gel	Invitrogen
One shot TOP10 E.Coli	Invitrogen
PacI	New England Biolabs
Paraformaldehyde 16% slution (PFA)	EMS
Paraplast Tissue Embedding Medium	McCormick scientific
Phenylmethylsulfonyl fluoride (PMSF)	Sigma
Placental Growth Factor	eBioscience
Polyethylenimine, branched (PEI)	Sigma
Potassium chloride (KCl)	Fisher
PrecisionPlus Protein Standards	BioRad
Protease inhibitor cocktail	Invitrogen
Propanol	Sigma
RNAse Zap	Ambion
Roswell Park Memorial Institute medium 1640 (RPMI 1640)	Cellgro

SacI	New England Biolabs
SalI	New England Biolabs
S.O.C medium	Invitrogen
Sodium chloride (NaCl)	VWR
Sodium Hydroxyde (NaOH) 2N Solution	Fisher
Sodium pyruvate ($C_3H_3NaO_3$) solution	Cellgro
Tris	Fisher
Triton X-100	Sigma
Trypan blue solution	Cellgro
Tween-20	BioRad
Vectorstain Elite ABC reagent	Vector Laboratories
Vector ImmPact DAB Peroxidase substrate	Vector Laboratories
Human VEGF-A (recombinant)	Sigma
Xanthine	Merck
Xylazine	Lloyd Laboratories
Xylene Substitute	Sigma
Z-fix	

3.1.3 Buffers and solutions

	Recipe
Acridine Orange staining (2x)	37 mM citric acid 126 mM Na_2HPO_4 150 mM NaCl 1 mM Na2EDTA Acridine Orange 6 mM ddH_2O
Agarose histology washing buffer	0.25% Triton X-100 1x PBS (pH 7.4)
Agarose histology blocking buffer	0.25% Triton X-100 5% Normal goat serum 1x PBS (pH 7.4)
Coomassie staining solution	40% Methanol 0.025% Coomassie Brilliant Blue R-250 7% Acetic acid 53% dd H2O
Citrate buffer	0.1 % Citric Acid 0.1 M Sodium Citrate dd H_2O (pH 6)
CMC overlay medium	1x DMEM medium

	1.5% Carboxymethylcellulose
	2% FBS
	1% Antibiotic-Antimycotic
Crystal violet staining solution	1.3g crystal violet
	5% ethanol
	30% formaldehyde (37%)
	dd H_2O
ELISA coating buffer	3.7g Sodium Bicarbonate
	0.64g Sodium Carbonate
	1L dd H_2O
Flag-tag immunoprecipitation washing buffer (10X)	0.5 M Tris HCl (pH 7.4)
	1.5 M NaCl (sterile)
His-Tag purification Buffer A	dd H_2O (up to 50 mL)
	50 mM NaH_2PO_4 (pH 8)
	300 mM NaCl
His-Tag purification Buffer B	ddH_2O (up to 50 mL)
	50 mM NaH_2PO_4 (pH 8)
	300 mM NaCl
	300 mM Imidazole
In-cell ELISA washing buffer	1x PBS (pH 7.4)

	0.1% Tween-20
In-cell ELISA blocking buffer	1x PBS (pH 7.4)
	1% Tween-20
Lysis Buffer	50 mM Tris-HCl, pH 3.5-5
	2 mM EDTA (pH 7.4)
	2 mM PMSF
RBM tissue homogenization buffer	1x PBS (pH 7.4)
	50 mM Tris-HCl
	2 mM EDTA
	1 tablet of complete protease inhibitor
Xylene cyanol loadding buffer (6x)	25 mg Xylene cyanol
	4 g Sucrose
	dd H_2O (up to 10 mL)

3.1.4 Antibodies

Primary Antibody	Origin	Manufacturer
anti-A27L (CAKKIDVQTGRRPYE)	rabbit	Genscript
anti-DDDDK	rabbit	Abcam
anti-MECA32	rat	
anti-b-actin	mouse	Sigma
anti-e-selectin	rabbit	Santa Cruz Biotechnology

anti-p-selectin	goat	Santa Cruz Biotechnology
anti-VCAM-1	goat	Santa Cruz Biotechnology
anti-ICAM-1	goat	Santa Cruz Biotechnology
anti-CD31	rat	BDPharmingen

Secondary antibody	Origin	Manufacturer
anti-rabbit-HRP	goat	BioRad
anti-goat-HRP	donkey	Santa Cruz Biotechnology
anti-goat-Alexa Fluor 594	donkey	Santa Cruz Biotechnology
anti-rabbit-Alexa Fluor	donkey	Santa Cruz Biotechnology
anti-rat-avidin	rabbit	

3.1.5 Kits

Kit	Manufacturer
Cell Profilefiration kit II (XTT)	Roche
DAB Map kit (RUO) Discovery ®	Ventana Medical
DC™ protein assay	BioRad
DNAse free™ DNAse treatment and removal	Ambion
Human Angiopoietin-2 ELISA	Life sciences
Human VEGF ELISA kit	Life sciences

Improm-II Reverse transcription system	Promega
Nucleobond Xtra Midi Plus	Mackey-Nagel
Plasmid Maxi kit	Qiagen
PlGF human ELISA kit	Abcam
Purelink DNA purification kit	Invitrogen
Purelink Quick gel extraction kit	Invitrogen
Purelink Quick Plasmid Miniprerp	Invitrogen
RNeasy Maxi kit	Invitrogen
VECSTASTAIN ABC kit	Vector Laboratories

3.1.6 Synthetic oligonucleotides

Name	Sequence
aPlGF SacI for	5'- GAG CTC CCA TGG AGA CAG AC -3'
aPlG SacI rev	5'- GAG CTC TTA CTT GTC GTC GTC ATC CTT -3'
aPlGF secR fw	5'- GQG CTC CCA CCA TGG GGA TCC TTC CCA GCC CTG GGA TGC CTG CGC TGC TCT CCC TCG TGA GCC TTC TCT CCG TGC TGC TGA TGGGTT TCG TAG CTG ATG AGA CAG ACA CAC TCC -3'
human b-actin fwd	5'- CCT CTC CCA AGT CCA CAC AG -3'
human b-actin rev	5'- CTG CCT CCA CCC ACT -3'
Plex-m sqcing fw	5'- GCA GAG TCC TTA AGT TGC -3'

Plex-m sqcing rev	5’- TCG AGG CAT GCG CCG -3’

3.1.7 Laboratory equipment and other material

Amicon Ultra-15 Centrifugal Filter Unit 10kDa cut-off	Millipore
Argus-100 Low Light Imaging System	Hamamatsu
Balance PL1501-S	Mettler-Toledo
Biosafety cabinet	The Baker Company
Carestream Imaging System	Carestream
Cell culture cluster 6-, 24- and 96-well Costar	Corning
Cell culture flasks	Corning
Cell Lab Quanta SC Flow Cytometer	Beckman Coulter
Cell scraper	Corning
Centrifuge Centra CL2	Thermo Scientific
Centrifuge CL 21	Thermo Scientific
Centrifuge Micro 1816	VWR
Centrifuge Sorvall RC 6 Plus	Thermo Scientific
Centrifuge Sorvall Legend RT	Thermo Scientific
Combitips Plus 1, 2, 5 and 25 mL	Eppendorf
Cryotubes 2 and 1 mL	Nalgene

CK30 culture microscope	Olympus
Digital caliper	VWR
Digital dry bath incubator	Boekel Scientific
Dish 100 mm	Fisher Scientific
Embedding Mold TISSUE-TEK ®	IMEB Inc.
Falcon 15 and 50 mL tubes	BD
Falcon centrifugation device 3K, 10k MWCO	Pall Corporation
Firewire DFC/IC monochrome CCD camera	Leica
Havels stainless steel surgical scalpel size 15	Braintree Scientific
Heater	VWR
Hotplate stirrer 375	VWR
Incubator	Forma Scientific
Incubator HERA Cell 150	Thermo Electron
Insulin syringe U-100 27G, 29G	BD
IX71 inverted fluorescence microscope	Olympus
MagNA Lyser	Roche
MagNA Lyser green beads	Roche
MicroAmp® Fast Optical 96-well reaction plate	Applied Biosystems

Microfuge tubes easy open cap 1.5 mL	Saarstedt
Microplate reader SpectraMax MS	Molecular Devices
Microscope cover glass	Fisher Scientific
Microslides Premium Superfrost®	VWR
Microtome Leica RM 2125	IMEB Inc.
Microwave Carousel	Sharp
Mini-Sub® Cell GT	BioRad
Multipipette	Eppendorf
MZ 16 FA stereo fluorescence microscope	Leica
Nikon Eclipse 6600 microscope	Nikon
Parafilm laboratory film	Pechiney Plastic Packaging
pH Meter Accumet AR15	Fisher Scientific
Photometer Biomate3	Thermo Spectronic
Pipette Aid	Drummond
Pipette Tips 10, 200, 300 and 1000 μL	VWR
Pipettes 20, 200 and 1000 μL	Rainin
Pipettes 1, 5, 10 and 25 mL	Corning
Repeater® stream pipette	Eppendorf

Rocking platform	VWR
Sonifier 450	Branson
StepOnePlus Real-Time PCR system	Applied Bisystems
Stereo Fluorescence macroimaging system	Lightools Research
Sterile disposable scalpel	Sklar Instruments
Syringe 1, 30, 60 Ml	BD
Syringe 20G	BD
Syringe Driven Filter Unit Millex®-VV PVDF 0.2 μm	Millipore
Tissue culture dish 60 mm	BD
Tissue Embedding Center	Reichert-Jung
Tissue Processing/Embedding Cassettes with Lid	Simport
Titer plate shaker	Thermo Scientific
Illumatool Tunable Lighting System	Lightools Research
Vibratome VT 1200S	Leica
Vortex VX100	Labnet
Water bath	Boekel Scientific
Water bath Isotemp202	Fisher Scientific
X Cell Sure Lock ™	Invitrogen

3.1.8 Recombinant vaccinia virus strains

In this study, seven recombinant vaccinia viruses derived from the wild-type (wt) Listeria Strain were used. All these viruses were constructed and produced at Genelux Corporation, San Diego. The parental virus GLV-1h68, used for the design of the anti-angiogenesis viruses evaluated in this study, was described in 2007 [59] (Figure .7).

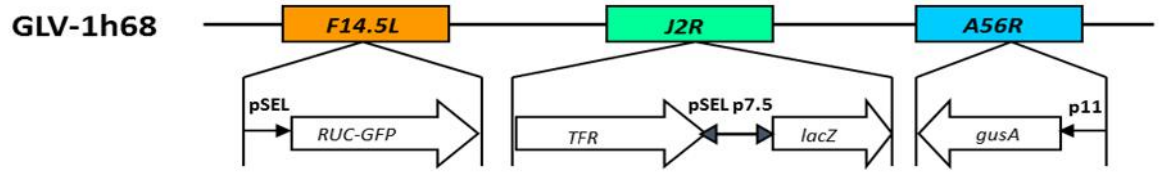

Figure 7: Therapeutic VACV GLV-1h68.
Schematic representation of the organization of the three foreign genes inserted in VACV genome

This virus was engineered by insertion of three expression cassettes, Renilla luciferase-Aequorea green fluorescent protein (Ruc-GFP) fusion, β-galactosidase (LacZ) and β-glucuronidase (GusA) respectively into the F14.5L, J2R (thymidine kinase) and A56R (hemagglutinin) loci of the LIVP genome.

The insertion of these three transgenes was shown to enable GLV-1h68 to selectively localize, enter, replicate and lyse tumor cells in a healthy organism; and thus validates GLV-1h68 as a suitable oncolytic treatment. As described previously, all tumor models treated did not respond significantly to GLV-1h68 treatment alone. Moreover, anti-angiogenesis strategies were shown to significantly impair tumor growth, facilitating their treatment. To improve the effect of the therapeutic vaccinia virus GLV-1h68, expression cassettes containing single chain antibodies (scAb)directed against VEGF, PlGF and Ang-2 have been inserted in the thymidine kinase and/or hemagglutinin loci of GLV-1h68 to create anti-angiogenesis vaccinia viruses (Figure 8, 9 and 10).

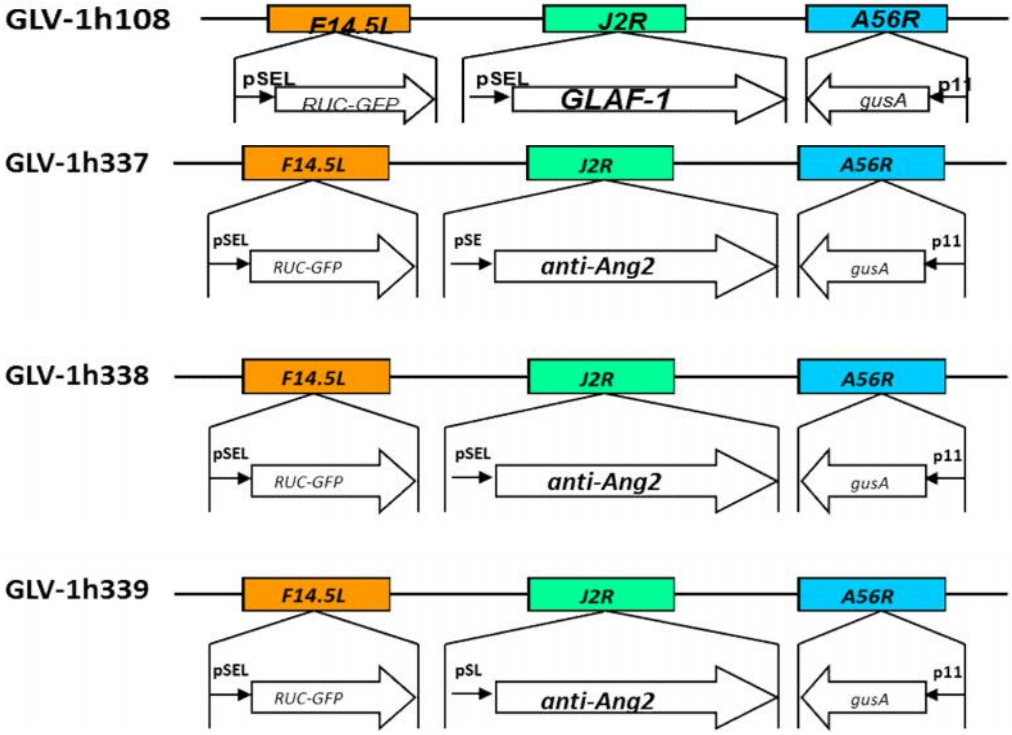

Figure 8: Anti-VEGF and anti-Ang-2 VACVs

Schematic representation of the three genes inserted in the anti-VEGF (GLV-1h108) and anti-Ang-2 (GLV-1h337, GLV-1h338, GLV-1h339) VACV genome, with their scAb in the J2R locus.

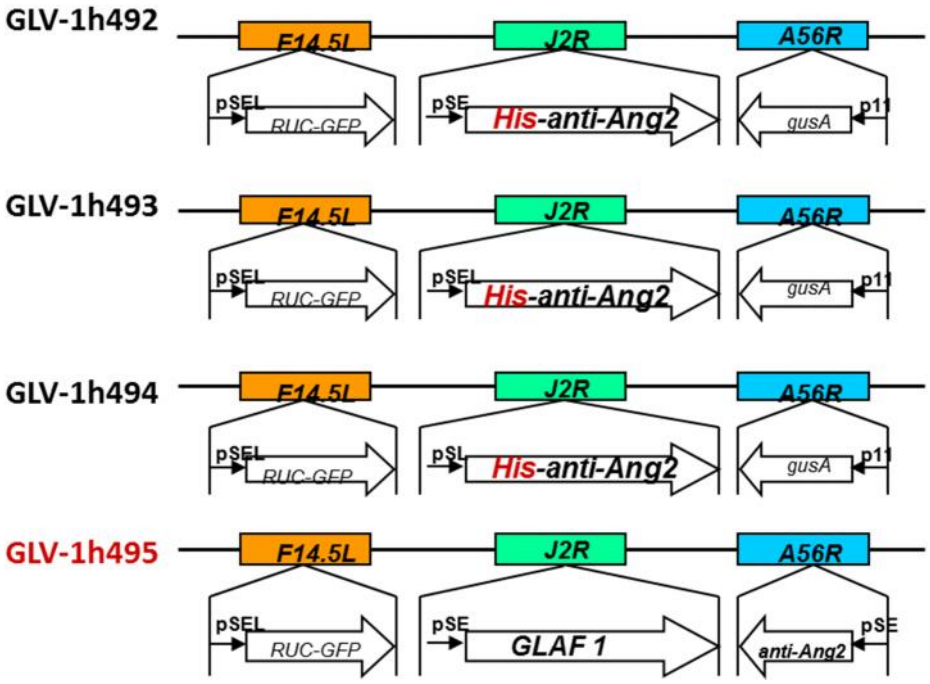

Figure 9: Schematic representation of Anti-Ang-2 VACVs.

GLV-1h492, GLV-1h493, and GLV-1h494 comprise an anti-Ang-2 scAb in their J2R loci. GLV-1h495 genome contains the GLAF-1 antibody (Ab) in its J2R locus, and the anti-Ang-2 Ab in in the A56R locus.

All the anti-angiogenesis viruses were constructed by Dr. Alexa Frentzen. The anti-VEGF virus GLV-1h108, using GLV-1h68 backbone and described in Frentzen et al., 2009 [60], has a genome enclosing the GLAF-1 expression cassette in lieu of the LacZ and inverted TFR genes. GLAF-1, a flag-tagged antibody targeting human and murine VEGF, is under the control of a synthetic early/late promoter.

Several sets of anti-angiogenesis viruses were made. For purification and detection purposes, two sets of anti-Ang-2 viruses, expressing an anti-Ang-2 scAb directed against human angiopoietin-2, were designed. GLV-1h337, GLV-1h338 and GLV-1h339 express flag-tagged anti-Ang-2 scAb; while GLV-1h492, GLV1h493 and GLV-1h494 express a His-tagged version of the antibody. Anti-PlGF viruses, expressing a scAb against human PlGF, under the control of early, early/late and late promoters, were also prepared (GLV-1h343, GLV-1h344 and GLV-1h345).

In order to evaluate the effect of combined anti-angiogenesis therapies, viruses expressing antibodies against VEGF and Ang-2 or against VEGF and PlGF were constructed. GLV-1h495 expresses GLAF-1 (flag-tagged) and the His-tagged antibody against Ang-2 under the control of the viral early promoter, when GLV-1h471 expresses GLAF-1 and the anti-PlGF scAb under the control of the early/late promoter.

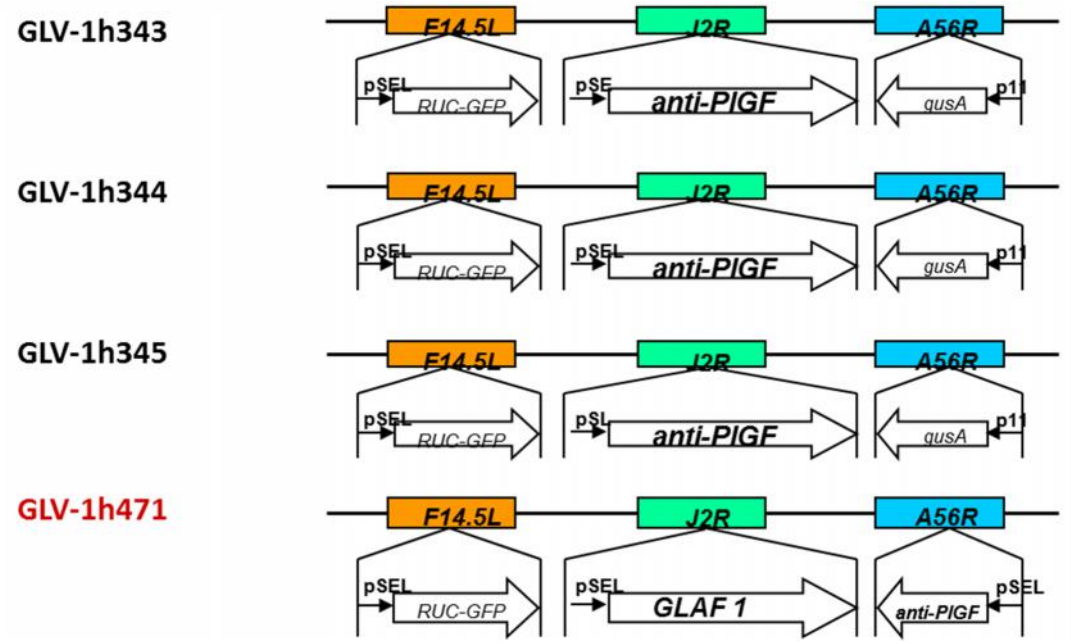

Figure 10: Schematic representation of Anti-PlGF VACVs.
GLV-1h343, GLV-1h344, and GLV-1h345 include an anti-PlGF scAb in their J2R loci. GLV-1h471 genome contains the GLAF-1 ab in its J2R locus, and the anti-PlGF scAb in ithe A56R locus.

3.1.9 Laboratories animals

Every animal study carried out in the San Diego Science Center was performed on male nude *Foxn1^{nu}* mice purchased from Harlan Laboratories. Mice were cared for in accordance with approved protocols by the Institutional Animal Care and Use Committee of LAB Research international Inc. and Explora Biolabs (San Diego, USA, protocol numbers ACUP EB14-043 and EB11-025.

The animal experiment carried out in Würzburg (Germany) has been done on female *Foxn1^{nu}* mice, in accordance with protocols approved by the government Unterfranken (Würzburg, Germany, protocol number AZ 55.2-2531.01-17/08).

Foxn1^{nu} mice (or nude mice) are characterized by a mutation of the *nu* locus of their 11th chromosome resulting in a rudimental thymus and an impaired T-cell production when B-cells and macrophages activity remains intact.

3.2 Methods

3.2.1 *Cell culture*

3.2.1.1 Maintenance and passaging of human and murine cells

All human and murine cells used in this study were handled inside a biosafety cabinet, under sterile conditions. CO_2 incubators were maintaining the cells in a 37°C, 95% humidity and 5% CO_2 environment. These incubators were regularly sanitized with a 70% ethanol solution and a virucidal solution, cells cultured in sterile flasks, plates, cell culture dishes and in medium containing an antibiotic-antimycotic solution.

3.2.1.2 Cell quantification

A hemocytometer was used to quantify the number of cells to be seeded, especially for angiogenic factor expression determination (see 3.2.2.1) and tube formation assays (see 3.2.1.4) for which the evaluation of the cell density is critical. Using an optical microscope, a counting grid engraved in the counting chamber permits the determination of the number of cells in a determined volume. The use of a Trypan blue, solution, that stains dead cells and debris in blue but not live cells, allows the distinction between living and dead cells. Cells concentration is determined as follows:

Number of cells counted per main squares × 10^4 × dilution factor = cell number/mL

3.2.1.3 Angiogenic factors levels modulation

Human lung adenocarcinoma cells (A549) VEGF expression per 10^6 was measured. A549 cells were then incubated with multiples of the basal amount of VEGF they expressed (2, 5, 8 and 10 times). For instance, if the basal amount of VEGF expressed is 5 units per 10^6 cells, A549 cells will be incubated with 10 units of VEGF, The angiogenic factor was added in the incubation medium prior to seeding.

In a different experiment, to determine the influence of angiogenic factors on tumor cells metabolism, murine endothelial cells 2H-11 as well as PC14PE6-RFP, HeLa, MEL1936 and A549 tumor cells were also incubated with 1 mg/mL of recombinant human VEGF, PlGF or Ang-2 prior to be seeded in 96-well plates (see 3.2.2.3).

3.2.1.4 Tube formation assay

Endothelial cells are able to build a tubular structure *in vitro* resembling the *in vivo* vascular network [61-65]. Therefore, 90% confluent murine 2H-11 cells were passaged 1 day prior to the assay at a 1:10 ratio in a new T-225 flask. The level of confluence and homogeneity of the cell layer is critical for the success of the assay. The next day, 2H-11 cells were harvested, counted (see 3.2.1.2) and seeded on 15 µL of matrigel when seeded in 96-well plate and 100 µL of matrigel when seeded in 24-well plates. The assay was performed in two different containers because 24-well plates allow a more accurate quantification of the phenomenon while 96-well plates require a shorter incubation time and amount of matrigel. The matrigel layer was prepared by pipetting under sterile conditions the desired amount of the viscous preparation in the container, without any air bubbles, and incubating it 30min at 37°C. According to the manufacturer protocol this gel needs to be gently thawed at 4°C, on ice, the gel aliquot should never reached a higher temperature in order not to impair the 3D matrix formation. After 3 hours and up to 24 hours post seeding, tubular structures are visible in 96-well plates.

The incubation time needed to observe the structures, the amount of cells seeded, and their confluence before and during the assay were determined experimentally. In all cases, experiments were performed in duplicates or triplicates to confirm the results.

3.2.2 Enzyme-Linked Immunosorbent Assays (ELISAs)

3.2.2.1 Binding activity assessment by ELISA.

Anti-angiogenesis VACVs express His- or Flag-tagged antibodies against VEGF, PlGF and Ang-2. The functionality of these antibodies, in other words their ability to bind to their target protein was evaluated before use. GLAF-1, anti-PlGF and anti-Ang-2 binding abilities have been assessed previously, but only data about GLAF-1 have been documented. Solutions of coating buffer containing either 1 μg/mL of PlGF or 1 μg/mL of Ang-2 or a serial dilution of flag-tagged BAP protein ranging from 1000 to 2 ng/mL have been pipetted in separate 96-well plates and incubated overnight at 4°C. After washing 1 time with distillated H_2O and 2 times with 1x PBS 0.05% Tween-20, the residual uncoated gaps were blocked with 200 μL of Blocker™ Casein in PBS for 4 hours at room temperature. The wells were then washed 4 times with 1x PBS 0.05% Tween-20, and the samples and standard serial dilutions added to their designated wells for a 2 hour incubation at room temperature. After removal of the samples and four washing steps with 1x PBS 0.05% Tween-20, a 1:5000 dilution of the primary anti-DDDDK antibody was added to the wells and incubated 1 hour at room temperature. The secondary antibody was then added for a 1 hour incubation at room temperature after removal of the primary antibody and washing the plate four times with 1x PBS 0.05% Tween-20. After removing the secondary antibody and washing the plates 4 times like described previously, the ELISA was developed by adding 100 μL of TMB substrate and stopping the color development by adding 100 μL of 2N HCl. The absorbance was read in a microplate reader at 450 nm and 550 nm for background noise.

The same protocol has been used to determine the functionality of aPlGF and quantify it.

3.2.2.2 Angiogenic profiles of tumor cells

Angiogenic factors are known to be over-expressed in several tumor cells types. In order to select the appropriate tumor model to evaluate the effect of their blockade on tumor progression and therapeutic vaccinia viruses, the expression of PlGF, Ang-2 and VEGF of several tumor cell lines was assessed by quantitative sandwich ELISA. For this purpose the mammalian cells were seeded in 6-well plates, at a concentration allowing them to reach 90% confluence in 48 hours. After 24 hours, when all the cells were settled in the wells, their medium was changed and the time noted. Precisely 24 hours

later, the supernatant of the cells was harvested, treated with proteinase inhibitors and immediately frozen in liquid nitrogen. The cells were collected, counted, lysed in presence of proteinase inhibitors and frozen in liquid nitrogen. All samples were stored at -80°C before being analyzed by ELISA.

ELISA is a well-known and acknowledged quantitative technique. Commercially available ELISA kits, with strips precoated with primary antibodies against the protein to detect, were used to quantify VEGF, PlGF and Ang-2 in the different cell samples collected. All the kits were used according to the manufacturers' protocols, the dilution used for the quantifications varied between cell lines and were determined experimentally after a first ELISA of serial dilutions of all the samples. The determination of the dilution is crucial for an accurate quantification. All the quantifications were confirmed at least once by repeating the experiment on an unthawed, unused and relatively fresh sample, always kept on ice, to avoid biased results due to protein degradation.

To evaluate the amount of angiogenic factors circulating in tumor bearing mice, sera of VACV-treated and -untreated mice were used in quantitative ELISAs. The dilutions used for quantification were determined experimentally and by considering manufacturer's instructions.

3.2.2.3 In-cell ELISA

The detection of proteins in and on cells is usually done by flow cytometry (FACS).This powerful tool allows the detection and quantification of the targets as well as the number of cells within the sample. However FACS analysis often requires a long and delicate preparation of the samples, especially when several targets are to be tested. Moreover, using this tool would have necessitated the transportation of samples to an appropriate facility. Consequently, the use of an ELISA technique would facilitate the detection and quantification of VCAM-1, ICAM-1, e- and p-selectin after incubation with VEGF, PlGF and Ang-2. In-cell ELISA enables the analysis of adherent cultured cells under different conditions in one assay. The cells (A549, 2H-11, HeLa, MEL1936 and PC14PE6-RFP) were cultured in presence of angiogenic factors as described previously (see 3.2.1.3). After 24 hours, the cells were fixed by adding an equal volume of an 8% PFA solution for 20 min at room temperature. The PFA solution was then gently

removed and cells gently washed three times on a plate shaker with 1x PBS 0.1% Tween-20. The cells were then permeabilized and additionally fixed by a 5 minutes treatment with ice cold methanol. After 4 washes with 1x PBS 0.1% Tween-20, the plates were blocked using 1x PBS 1%Tween-20 for 2 hours at room temperature. After another washing step (x4), the cells were ready to be incubated with the designated primary antibody (anti-VCAM-1, -ICAM-1, -e-selectin and -p-selectin) at a dilution of 1:1500, for 2 hours at room temperature. Once the primary antibody was gently removed and the plates washed 4 times, the cells were incubated with a 1:1000 dilution of the appropriate secondary antibody for 1 hour at room temperature. The secondary antibody was then removed and the plates washed 4 times before adding 100 μL of the TMB solution at room temperature, in the dark for 5 min. A 2N HCl stop solution was then used to give the final coloration (100 μL per well). The absorbance was read at 450 and 550 nm.

In order to normalize the data according to the cell density, the cells can be treated with Acridine Orange staining after washing the plates 4 times with 1x PBS 0.1% Tween. Acridine Orange (AO) is a metachromatic dye which differentially stains double-stranded (ds) and single-stranded (ss) nucleic acids. When AO intercalates into dsDNA it emits green fluorescence upon excitation at 480-490 nm. On the contrary, it emits red fluorescence when interacting with ssDNA or RNA. By looking at the green fluorescence emission, the relative amount of cells can be evaluated, and the expression of the protein obtained can be normalized by the number of cells. On ice, washed 96-well plates were incubated for 5 min, in the dark with 100 μL per well of AO staining solution (2x)

3.2.3 Protein production and purification

3.2.3.1 Purification GLAF-1, anti-PlGF and anti-Ang-2 antibodies from VACV infected cells

To evaluate the functionality of the scAb expressed by the anti-angiogenesis VACVs (see 3.2.2.1), 4×10^7 CV-1 cells were infected at MOI 2 (see 3.2.4.1) for 24 hours in T-225 flasks with 15 mL of infection medium. Supernatants have been harvested, filtered with 0.4 and 0.2 μm filters to remove the virus and any dead cells, treated with the

appropriate amount of proteinase inhibitors, and concentrated in 1 to 1.5 mL using a 10k or 3k MWCO device and a centrifuge at 3000 rpm. The purification resin (specific to flag or his-tagged proteins) was washed 3 times with the adapted washing buffer. The concentrated supernatant was then incubated 2 hours at 4°C for the tagged protein to bind to the resin. The concentrated supernatant was then removed, the resin washed, and the tagged protein eluted by a 30 min incubation with the elution buffer. The purified protein was quantified using the DC protein assay and stored for later use.

3.2.3.2 Production and purification of aPlGF antibody

3.2.3.2.1 Synthesis of an aPlGF expressing plasmid

The plex-m plasmid for transient protein expression in mammalian cells has been generously provided by Prof. Dr. Jones and Dr. Zhao (University of Cambridge). This plasmid allows the expression of proteins by transfection of mammalian cells and is not transmitted by mitosis to the daughter cell [66].

3.2.3.2.2 Production and purification of aPlGF

To evaluate the functionality of aPlGF, CV-1 and HEK293 cells were transfected in 6-well plates using PEI branched and 0.5 and 5 µg of plasmid, using the protocol provided in [66]. After 24 hours, supernatants of the transfected cells have been harvested and aPlGF purified using the Flag immunoprecipitation resin (see 3.2.3.1). Repeated ELISA assays showed that aPlGF can bind to PlGF and be detected by an anti-DDDDK (flag-tag) antibody, in conclusion the antibody is functional.

3.2.4 Virological methods

3.2.4.1 Infection of mammalian cells using therapeutic VACV

Eighty to ninety-five percent confluent tumor and endothelial cells were seeded at a multiplicity of infection (MOI) adapted to the assay. The MOI unity represent the theoretical number of virus particles available to infect one cell. The amount of virus needed for each experiment was calculated as follow:

$$Input\ Virus = \frac{Number\ of\ Wells\ x\ MOI\ x\ Cell\ Count/\ Well}{Viral\ Titer}$$

Virus aliquots or samples suspected to contain virus were either thawed rapidly in a 37°C water bath or on ice, before being sonicated three times for 30 seconds to disperse any virus aggregates. The desired amount of virus or sample was then added to a fresh infection medium and dispensed onto the cells to be infected in place of the culture medium.

3.2.4.2 Vaccinia virus titration using plaque assay

Plaque assay is a common procedure for titrating the amount of virus in a sample, it was used to titrate virus stocks (data not shown) and evaluate the amount of virus in murine biological samples. The first step of this procedure consist in growing CV-1 cells to 90-95% confluence in 24-well plates, before infecting them with serial dilutions of the sample to titrate. Samples were diluted in 250 µL of infection medium and poured gently onto the CV-1 cells. After a one hour incubation at 37°C, the infection medium was replaced by a CMC overlay medium (1mL/well) and the CV-1 cells placed back into the 37°C incubator. Staining of the cell layer and visualization of viral plaques was performed 48 hours post infection by adding 250mL per well of a crystal violet solution. After several hours CV-1 plates were rinsed in a water bath and dried. The number of plaques was counted manually and the viral titer calculated according to the following formula:

$$\frac{Number\ of\ plaques}{Dilution\ factor\ x\ infection\ volume} = Virus\ titer\ (pfu/ml)$$

3.2.5 *In vivo* experiments

3.2.5.1 Xenograft tumors implantation and monitoring

Four- to six-week old male nude-Foxn1^{nu} mice were implanted with 5 × 10^6 A549 and 4 × 10^6 PC14PE6-RFP, Colo205, or MEL1936 cells. Tumor cells were implanted by a subcutaneous injection of cells diluted in 100 µL of 1x PBS per implant. Therapeutic VACVs were administered when tumors reached a size of 200-400 mm^3 (depending of the tumor model). To assess the therapeutic efficacy of each treatment, tumor growth was monitored twice a week by measuring the tumor in three dimensions using a digital caliper and calculating the tumor volume using the following formula:

$$Tumor\ Volume = \frac{length \times width \times width}{2}$$

Tumor size is reported as relative tumor volume corresponding to the tumor volume at the given time point divided by the tumor volume at the initiation of the treatment.

3.2.5.2 Organs and tumors preparation for virus and human cells detection

Tumors and organs were dissected, using sterilized scissors and tweezers to avoid any contamination, and their weight was recorded. Two different protocols were used to homogenize the samples, they were either placed in MagNA Lyser Green Beads tubes® or in Swirl bags®. When placed in MagNA Lyser Green Beads tubes®, samples were shredded at 3000 rpm for 30 seconds using the MagNA Lyser®. Alternatively, when placed in Swirl bags®, samples were subjected to manual compression, until sample was appropriately homogenized. In all cases 1mL of PBS containing a proteinase inhibitor cocktail was added to each sample before homogenization and this volume was taking into account for weight related quantifications. The samples were then stored at -80°C until use.

For viral titration, samples underwent 3 rapid freeze-thaw cycles before being sonicated three times 30 seconds to complete the destructuration of the tissues and to separate virus aggregates. The samples were then titrated on CV-1 cells as described previously (see 3.24.2.).

3.2.5.3 Human cell detection

Human β-actin is one of the ubiquitous gold standard genes used to detect human cells in biological samples. The detection of human β-actin RNA in a murine organs indicates the presence of at least one human cell with a functional translation machinery. In other words, the detection of β-actin implies the presence of at least one living human cell in the organ analyzed. Total RNA of organs, harvested from tumor-bearing mice, and treated with different therapeutic VACVs, were extracted using the RNeasy® Maxi kit according to the manufacturer protocol. DNA, DNAses and RNAses were removed using RNeasy and Ambion kits. The RNAs extracted were retro-transcribed according to a protocol previously described [67] and using the Improm-II retrotranscription kit to

form cDNAs. The presence of the human b-actin gene was then assessed by PCR using human β-actin primers and the following reaction steps:

PCR program:
- Denaturation at 95°C for 30 seconds
- Annealing at 58°C for 30 seconds
- Elongation at 72°C for 15 seconds
- This sequence of steps have been repeated 29 times

PCR reaction mix:
- 1 mL of cDNA
- 1 μL of human β-actin fw primer (200 pmolar/mL)
- 1 μL of human β-actin rev primer (200 pmolar/mL)
- 22 μL of *Pfx* supermix

3.2.5.4 Histological preparations

3.2.5.4.1 Sample preparation and immunostaining of paraffin sections

As for viral titrations, tumors and organs were dissected using sterilized scissors and tweezers to avoid any contamination. Following dissection, samples were placed into a 10% neutral buffered formalin solution for overnight fixation at 4°C. Before undergoing dehydration, samples were directly placed in embedding cassettes if they were no thicker than 5 mm or sliced accordingly to an appropriate size before being placed in the cassettes. The dehydration process comprised the following steps: on a rocking platform, 0.9% NaCl, 30% EtOH in 0.9% NaCl, 50% EtOH in 0.9% NaCl, 70% EtOH in H_2O, 90% EtOH in H_20, 100% EtOH (2 times). Fresh paraffin wax was melted ahead of time, and samples were incubated in the following solutions: 100% EtOH, EtOH-xylene 1:1, xylene, xylene-wax 1:1, wax (3 times). Samples were then embedded in paraffin, cut in sections of 5 to 10 μm thickness using a microtome, placed on microscopic slides. Sections were dewaxed and rehydrated for immune-staining. Antigens were retrieved using a steamed 10μm sodium citrate buffer solution (pH 6.0), and after a washing step,

endogenous peroxidase activity was quenched with 3% hydrogen peroxidase. Sections were finally stained for vaccinia virus using an anti-A27L antibody (Genelux custom-made rabbit polyclonal antibody, 1:1000 dilution), or blood vessels using an anti-MECA32 antibody (dilution 1:30) and revealed using biotinylated secondary antibodies and horseradish peroxidase.

3.2.5.4.2 Sample preparation and immuno-staining of agarose sections

To embed biological samples in agarose, freshly dissected tumors were snap frozen in liquid nitrogen before being fixed in a 4% paraformaldehyde (PFA) solution, overnight at 4°C. Subsequent to fixation, samples were washed 5 times to remove any remaining PFA and embedded into a 5% low melting point agarose matrix. Embedded tumors were then cut into 100 μm sections using a Leica RM 2125 microtome and blocked with 5% goat serum 1 hour at room temperature prior to immunostaining. VCAM-1 and endothelial cells are stained using anti-VCAM-1 and anti-CD31 antibodies primary antibodies and Alexa-fluor 594 secondary antibody.

3.2.6 Statistical analysis

One way ANOVA tests were used to determine the statistical relevance of experimental data involving several populations (tumor volumes, protein expression, viral replication, etc.)

4 Results

4.1 Angiogenic factors VEGF, Ang-2 and PlGF are expressed by various tumor cell types.

Tumor-induced angiogenesis is widely accepted as a requirement for tumor progression [4]. The important role and prevalence of VEGF in tumor development was shown in numerous studies [13, 14]. However, the significance of Ang-2 and PlGF is still controversial [68]. Several tumor cell lines were tested for VEGF, Ang-2 and PlGF expression by ELISA (Figure 1.1, Figure 1.2). For that purpose, selected cell lines and their supernatants were harvested and conditioned for ELISA when cells reached 95% confluence. The protein expression was evaluated per 10^6 cells.

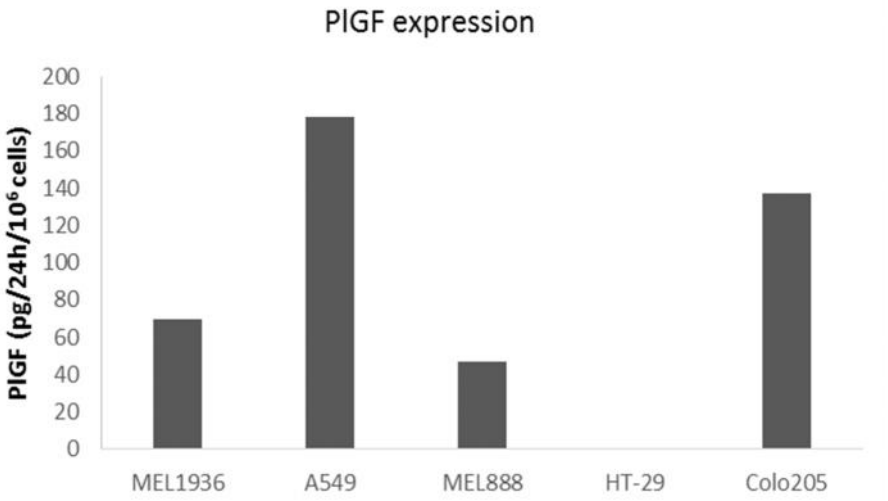

Figure 11.1: Angiogenic profiles of human tumor cells. Supernatants of MEL1936, A549, MEL888, HT-29 and Colo205 cells confluent at 95% were harvested from 6-well-plates after 24 hours of culture, and the number of cells counted. The level of expression of PlGF was determined by ELISA.

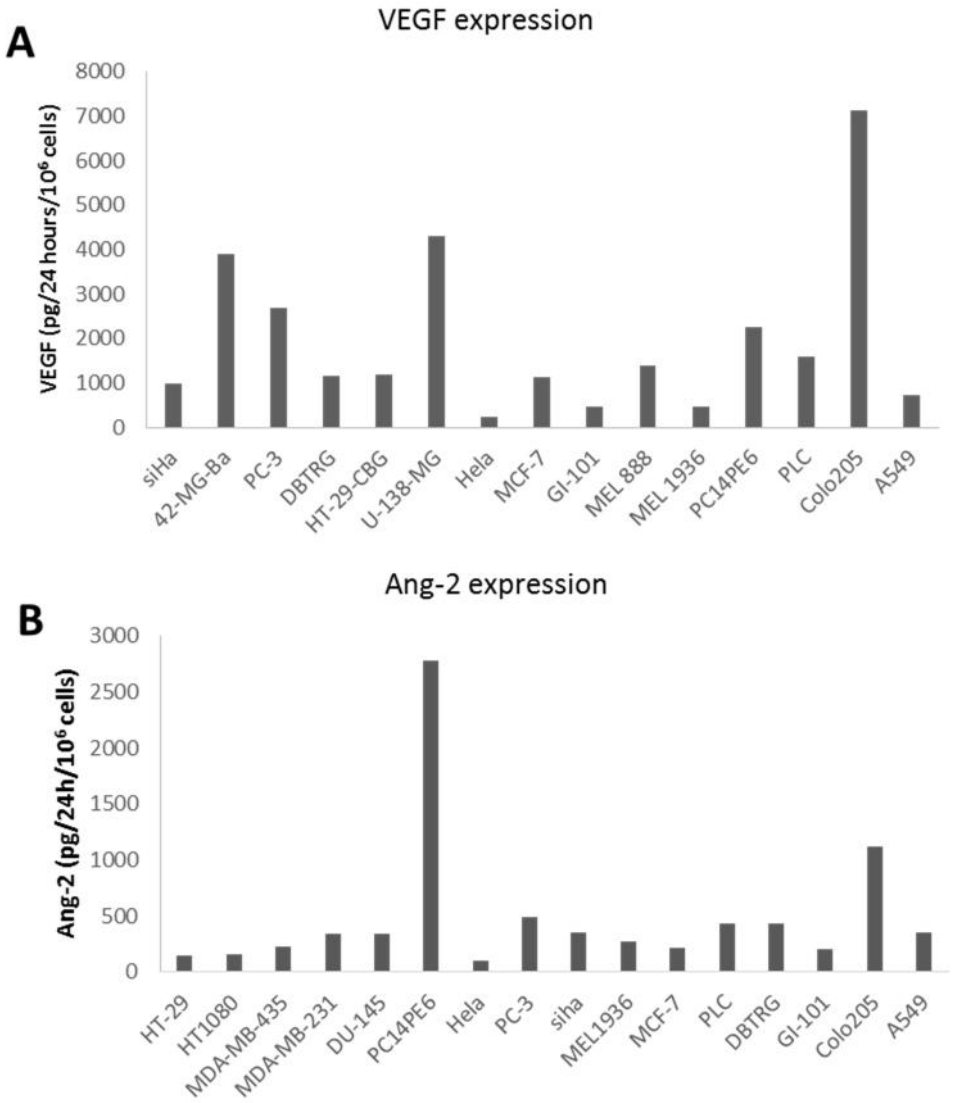

Figure 11.2: Angiogenic profiles of human tumor cells. Supernatants of Siha, 42-MG-Ba, PC-3, DBTRG, HT-29-CBG, U-138-MG, HeLa, MCF-7, GI-101, MEL888, MEL1936, PC14PE6-RFP, PLC, Colo205, A549 HT-1080 MDA-MB-435 and 231, DU-145 and GI-101 cells confluent at 95% were harvested from 6-well-plates after 24 hours of culture, and the number of cells determined. The expression level of (A) VEGF and (B) Angiopoietin-2 were measured by ELISA.

These results confirmed that a wide range of tumor types are abnormally expressing VEGF, PlGF and Ang-2. To determine the importance of each of these angiogenic factors, five cell lines expressing relatively high and low levels of VEGF were selected for further studies.

4.2 Therapeutic VACVs lyse efficiently human tumor cells and produce functional anti-PlGF, anti-Ang-2 and anti-VEGF single chain antibodies.

GLV-1h108 is an attenuated vaccinia virus expressing the GLAF-1 single chain antibody (scAb) targeting VEGF, as described in Frentzen et al., 2009 [60]. It was shown to treat DU-145 and A549 tumors more efficiently than the parental VACV GLV-1h68 (not expressing the scAb). Using a similar strategy, a line of anti-angiogenesis viruses targeting either Ang-2 or PlGF were constructed, as well of viruses combining either PlGF blockade with VEGF blockade, or Ang-2 blockade with VEGF blockade (Table 1). The ability of these viruses to infect and lyse tumor cells has been successfully evaluated *in vitro* (Figure 12).

Table 1: List of therapeutic vaccinia viruses.

Virus	Antibody expressed	Promoter strengh
GLV-1h68	None	
GLV-1h108	GLAF-1 (anti-VEGF, flag-tagged)	Early late
GLV-1h343	Flag-tagged anti-PlGF scab	Early
GLV-1h344	Flag-tagged anti-PlGF scab	Early late
GLV-1h345	Flag-tagged anti-PlGF scab	Late
GLV-1h471	Flag-tagged anti-PlGF scab and GLAF-1	Early late
GLV-1h337	Flag-tagged anti-Ang-2 scab	Early (weak)
GLV-1h338	Flag-tagged anti-Ang-2 scab	Early late (strong)
GLV-1h339	Flag-tagged anti-Ang-2 scab	Late (intermediate)
GLV-1h492	His-tagged anti-Ang-2 scab	Early (weak)
GLV-1h493	His-tagged anti-Ang-2 scab	Early late (strong)
GLV-1h494	His-tagged anti-Ang-2 scab	Late (intermediate)
GLV-1h495	His-tagged anti-Ang-2 scab and GLAF-1	Early (weak)

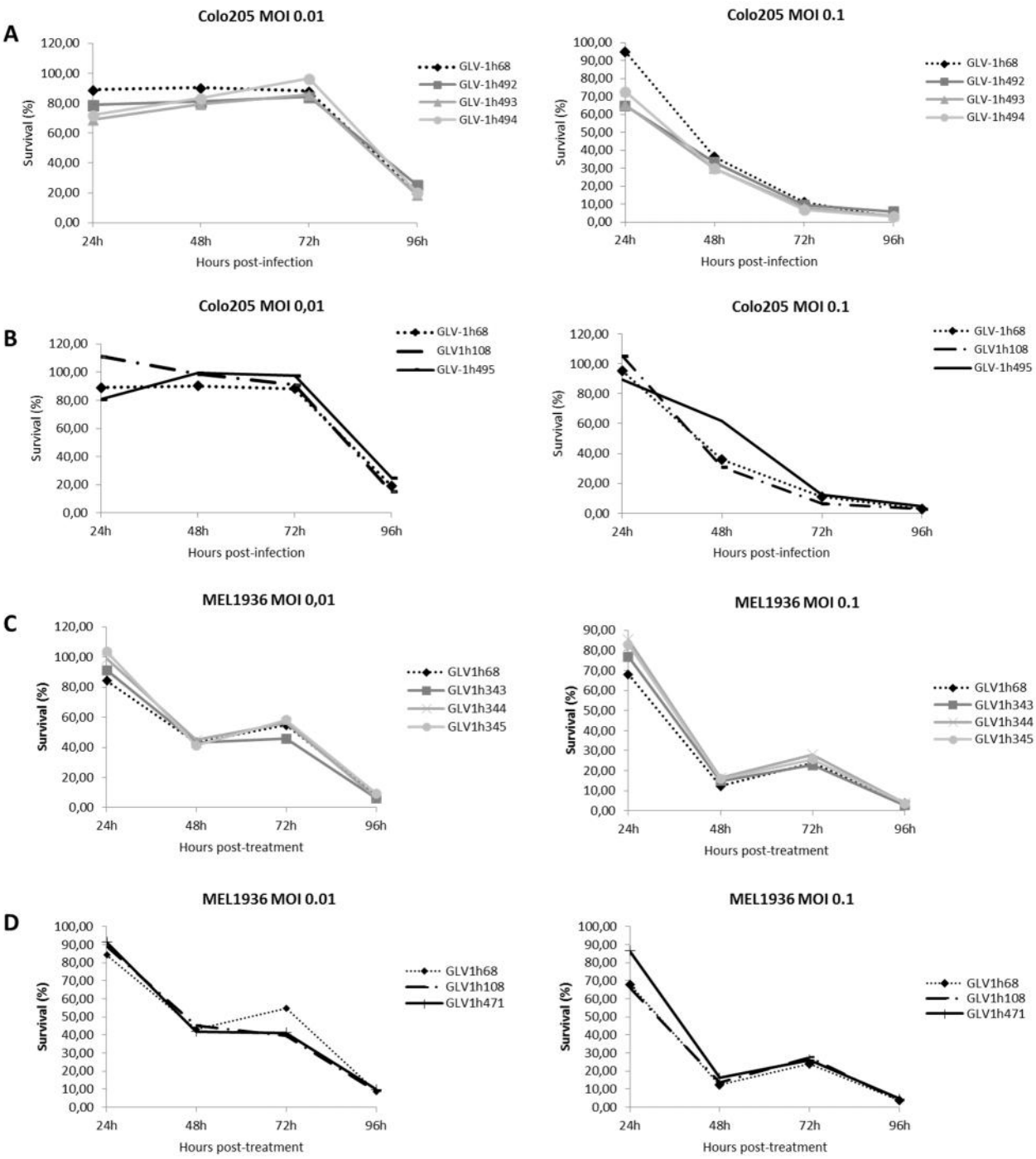

Figure 12: Oncolytic activity of anti-angiogenesis vaccinia viruses in MEL1936 and Colo205 tumor cells. Anti-PlGF viruses oncolytic effect was compared to GLV-1h68, (A) MEL1936 cells were infected with two MOIs, 0.1 and 0.01. The anti-VEGF (GLV-1h108) and combination treatments (GLV-1h471) were also tested in the same cell line (B). Colo205 cells were infected with anti-Ang-2 viruses (C) and the anti-ang-2/VEGF virus (GLV-1h495) (D). Colo205 cell survival was monitored up to 96 hours.

GLV-1h493, expressing the His-tagged anti-Ang-2 scAb under the vaccinia virus early-late promoter, and GLV-1h344, expressing a flag-tagged anti-PlGF scAb under the

vaccinia virus early-late promoter were used to evaluate the functionality of the anti-Ang-2 and anti-PlGF antibodies.

To produce and purify the antibodies, 4 × 10^7 CV-1 cells were infected either with GLV-1h493 or with GLV-1h344 at MOI 2 for 24h. Supernatants have then been harvested, conditioned and concentrated for antibody purification. The purification products were used as primary antibodies in ELISA (Figure 13). The anti-Ang-2 and anti-PlGF scAb expressed by GLV-1h493 and GLV-1h334 infected cells were found to bind to their target proteins and be detected by the anti-His and anti-flag secondary antibodies, respectively.

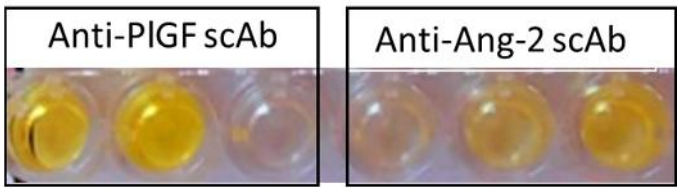

Figure 13: Anti-PlGF and Anti-ang-2 scAb binding. The right inset displays the ELISA results of wells coated with, from left to right, the protein purification product issued from GLV-1h344 infection, a 1:2 dilution of the same solution, a 1x PBS solution. The left inset shows the ELISA results of wells coated with, from left to right, a 1x PBS solution, a 1:2 dilution of the protein purification product issued from GLV-1h493 infection, the same undiluted purification product.

4.3 Human angiogenic factors stimulate tube formation by murine endothelial cells *ex vivo*

Before evaluating anti-angiogenesis VACV *in vivo*, murine endothelial cell responsiveness to human angiogenic factors needed to be confirmed. Consequently, the ability of 2H-11 murine endothelial cells to form vascular-like structures and their reaction to tumor cell stimulation has been measured on an artificial support matrix, under different conditions. The murine endothelial cell line 2H-11 was cultured with conditioned supernatant of either PC14PE6-RFP cells, or PC14PE6-RFP cells infected for 24 hours with GLV-1h68 or GLV-1h108 (expressing GLAF-1). The structures formed by endothelial cells were then fixed and imaged (Figure 14). The absence of tumor cell lysis was verified to ensure that the presence of free proteases did not interfere with the reduction of tubular structures (Figure 15). For that, the presence of human β-actin

protein was tested by Western blot. Tube density was quantified and the statistical significance determined using a One-way ANOVA test (Figure 16).

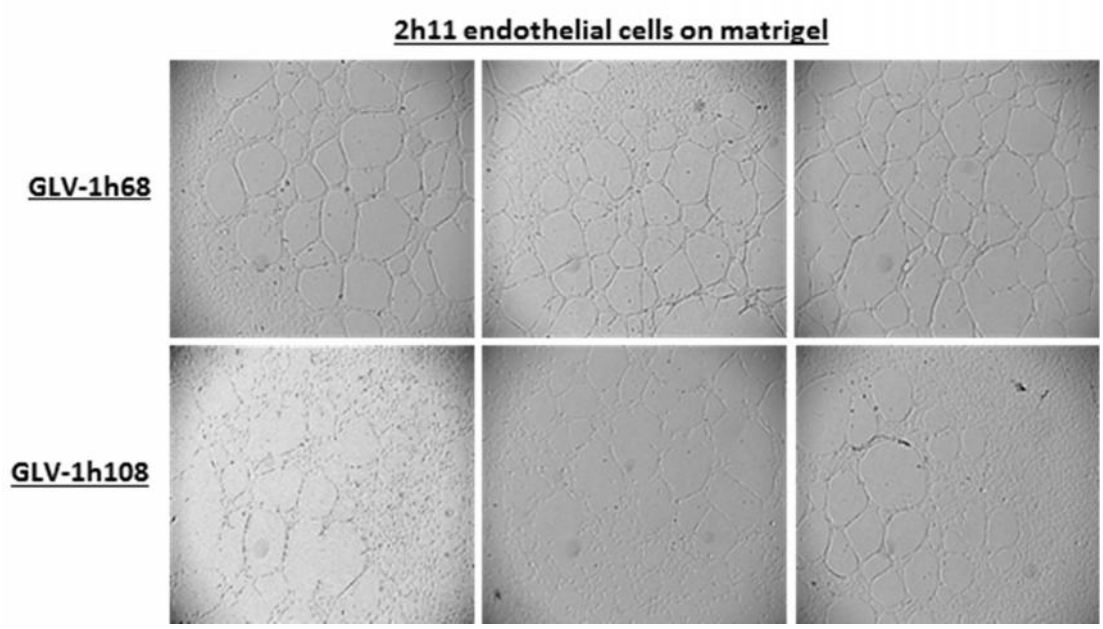

Figure 14: Blood vessel-like structures formed by murine endothelial cells.
2H-11 cells were seeded on an artificial basement membrane matrix in a 24-well-plate. After 14 hours at 37°C, the structures were imaged using a Leica TCS SP2 confocal microscope.

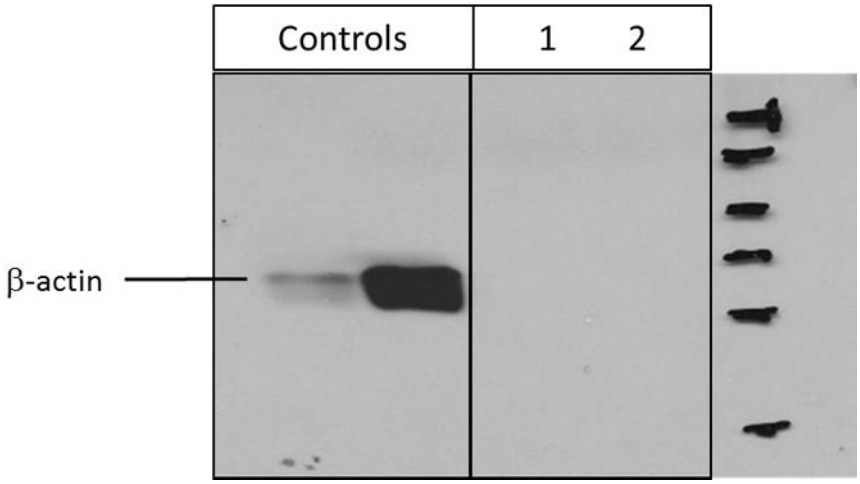

Figure 15: PC14PE6-RFP supernatant does not contain cell lysis products.
The supernatant of PC14PE6-RFP infected by GLV-1h68 (1) and GLV-1h108 (2) were tested for β-actin protein using western blotting.

When cultured in PC14PE6-RFP supernatant or supernatant of PC14PE6-RFP cells treated with GLV-1h68, 2H-11 blood vessel-like network displayed a higher density than when cultured in DMEM 2% FBS medium. On the contrary, in presence of GLAF-1

(anti-VEGF scAb) 2H-11 tubular network was reduced by 64.7% and 59% compared to GLV-1h68 and PC14PE6-RFP supernatants.

This experiment confirmed, first, that murine endothelial cells can be stimulated by human angiogenic factors expressed by tumor cells [60], then that the anti-VEGF scAb derived from tumor cells infected with GLV-1h108 impairs blood vessel formation as described in [60]. Finally, this experiment suggested that the viral VEGF expressed by VACV may have an effect on the tumor vasculature.

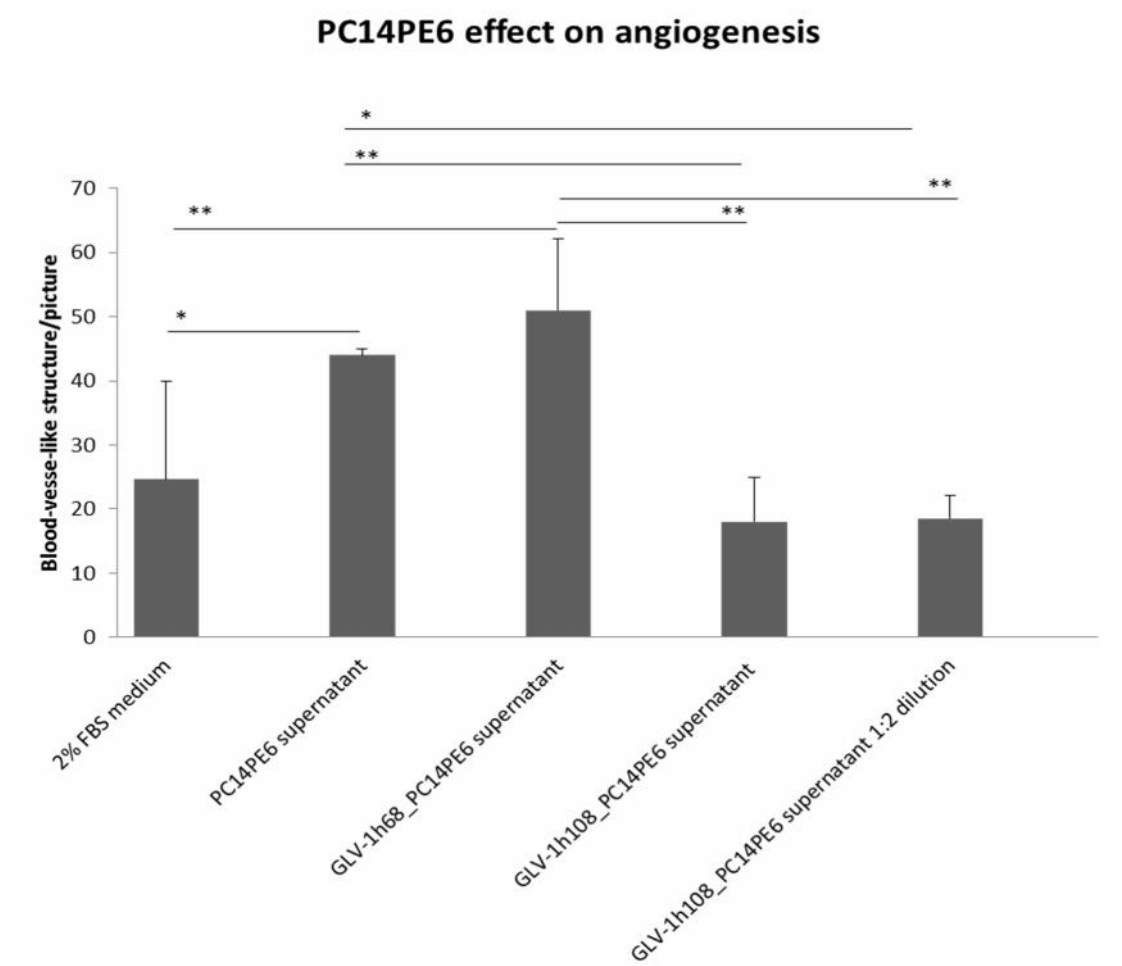

Figure 16: Quantification of 2H-11 blood vessel-like structures. Murine endothelial cells were seeded with a standard 2% FBS medium PC14PE6-RFP supernatant treated or not with GLV-1h68 or GLV-1h108. The statistical significance has been determined by a One-way ANOVA Fisher test ($p<0.05$:*, $p<0.01$:**, $p<0.001$:***).

To analyze and understand the effect of the viral VEGF on the vasculature, a purification and quantification method would be required. Unfortunately, this protein has not been studied extensively, making these requirements hardly accessible.

4.4 Angiogenic factors modulate tumor cell adhesion patterns

Following completion of bevacizumab treatment, some patients displayed an increased risk to develop metastases [39]. The study of adhesion proteins by endothelial cells was used to document the transendothelial migration of tumor cells to escape the primary tumor site and reach one of the major routes implicated in the development of metastases [69].

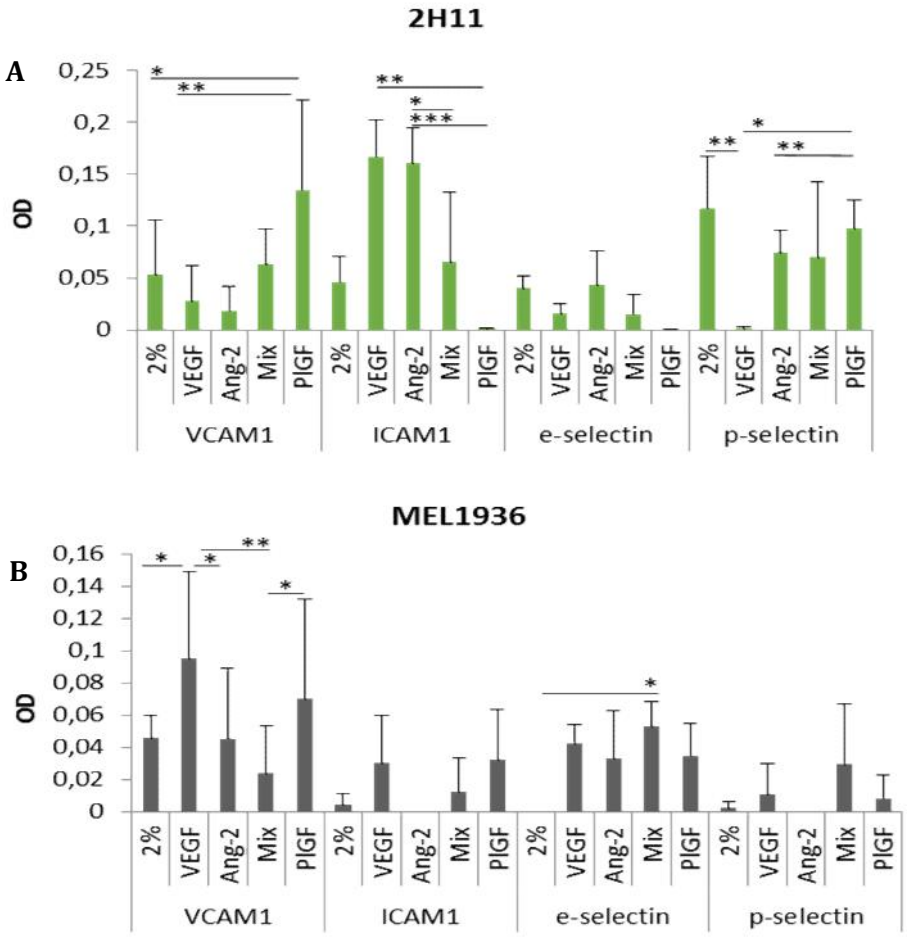

Figure 17.1: Effect of VEGF, Ang-2 and PlGF on VCAM-1, ICAM-1, e-selectin and p-selectin expression. VCAM-1, ICAM-1, e-selectin and p-selectin quantification after a 24 hours treatment with PlGF, VEGF and or Ang-2 in (A) 2H-11 murine endothelial cells and (B) MEL1936 tumor cells. Statistical significance was determined using a One-way ANOVA Fisher test ($p<0.05$ represented by *, $p<0.01$ by **, and $p<0.001$ by ***)

ICAM-1, VCAM-1 e- and p-selectin are adhesion proteins implicated in the recruitment and migration of leukocytes from the vasculature to the inflamed tissue [34, 70]. These adhesion proteins were shown to be overexpressed in cancer patients [29, 32-33].

Therefore we analyzed the expression of ICAM-1, VCAM-1, e-, and p-selectin by tumor cells upon VEGF, Ang-2 and PlGF stimulation.

Endothelial cells are known to respond to VEGF, PlGF and Ang-2 stimulation and migrate or release pericytes, respectively [12, 23, 71]. These processes could be achieved by a modulation of the expression of adhesion proteins and thus observing the variation of these proteins on tumor endothelial cells served as a control. The expression of e-selectin, p-selectin, ICAM-1 and VCAM-1 proteins was evaluated in 2H-11 endothelial cells (Figure 17.1A) MEL1936 (Figure 17.1B), PC14PE6-RFP (Figure 17.2), HeLa (Figure 17.3A) and A549 (Figure 17.3B) tumor cells. Tumor cells and murine endothelial cells were incubated with 2% FBS medium, to determine the basic expression levels of the target protein, and with either VEGF, PlGF, Ang-2 or a mix of Ang-2 and VEGF (Figure 17.1).

A

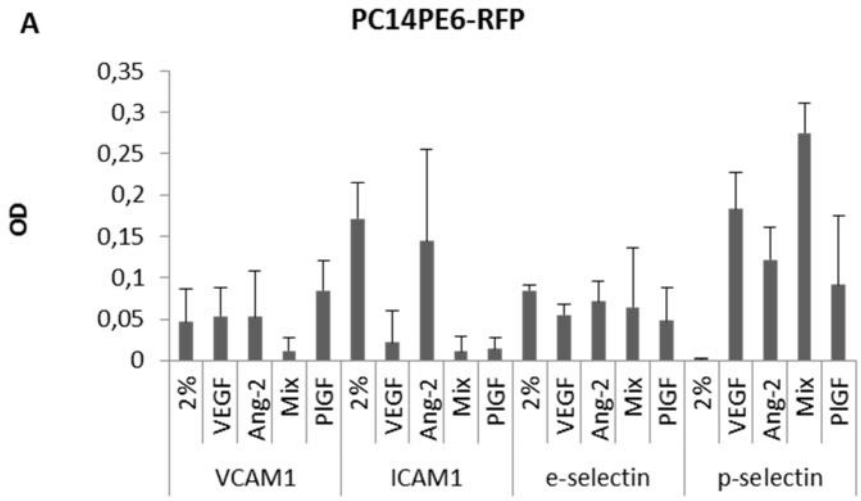

B

		P-selectin				
		2%	VEGF	Ang-2	Mix	PlGF
ICAM-1	2%		p<0,001	p<0,01	p<0,001	p<0,05
	VEGF	p<0,001			p<0,05	p<0,05
	Ang-2		p<0,01		p<0,001	
	Mix	p<0,001		p<0,01		p<0,001
	PlGF	p<0,001		p<0,01		

Figure 17.2: Effect of VEGF, Ang-2 and PlGF on VCAM-1, ICAM-1, e-selectin and p-selectin expression in PC14PE6-RFP tumor cells. (A) In-cell ELISA results. (B) Statistical relevance was determined by a One-way ANOVA Fisher test.

Depending of the cell line observed, angiogenic factors had various effects on the protein tested. For instance, after VEGF stimulation an increase in p-selectin level was

observed in PC14PE6-RFP cells (Figure 17.2) however the detectable level of this same protein decreased in 2H-11 cells (Figure 17.1A).

Although VEGF is known to be the most potent angiogenic factor, we could observe that PlGF and Ang-2 had significant, and in some cases, comparable effects on ICAM-1, VCAM-1, e-selectin and p-selectin expression.

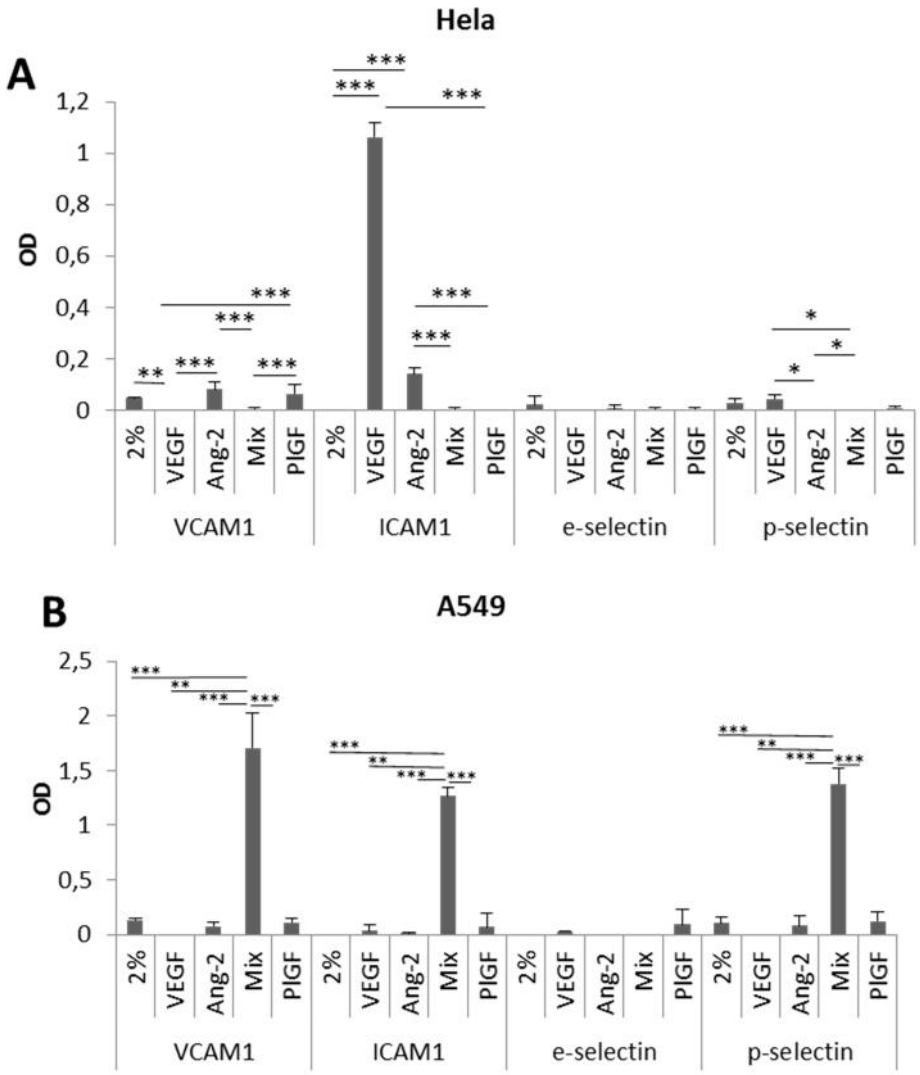

Figure 17.3: Effect of VEGF, Ang-2 and PlGF on VCAM-1, ICAM-1, e-selectin and p-selectin expression in tumor cells. In-cell ELISA quantification in (A) A549 and (B) HeLa tumor cells. Statistical relevance determined using a One-way ANOVA Fisher test ($p<0.05$:*, $p<0.01$:**, $p<0.001$:***).

It suggests that anti-angiogenesis therapy does not only affect the number of blood vessels but could also alter the tumor vasculature structure, tumor cell migration and immune cell docking, since tumor cells expressed adhesion proteins normally found on activated endothelial cells. It could also explain one of the mechanisms used by tumor cells to circumvent anti-angiogenic therapies, the selection of angiogenic immune cells to help restore the tumor vasculature during VEGF blockade and regulate the activation of anti-tumoral immune cells.

We also observed that VEGF tended to increase ICAM-1 expression by HeLa cells, while notably decreasing its expression by the PC14PE6-RFP cell line. The intercellular cell adhesion molecule 1 is known to be responsible for the docking of immune cells, and the loosening of inter-endothelial junctions for immune cell transmigration.

The over-expression of ICAM-1 induced by VEGF in HeLa cells (Figure 17.3A), can allow the transmigration of tumor-promoting immune cells [72] but also ease the integration of tumor cells to other tissues. This increased expression can also stimulate the angiogenesis process by recruiting immune angiogenic factor expressing cells [73], since we observed previously that VEGF production by HeLa cells was limited. On the contrary, highly angiogenic cells like PC14PE6-RFP, experienced a decrease of ICAM-1 expression that can potentially impair the recruitment of leukocytes targeting tumor. This finding confirmed that VEGF can protect tumors from certain immune cells [74]. The relative over-expression of e- and p-selectin by MEL1936 and PC14PE6-RFP enables tumor cells to bind more easily to endothelial cells and roll on the vasculature to use the existing vasculature as a blood supply [75].

Additionally, the increase of VCAM-1, ICAM-1, e- and p-selectin expression in A549 tumor cells after treatment with a solution containing VEGF and Ang-2 factors further confirmed the importance of Ang-2 in the tumoral development [76]. VEGF alone was not able to induce any variation but when combined to Ang-2 it led to the increase of the adhesion proteins tested.

The expression of VCAM-1, ICAM-1, e- and p-selectin by tumor cells followed various strategies. Nevertheless, we proved that tumor cells express adhesion proteins normally

expressed by activated endothelial cells and that this expression is modulated by angiogenic factors.

4.5 Specific tumor cell lines form blood vessel-like structures

Since tumor cells reacted to angiogenic factors by expressing ICAM-1, VCAM-1, e- and p-selectin, adhesion proteins normally expressed by endothelial cells, their capacity to mimic the endothelial cell function of blood transporter has been evaluated. Blood vessels constituted of tumor cells have been observed in melanoma biopsies of patients [77]. Vascular structures formed by melanoma tumor cells were localized preferentially in aggressive and invasive areas of the tumor. Tube formation assay was shown to be an appropriate *in vitro* tool to evaluate the potential of tumor cells to form vascular structures [78-81]. The human derived fibrosarcoma cell line HT1080 as well as C8161 melanoma cells were found to form vascular-like networks when seeded on matrigel [78, 83] Moreover melanoma vascular structures formed on matrigel were successfully injected with a fluorescent fluid [81].

Therefore, the same four human tumor cell lines PC14PE6-RFP, MEL1936, A549 and HeLa, and the endothelial murine cell line 2H-11 were seeded on matrigel and imaged (Figure 18). Unexpectedly, in addition to 2H-11 and MEL1936, A549 tumor cells were also able to form blood vessel-like structures. This phenomenon is described here in the A549 lung adenocarcinoma tumor cell line for the first time.

As shown in Figure 18 MEL1936 and A549 cells were, in addition to expressing hematopoietic proteins, able to mimic endothelial cell function (blood vessel formation). These data suggest that MEL1936 and A549 tumors can create alternative vascular structures as described in melanoma tumors [77]. PC14PE6-RFP cells did not exhibit the same ability to form defined tubular networks but were organized differently than when seeded on an empty 96 well-plate.

Consequently, to further investigate the relationship between PC14PE6-RFP and the endothelium, the next experiment was performed cultivating a mixture of 2H-11 and PC14PE6-RFP cells on the same artificial extracellular matrix. After 3 hours, 2H-11 cells were forming a tubular network and PC14PE6-RFP cells participated in the structure. It appeared that this tumor model is not able to form a tubular network by itself, but

PC14PE6-RFP cells can bind to endothelial cells like pericytes [83-84] and be integrated in the tumor vasculature.

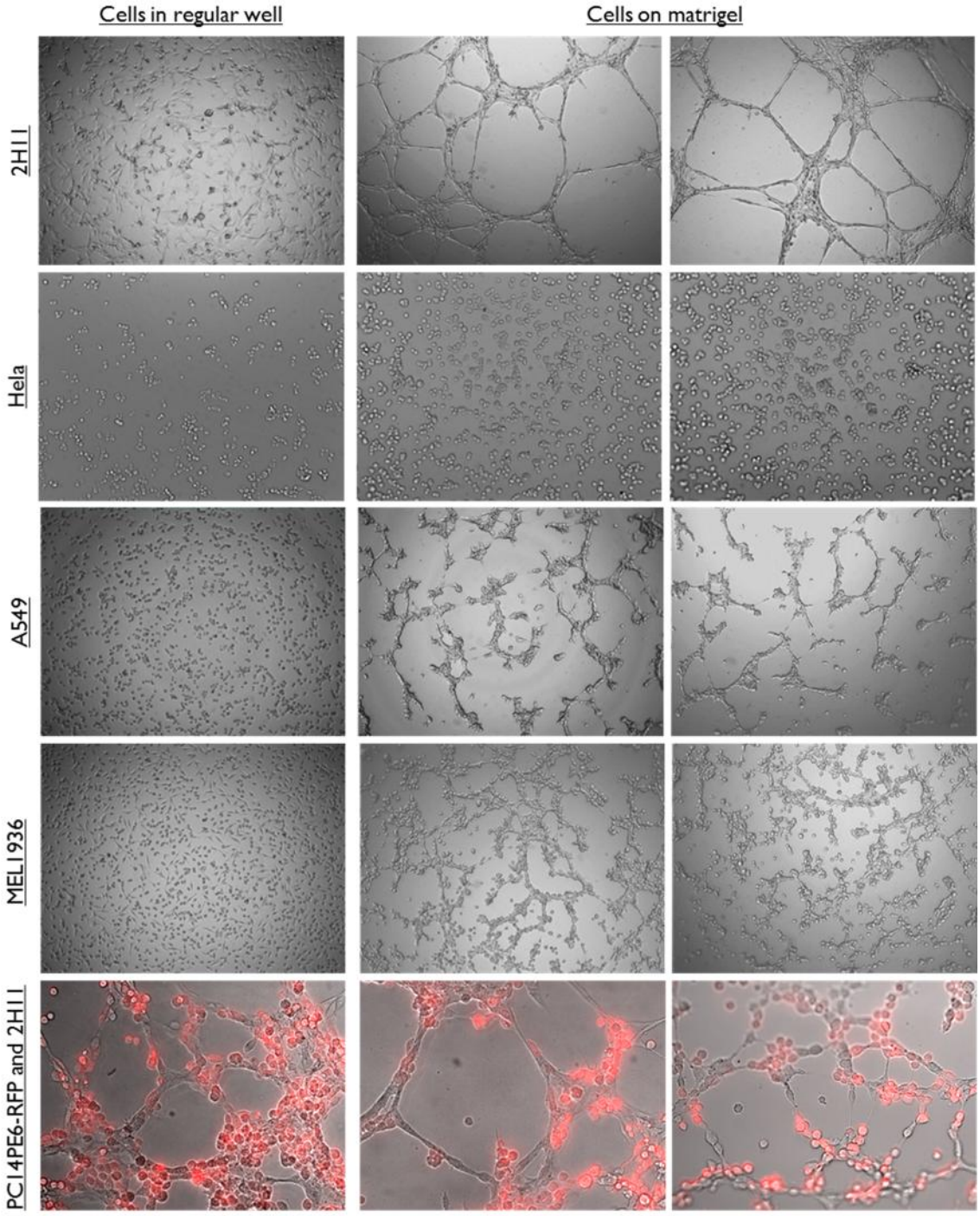

Figure 18: Human tumor cells forming blood vessel-like structures. PC14PE6-RFP, MEL1936, A549, HeLa and 2H-11 cells were seeded 3 hours on a regular 96-well-plate or a 96-well-plate coated with matrigel. PC14PE6-RFP cells appear in red.

4.6 VACV mediated anti-angiogenesis therapies reduce tumor induced vascular leakage

The next step of the project was to assess the effect of VACV mediated anti-angiogenesis therapy on tumor induced vasculature *in vivo*. Thirty-nine mice were implanted with 4×10^6 PC14PE6-RFP cells and treated with different anti-angiogenic VACVs when the tumor size reached 200 mm^3. The mice were divided in 7 groups of eight, and each group received a different anti-angiogenesis VACV or 1x PBS. GLV-1h68 was used as a control.

Description of the cohorts:

- Group 1: 8 mice treated with GLV-1h108 (anti-VEGF)
- Group 2: 7 mice treated with GLV-1h493 (anti-Ang-2)
- Group 3: 8 mice treated with GLV-1h344 (anti-PlGF)
- Group 4: 8 mice treated with GLV-1h68 (VACV control, it doesn't express any Ab)
- Group 5: 8 untreated mice

The different groups were imaged on days 0, 4, 7 and 10 post-treatment. The PC14PE6-RFP tumor model, by over-expressing various angiogenic factors, induces a strong vascular leakage in the tumor micro-environment visible by an accumulation of blood around the tumor [85]. By monitoring the evolution of the blood accumulation (purple color) the effect of the different anti-angiogenic viruses on the tumor induced vasculature could be evaluated (Figure 19).

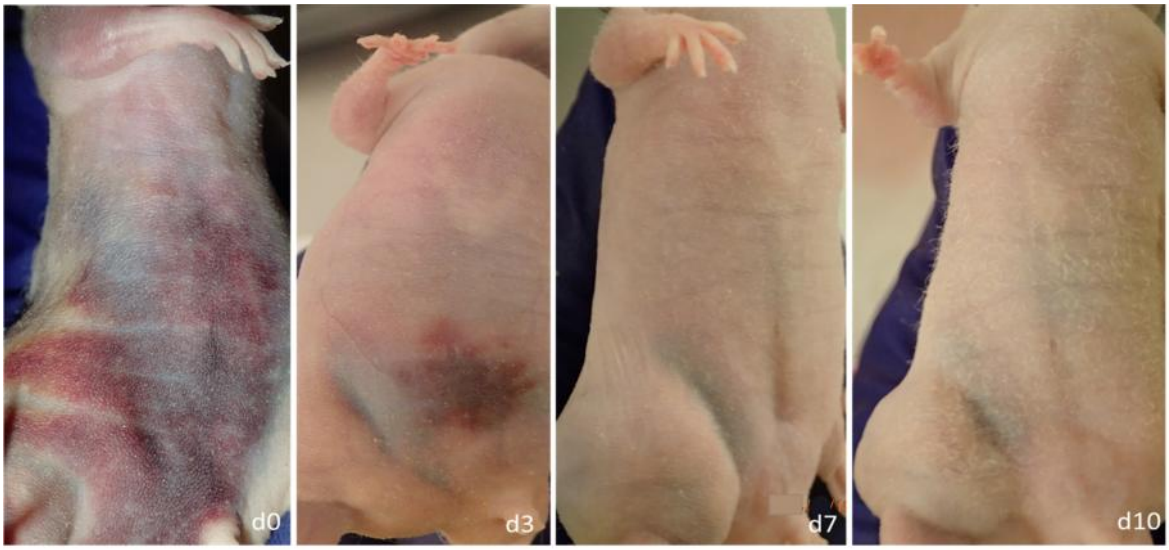

Figure 19.1: Reduction of an extended hematoma by VEGF blockade (group 1). A PC14PE6-RFP tumor-bearing mouse hematoma was imaged before GLV-1h108 treatment and 3, 7 and 10 days post-treatment.

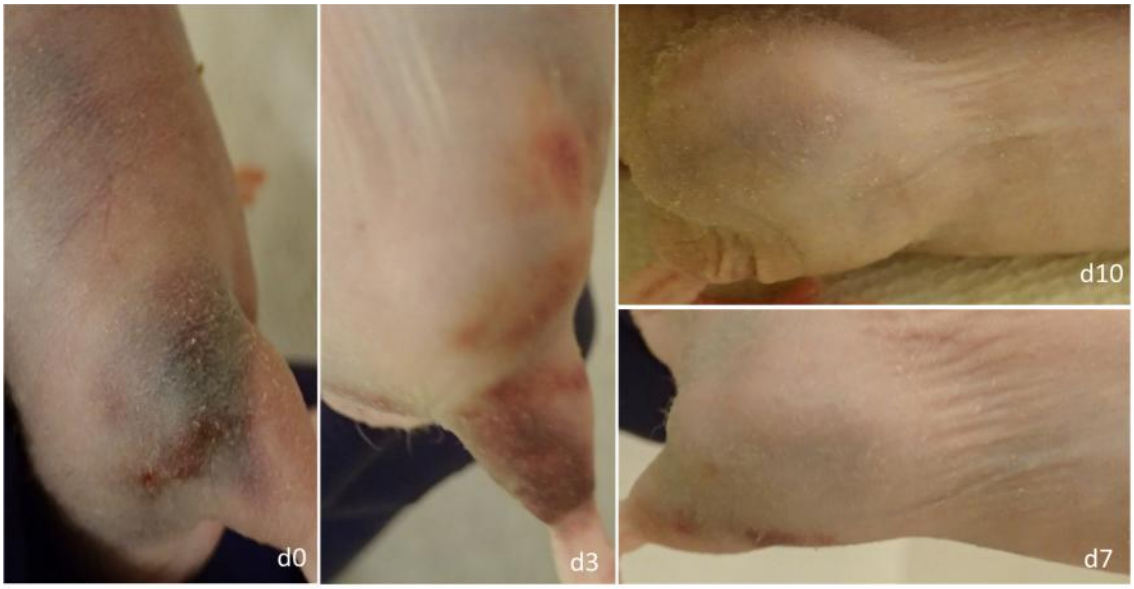

Figure 19.2: Reduction of a PC14PE6-RFP tumor-induced hematoma by Ang-2 blockade (group 2). A PC14PE6-RFP tumor-bearing mouse hematoma was imaged before GLV-1h493 treatment and 3, 7 and 10 days post-treatment.

All the viruses tested were efficient against tumor-induced vascular-blood-leakage, proving their effect on the tumor vasculature.

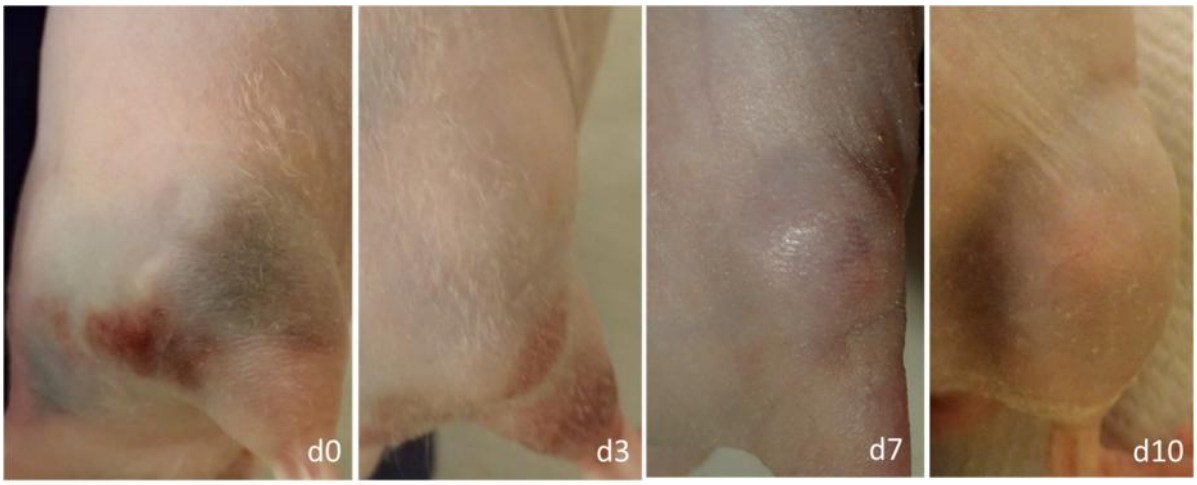

Figure 19.3: Reduction of a PC14PE6-RFP tumor-induced hematoma by PlGF blockade (group 3). A PC14PE6-RFP tumor-bearing mouse hematoma was imaged before GLV-1h344 treatment and 3, 7 and 10 days post-treatment.

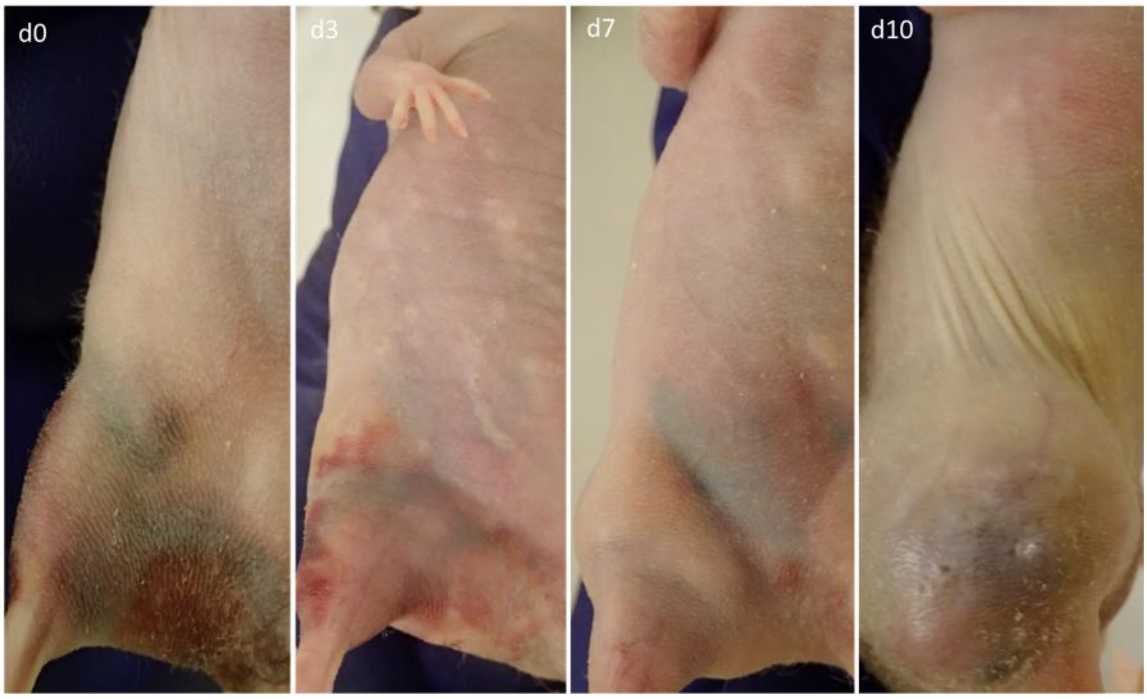

Figure 19.4: Slight reduction of a PC14PE6-RFP tumor-induced hematoma by oncolytic VACV treatment (group 4). A PC14PE6-RFP tumor-bearing mouse hematoma was imaged before GLV-1h344 treatment and 3, 7 and 10 days post-treatment.

The blockade of PlGF and VEGF using GLV-1h344 and GLV-1h108, respectively, target endothelial cells while the blockade of Ang-2 by GLV-1h493 target pericytes, nevertheless all viruses tested resolved PC14PE6-RFP-induced hematomas more efficiently than the GLV-1h68 treatment. Additionally, we observed that VEGF blockade

by GLV-1h108 resorted an extended hematoma confirming once again the strong effect of VEGF on endothelial cells.

4.7 VACV is able to infect murine tumor endothelial cells.

The effect of GLV-1h108 on tumor-induced angiogenesis has been described in the literature [60], and we demonstrated in this study that Ang-2 and PlGF blockade, mediated by vaccinia virus, was also able to impair the tumor vasculature significantly. GLV-1h68 replication in tumor endothelial cells has been documented. VACV replication was undetectable up to 48 hours post GLV-1h68 infection [86]. Therefore, we investigated the effects of VEGF, PlGF and Ang-2 blockades on VACV replication in the 2H-11 tumor endothelial cell line.

Murine endothelial cells extracted from a mouse after human Kaposi Sarcoma implantation (2H-11) were infected either with GLV-1h68, or VACV targeting Ang-2 or PlGF alone and their replication monitored by GFP quantification. The effect of a combined anti-angiogenesis therapy on the tumor-endothelium has also been tested by infecting 2H-11 cells with GLV-1h495 (Ang-2 and VEGF blockade) or with GLV-1h471 (PlGF and VEGF blockade). The GFP quantification confirmed the results obtained by viral plaque assays and described in the literature, during the first 48 hours the GLV-1h68 virus is almost undetectable [86]. We observed that VEGF blockade, alone or in combination with PlGF or Ang-2 blockade, improved VACV replication in 2H-11 cells. VACV replication during VEGF blockade, alone or combined with PlGF blockade appeared to be more important during the first 48 hours. Conversely, when combined with VEGF blockade, Ang-2 blockade notably improved VACV replication starting 72 hours post-infection. Twenty-four hours post-infection, when both PlGF and VEGF were inhibited (GLV-1h471), we observed 3 fold more VACV than during GLV-1h344 infection, and 24 fold more than during GLV-1h68 infection. Seventy-two hours post-infection, GLV-1h495 (anti-VEGF and anti-Ang-2) showed a 4 fold and 41% increase in VACV replication compared to GLV-1h108 and GLV-1h68, respectively (Figure 20.1C).

GLV-1h493 displayed a particular replication pattern. When 2H-11 cells were infected with GLV-1h493 at MOI 0.01, the amount of VACV detected was higher than when infected at MOI 0.1. In other words a small amount of GLV-1h493 virus and thus a

moderate blockade of Ang-2 was more beneficial for murine tumor endothelial cells colonization by VACV.

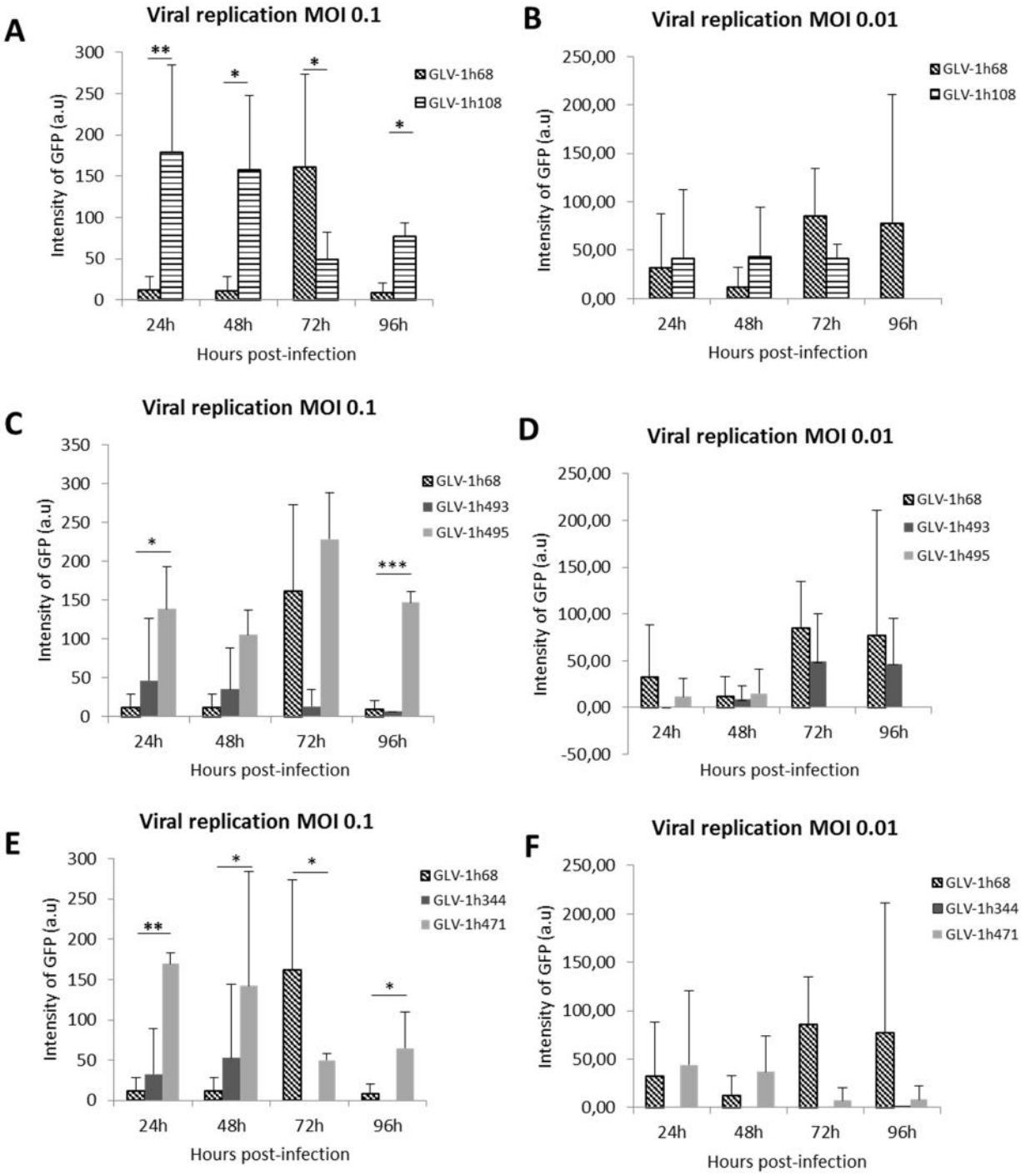

Figure 20.1: Replication of therapeutic VACV in tumor endothelial cells. The replication of (A, B) GLV-108, (C, D) GLV-1h493, GLV-1h495, (E, F) GLV-1h344 and GLV-1h471 was compared to GLV-1h68 in murine tumor-endothelial 2H-11. Viral amounts were quantified by GFP emission readings.

With the exception of GLV-1h493, the infection of murine endothelial cells with low MOIs (0.01) of scAb-expressing VACVs was not sufficient to induce a significant replication in this cell line (Figure 20.1B). We can infer that the expression of the antibodies slightly delayed VACV replication in murine tumor endothelial cells. Consequently, to induce a consistent replication in the tumor endothelium, a higher MOI was necessary for anti-angiogenesis viruses (Figure 20.1A).

Nevertheless, the GFP detected in GLV-1h493 and GLV-1h344 infected cells 24 and 48 hours post-infection showed that Ang-2 and PlGF blockade alone improved VACV replication in tumor endothelial cells compared to the parental GLV-1h68.

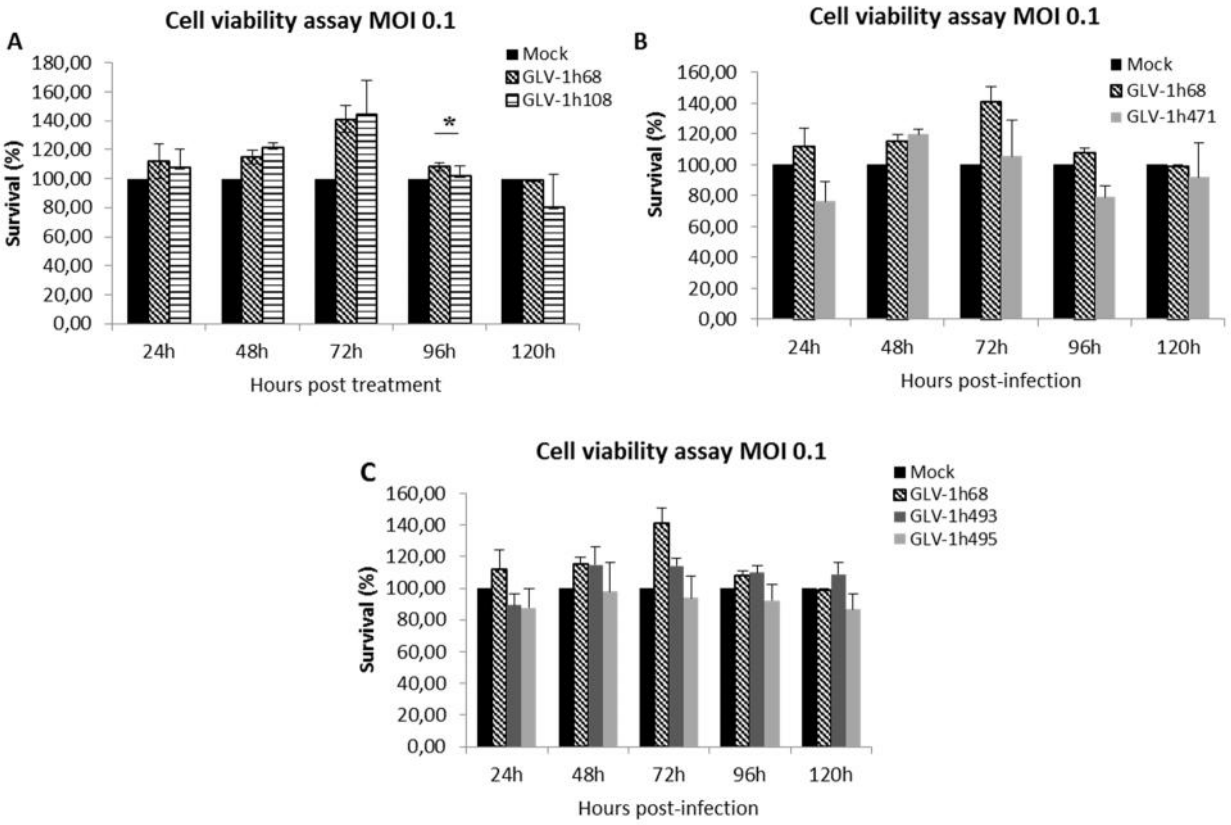

Figure 20.2: Cytotoxic effect of therapeutic VACVs in tumor endothelial cells. The percentage of 2H-11 survival was monitored every 24 hours for 120 hours after infection with (A) GLV-108, (B) GLV-1h344 and GLV-1h471, (C) GLV-1h493 and GLV-1h495.

The effect of VACV replication on 2H-11 cells survival was assessed using an XTT assay (Figure 20.2). However only a time-limited effect was observed with 23.43, 12.41, and 10,71% cytotoxicity 24 hours post-infection for GLV-1h471, GLV-1h495 and GLV-

1h493, respectively, and 20% cytotoxicity after 96h for GLV-1h108. 2H-11 cells appear to be able to survive the infection longer than regular tumor cells. Interestingly, in spite of an efficient replication, GLV-1h108 cytotoxicity in 2H-11 was significant only 96h post-infection.

4.8 Anti-VEGF scAb expression increases VACV replication and/or entry.

We established that anti-angiogenesis viruses have an effect on tumor-induced angiogenesis (see 4.6).

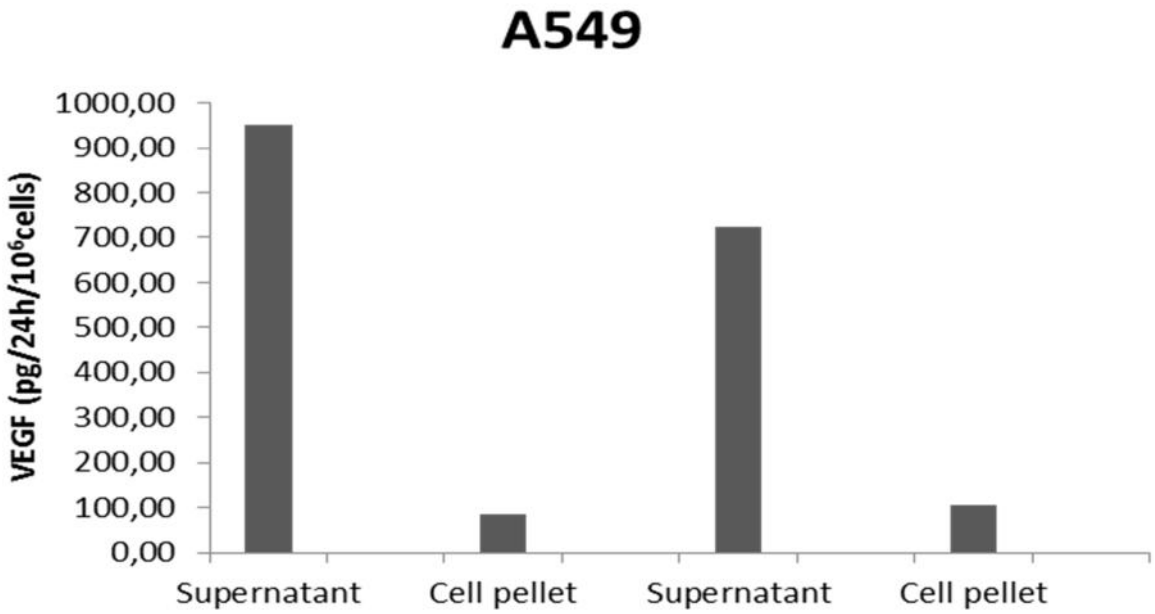

Figure 21: VEGF expression by A549 cells.
VEGF expression of A549 supernatant and cell pellet determined by ELISA.

The next step was to evaluate whether, on the one hand, angiogenic factors and more specifically VEGF have an influence on tumor cell colonization by VACV, and on the other hand if the expression of GLAF-1 scAb can impact this colonization.

The replication and cytotoxic effects of the anti-VEGF virus were compared to the parental VACV, in A549 cells. For quantification and imaging purposes, different versions of the VACV strains were used, GLV-1h189 is a version of GLV-1h68 expressing RFP, and GLV-1h413 is a version of GLV-1h108 expressing GFP and RFP. The amount of VEGF secreted by the A549 adenocarcinoma cell line was assessed by ELISA (Figure 21). Briefly after 24 hours of culture A549 cells and supernatant were harvested for VEGF quantification. To observe the effect of VEGF and GLAF-1 on VACV replication, the amount of VEGF per 10^4 cells was calculated, and A549 cells were then seeded at 1×10^4

cells per well, and infected in presence of 2, 5, 8 and 10 times the amount of VEGF measured, 800 pg/24h/10^6 cells (Figure 22).

The amount (RFU) of TurboFP635 quantified reflects the amount of the GLV-1h413 and GLV-1h189 viruses present within A549 cells. Despite the fact that when infected with a smaller MOI (0.01), 24 hours post-infection, GLV-1h413 amount was lower to the parental GLV-1h189, most likely due to the production of the GLAF-1 antibody (Figure 23.1A), the VEGF blockade by GLAF-1 improved VACV replication.

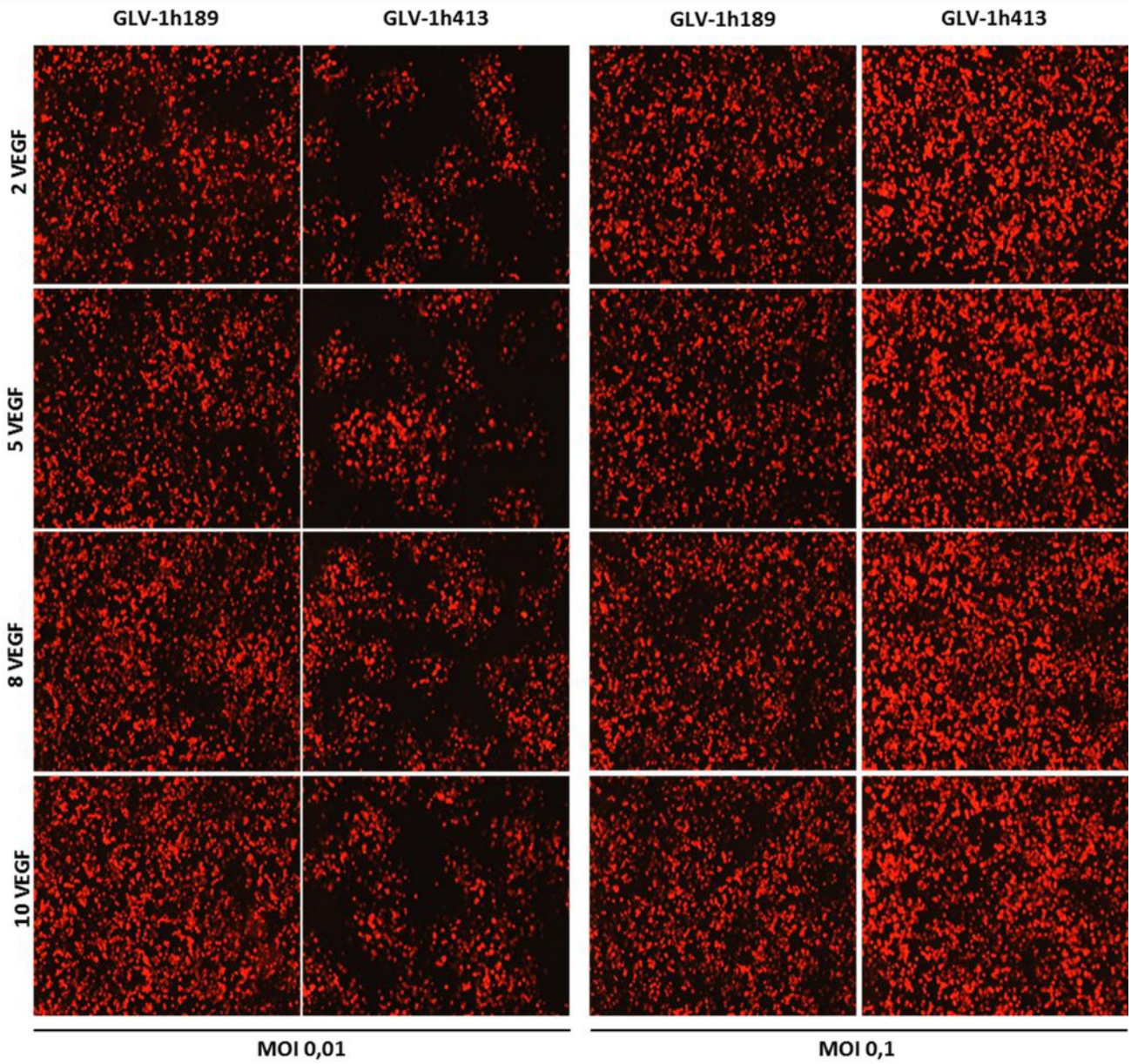

Figure 22.1: A549 cells 24 hours post-treatment with GLV-1h189 or GLV-1h413 (anti-VEGF). A549 cells seeded with increasing levels of VEGF (2 VEGF, 5 VEGF, 8 VEGF and 10 VEGF) were infected at low (0.01) or high (0.1) MOI of GLV-1h189 and GLV-1h413 viruses.

This trend was confirmed over time, despite an early delay in replication when using the low 0.01 MOI, the amount of the anti-VEGF VACV GLV-1h413, is two-fold higher than GLV-1h189 (p values <0.001). Starting 48 hours post-infection, A549 cells infected at an MOI of 0.01 with GLV-1h413 displayed a quantity of virus two-fold higher than A549 cells infected with GLV-1h189 at an MOI of 0.1 (Figure 23.1B).

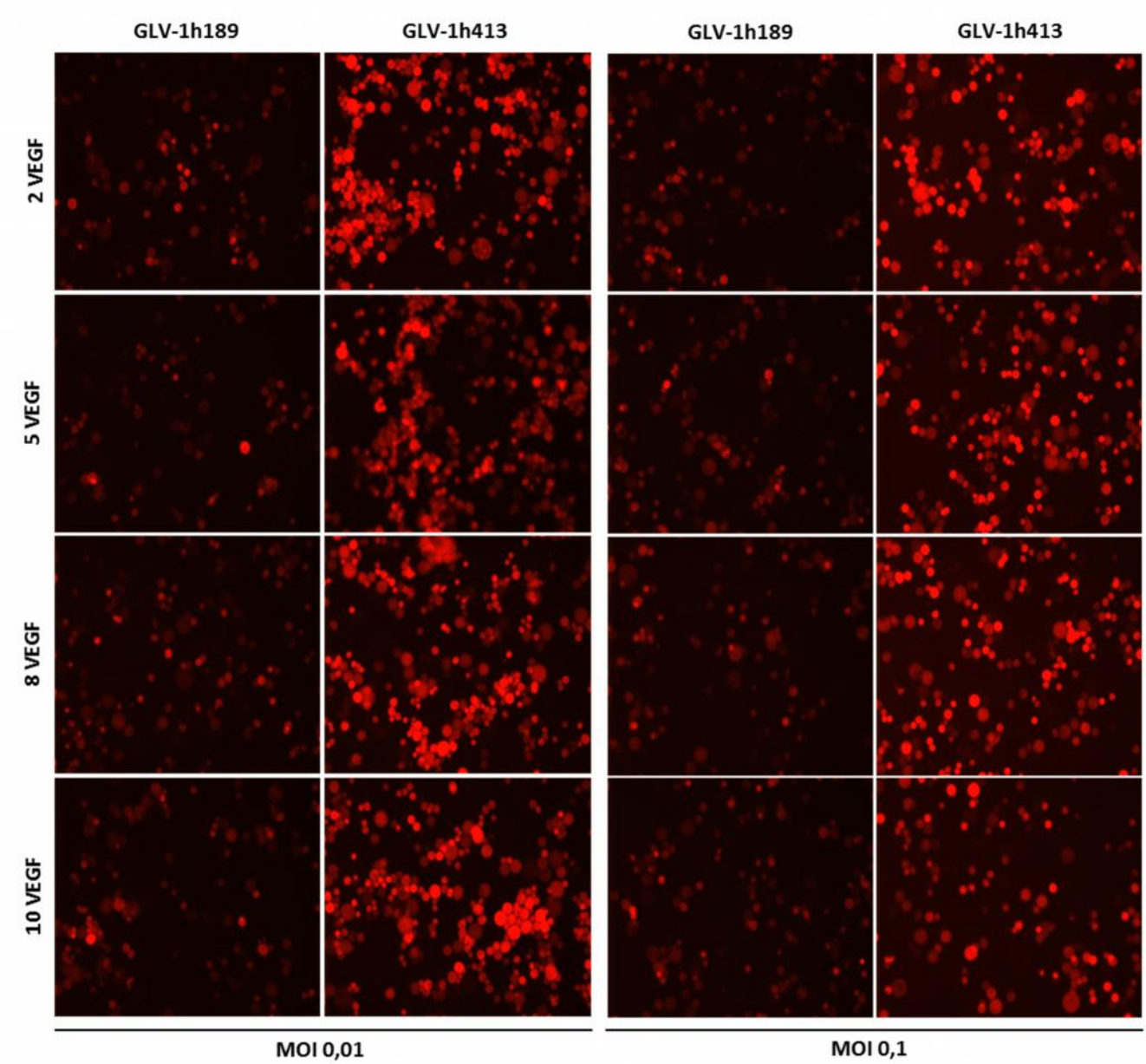

Figure 22.2: A549 cells 72 hours post-treatment with GLV-1h189 or GLV-1h413 (anti-VEGF). A549 cells seeded with increasing levels of VEGF (2VEGF, 5VEGF, 8 VEGF and 10VEGF) were infected at low or high MOI of GLV-1h189 and GLV-1h413 viruses.

To colonize the same amount of A549 cells, we would need 20 times less GLV-1h413 (anti-VEGF) virus than when using GLV-1h189. We also observed that the amount of VEGF slowed down the replication of GLV-1h413, the amount of this virus is significantly lower when cultured with 8 times VEGF than when cultured with 2 times ($p<0.00001$).

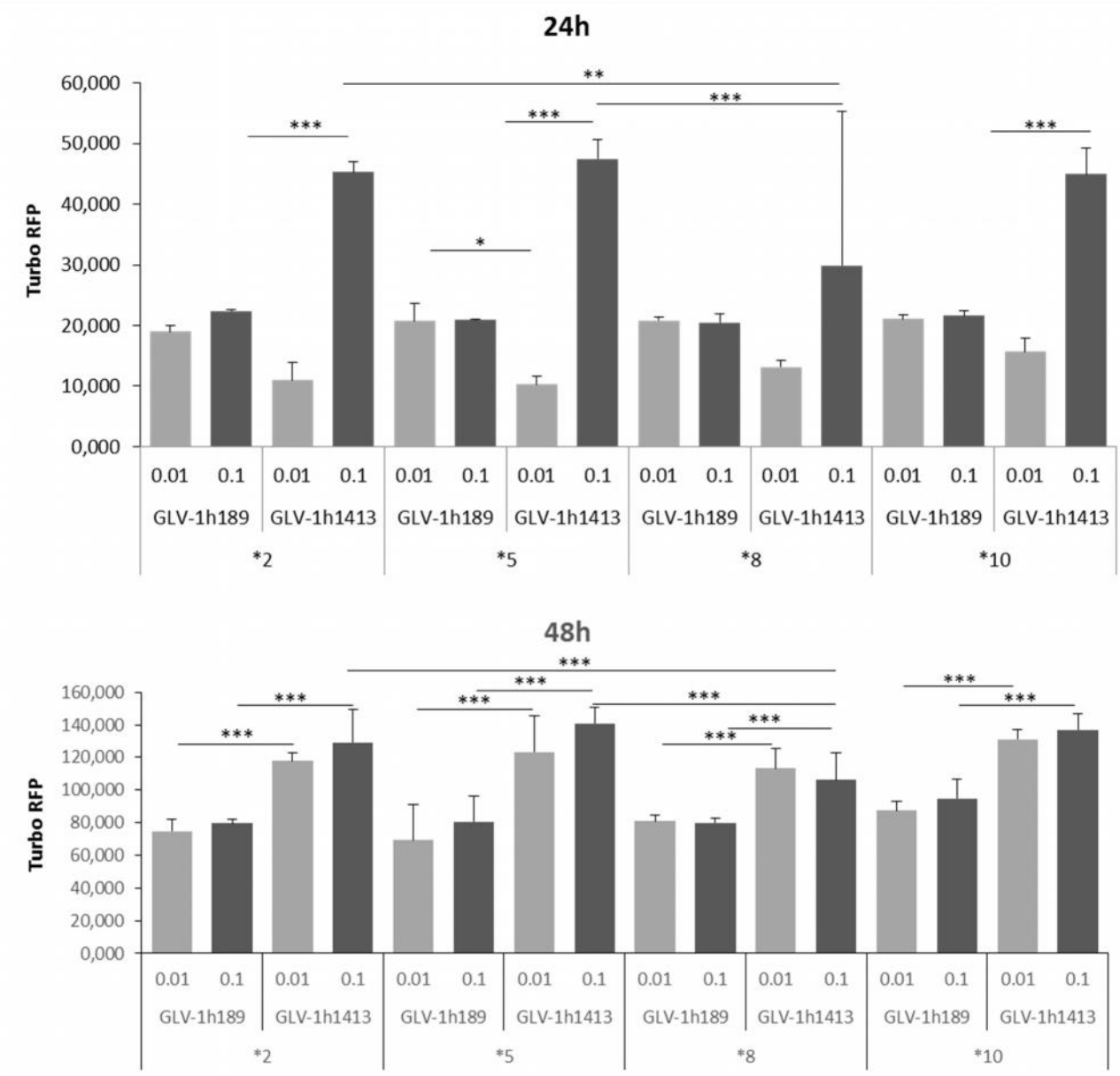

Figure 23.1: Quantification of TurboFP635 in A549 cells infected with GLV-189 and GLV-1h413 (anti-VEGF). A549 cells seeded with increasing levels of VEGF were infected at low (0.01) or high (0.1) MOI of GLV-1h189 and GLV-1h413 viruses. The expression of TurboFP635 induced by both viruses was quantified 24 (A), 48 hours (B) post-infection.

These results suggest that the blockade of VEGF by GLAF-1 conferred to GLV-1h413 an advantage for A549 cells colonization more susceptible to VACV infection and/or replication.

Since we observed that angiogenic factors had an effect on the expression of adhesion molecules, we hypothesized that VEGF stimulation down-regulated the expression of a membrane protein implicated in VACV entry. However, since VACV receptor and mode of entry are still unknown verifying this hypothesis was challenging.

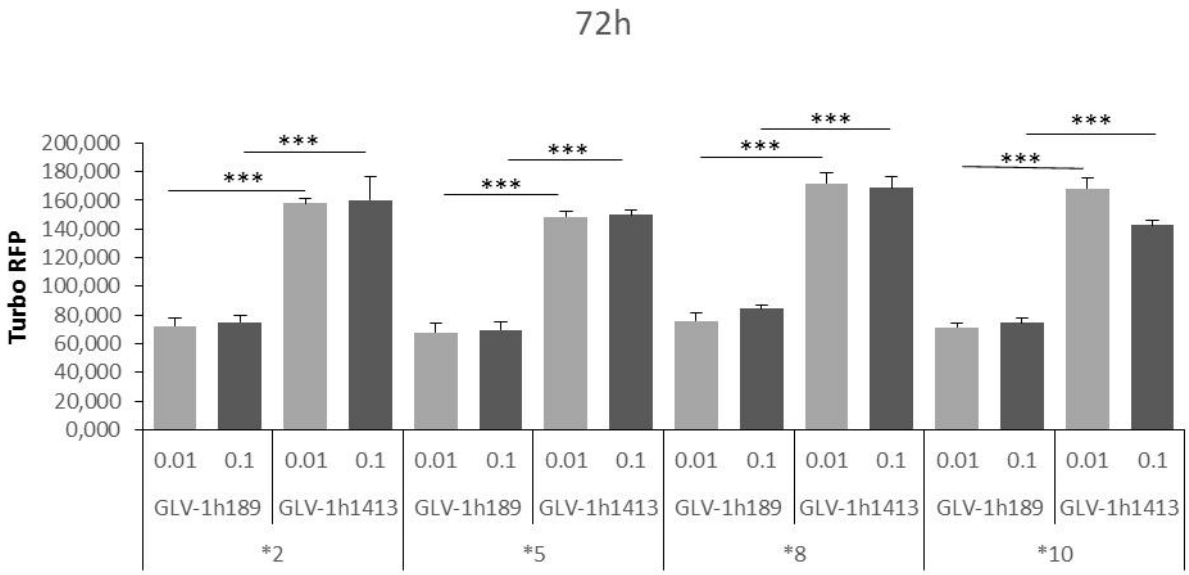

Figure 23.2: Quantification of TurboFP635 in A549 cells infected with GLV-189 and GLV-1h413 (anti-VEGF). A549 cells seeded with increasing levels of VEGF were infected at low (0.01) or high (0.1) MOI of GLV-1h189 and GLV-1h413 viruses. The expression of TurboFP635 induced by both viruses was measured 72 hours post-infection.

To determine whether VEGF blockade also improved VACV replication *in vivo*, 14 nude mice were implanted subcutaneously with PC14PE6-RFP cells and 14 days later, treated with either the anti-VEGF strain GLV-1h108 or the parental GLV-1h68. The amount of RFP expressed by PC14PE6-RFP tumors and the GFP produced by GLV-1h108 and GLV-1h68 were quantified 7, 14 and 21 days post-infection. The percentage of tumor infected by the virus has been calculated using the amount of GFP and RFP detected (Figure 24). It could clearly be observed that the anti-VEGF VACV (GLV-1h108) colonized PC14PE6-RFP tumors more efficiently than GLV-1h68, with up to 78% of infection rate 14 days post-treatment (GFP), while GLV-1h68 only colonized half of the

PC14PE6-RFP tumors. This results confirmed the data observed in A549 tumor cells *in vitro* (see 4.8), and indicate that VEGF blockade eased PC14PE6-RFP tumor colonization and thus improved VACV infectivity.

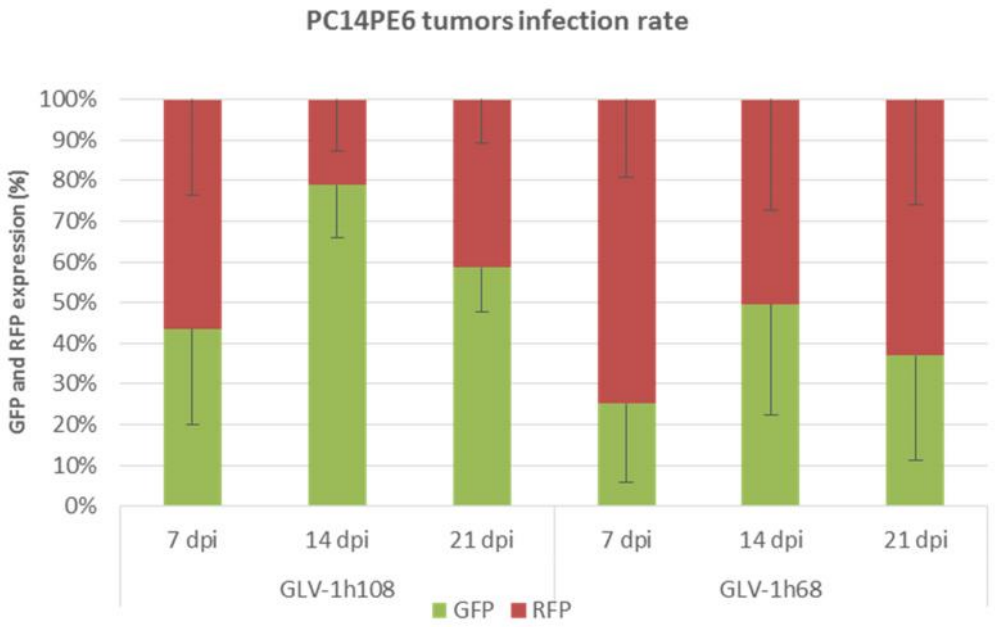

Figure 24: PC14PE6-RFP tumors colonization rate.
PC14PE6-RFP tumor-bearing mice were treated with GLV-1h108 (anti-VEGF) and GLV-1h68 viruses. The GFP emission of the VACV infected tumor cells, and the RFP emission of the PC14PE6-RFP tumors were measured weekly.

VEGF blockade was shown to improve VACV infectivity and PC14PE6-RFP tumor colonization. Nonetheless several clinical studies reported accelerated metastases development after VEGF blockade [42]. Therefore we evaluated the effect of VEGF and Ang-2 blockades on tumor cell colonization.

4.9 VACV mediated anti-VEGF and anti-Ang-2 therapies target and lyse PC14PE6-RFP primary tumors and metastases more efficiently than GLV-1h68

GLV-1h68 was shown to colonize preferentially PC-3 metastases the primary tumors [67]. To determine whether VEGF and Ang-2 blockade affect lung adenocarcinoma dissemination, 30 nude mice were implanted subcutaneously with 4×10^6 PC14PE6-RFP cells and treated intravenously with 1×10^7pfu of different anti-angiogenic viruses. Ten days post treatment, the mice were sacrificed and their organs harvested. The

amount of virus in tumors and organs was titrated by viral plaque assay, and the amount of human β-actin RNA estimated in mice lungs. After reverse transcription and amplification, an electrophoresis gel of the PCR products has been made to compare the amounts of human β-actin RNA in each group, and therefore the amount of human cells present in mice lungs.

Results demonstrated that the anti-angiogenesis viruses reduced more efficiently PC14PE6-RFP cells homing than GLV-1h68 (Figure 25) [87]. The signal emitted by GLV-1h68 samples was stronger than those of the anti-angiogenesis viruses. Moreover we noticed that a light blockade of Ang-2 (GLV-1h337) led to weaker β-actin signals compared to a strong (GLV-1h338) or moderate (GLV-1h339) blockade of Ang-2. When treated with anti-Ang-2 viruses, PC14PE6-RFP cell migration to the lungs was reduced more efficiently than when treated with the anti-VEGF VACV, GLV-1h108, with the exception of GLV-1h338.

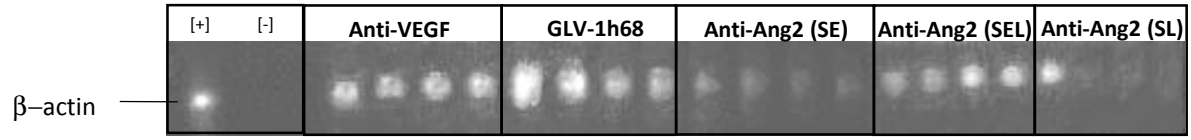

Figure 25: -actin expression in lungs of PC14PE6-RFP tumor-bearing mice 10 days post-treatment. RNA was extracted from lungs of PC14PE6-RFP tumor-bearing mice and amplified by rtPCR. The DNA fragments obtained were processed on an electrophoresis gel. The gel is annoted as follows [+]: positive control (human tumor cells β-actin); [-]: negative control (RNA input replaced by water); Anti-Ang2 (SEL): lungs of mice treated with anti-Ang-2 VACV under SEL promoter, Anti-Ang2 (SL): lungs of mice treated with anti-Ang-2 VACV under SL promoter, Anti-VEGF (SEL): lungs of mice treated with anti-VEGF VACV under SEL promoter, Anti-Ang2 (SE): lungs of mice treated with anti-Ang-2 VACV under SE promoter. GLV-1h68: lungs of mice treated with GLV-1h68.

These data confirmed the previous hypothesis according to which angiogenic factors, including Ang-2, have a strong effect on tumor cell adhesion proteins, but they also showed that to set up an optimal anti-Ang-2 treatment, Ang-2 mode of action and availability compared to other angiogenic factors need to be further studied.

To determine whether anti-angiogenesis VACVs are able to follow PC14PE6-RFP cell dissemination more efficiently or just limit their migration, the amount of virus in organs more likely to be metastatic niches for lung adenocarcinoma tumor cells was determined. It was interesting to notice that despite the low level of β-actin estimated, the GLV-1h337 virus seemed to be present at higher levels compared to GLV-1h108 in murine lungs (Figure 26). One explanation would be that the drastic reduction of VEGF and thus of the tumor vasculature impaired significantly the PC14PE6-RFP cell migration but also slowed down VACV migration to metastatic sites. On the contrary, Ang-2 blockade, under the viral early promoter, significantly increased the amount of virus in the metastatic site and decreased the amount of β-actin detected.

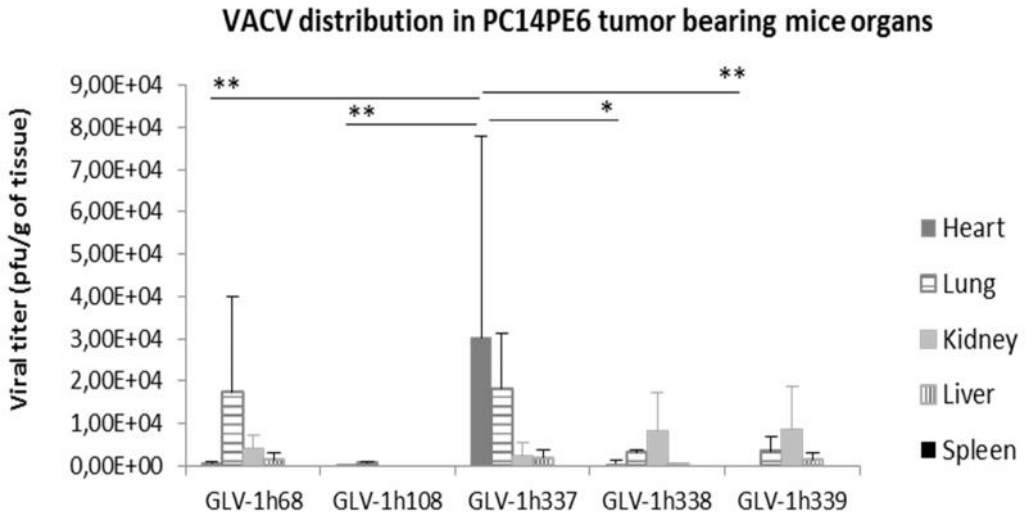

Figure 26: Viral distribution of anti-angiogenesis and parental GLV-1h68 vaccinia viruses in PC14PE6-RFP tumor-bearing mice 10 days post-treatment. Viral amounts were assessed by viral plaque assay. The statistical relevance have been determined by a One-way ANOVA test and represented by * if $p<0.05$ and ** if $p<0.01$.

These data suggest that Ang-2 reduction by GLV-1h337 is more efficient than GLV-1h68 and GLV-1h108 in the reduction of tumor cell migration by facilitating VACV dissemination in the circulation. The reduction of Ang-2 in the tumor micro-environment, improved VACV dissemination and metastases treatment, in PC14PE6-RFP tumor-bearing mouse organs.

The vascular micro-environment was shown to be important for tumor cells and VACV dissemination. One explanation would be that more pericytes coverage, led to less tumor cells being able to cross the endothelium and migrate to form metastases.

Moreover, the reduction of Ang-2 availability facilitated VACV access to metastatic sites, improving oncolytic treatment of PC14PE6-RFP tumor-bearing mice.

4.10 Angiogenic factor blockade improved VACV oncolytic therapy in different tumor models

The anti-tumor effect of the anti-angiogenesis viruses was assessed *in vivo*, in nude mice, using different tumor models. The tumor evolution, as well as the survival of the tumor-bearing mice, and the metastatic abilities of tumors were monitored to determine the tumor response to VACV mediated anti-angiogenesis treatment.

4.10.1 Angiopoietin 2 blockade improved oncolytic VACV treatment of Colo205 tumors

The first study aimed to evaluate the effect of Ang-2 blockade on the evolution of a highly vascularized tumor model Colo205. Thirty-three nude mice were implanted subcutaneously, on the right flank, with 4×10^6 Colo205 cells. When tumors reached 150 to 200 mm^3, mice were treated with VACV by intravenous tail vein injection, six groups of 5 (GLV-1h108, GLV-1h68, untreated control) and 6 mice (GLV-1h492, GLV-1h493, GLV-1h494) were made. Tumor size measurements showed that VEGF blockade by GLV-1h108 stabilized the tumor progression starting as early as 3 days post treatment (Figure 27.A). This again confirms the crucial role of VEGF in the tumor progression.

Ang-2 blockade led to two different situations depending of the level of expression of the anti-Ang-2 scAb. As explained previously, VACV produces three types of proteins, early, early late and late proteins, under the control of three different promoters. When the anti-Ang-2 promoter is under the control of the synthetic early-late promoter of VACV, in other words produced at a high quantity, Ang-2 blockade profited Colo205 tumor growth, and allowed tumors to grow even faster than the untreated ones (data not shown).

A

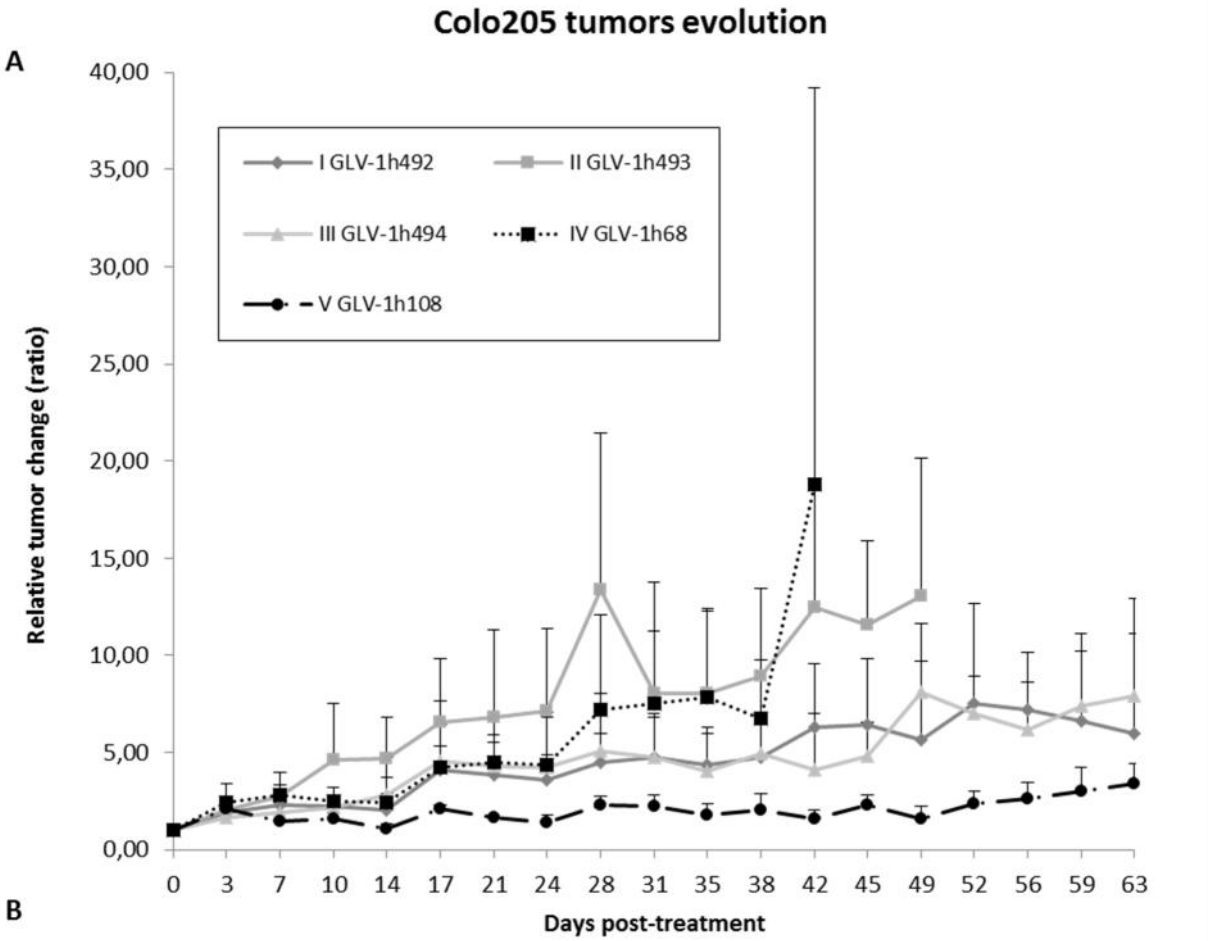

B

	d3	d7	d21	d24	d28	d31	d35	d42
GLV-1h108		p <0.001	p <0.05	p <0.05	p <0.01	p <0.01	p <0.001	p <0.001
GLV-1h492	p<0,05	p <0.05				p <0.05	p <0.05	p <0.05
GLV-1h494	p<0,01	p<0,01						p <0.05

Figure 27: Colo205 tumors relative tumor size. Tumor sizes were measured 2 times a week for 63 days (A). The statistical relevance of the difference between anti-angiogenesis treated groups and GLV-1h68 virus was determined by a One-way ANOVA test (B).

However, when treated with GLV-1h492 (weak promoter) and GLV-1h494 (intermediate promoter), we can observe a steady and statistically significant tumor growth delay at different stages of the tumor development. Starting 31 ($p<0.05$) and 42 days ($p<0.05$) post-treatment, GLV-1h492 and GLV-1h494, respectively displayed a late stage tumor growth delay and at 3 and 7 days these viruses induced an early tumor growth delay, compared to the GLV-1h68 treated group. Anti-angiogenesis treatments had a prompt and long lasting effect on tumor progression, an effect visible until 42 days post-treatment, when the number of GLV-1h68 treated mice left did not allow

statistical relevance assessment. These data confirmed the observations made previously on PC14PE6-RFP tumor-bearing mice, a moderate inhibition of Ang-2 is efficient for cancer treatment, thus the use of Ang-2 blockade for tumor therapy entails a good understanding and control of the balance of Ang-2 with others angiogenic factors like VEGF, for it can change completely the outcome of the treatment (see 4.9).

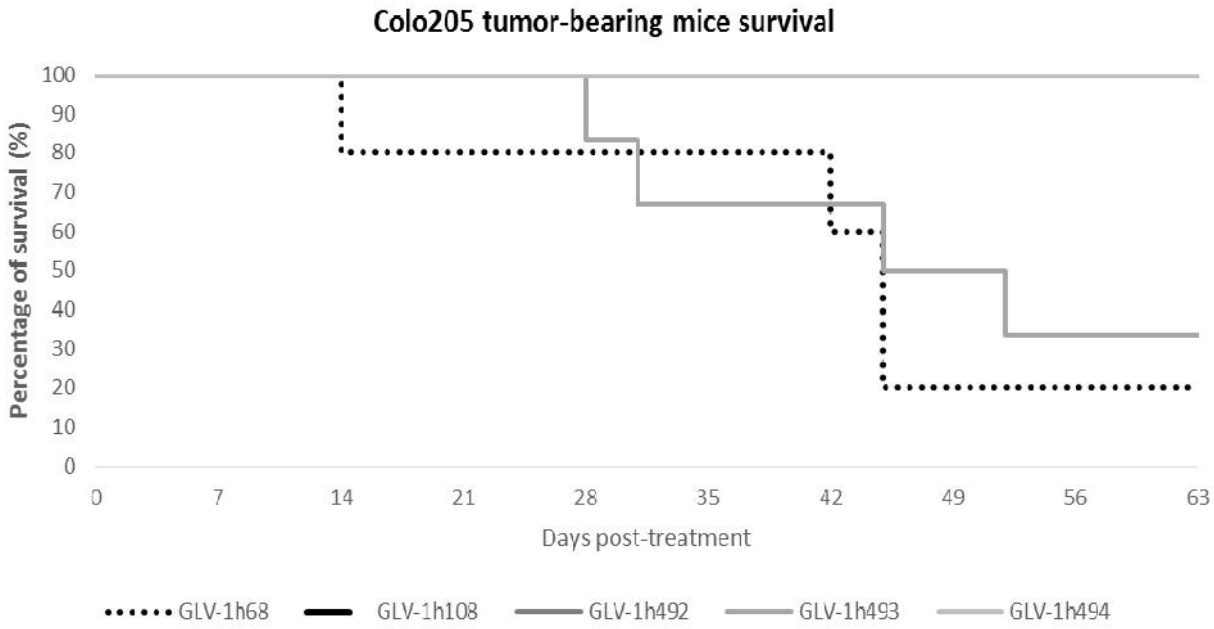

Figure 28: Colo205 tumor-bearing mice survival after VACV oncolytic treatment.

In spite of mixed results on tumor growth delays, all VACV expressing an anti-Ang-2 scAb improved Colo205 tumor-bearing mice survival compared to the group treated with GLV-1h68 (Figure 28). Nevertheless, GLV-1h492 and GLV-1h494, which express the anti-Ang-2 scAb under the weak and intermediate promoters, respectively, allowed the survival of 100% of the mice when 33,33% of GLV-1h493 treated mice survived. These data proved again that Ang-2 needs to be reduces and not completely inhibited to be efficient against tumors.

All anti-angiogenesis VACV improved Colo205 tumor-bearing mice survival compared to GLV-1h68-treated mice.

4.10.2 PlGF blockade improves VACV treatment of MEL1936 tumors

The impact of PlGF blockade on tumor progression, was assessed in the MEL1936 tumor model.

MEL1936 is a melanoma cell line known as a slow responder to GLV-1h68 treatment [88]. To determine whether PlGF blockade improve MEL1936 treatment, 47 nude mice were implanted subcutaneously with 4×10^6 MEL1936 cells and treated with either 1x PBS, GLV-1h68, GLV-1h108, or the anti-PlGF viruses GLV-1h343, GLV-1h344 and GLV-1h345.

We observed that the anti-VEGF GLV-1h108 induced a statistically significant tumor growth delay of MEL1936 tumors ($p<0.001$) and that the anti-PlGF GLV-1h343 followed the same trend (Figure 29). These results are encouraging since none of the anti-angiogenic viruses tested so far shown comparable results to GLV-1h108. Additionally, they confirmed the impact of PlGF on tumor development.

When observing the overall survival of the different groups, we noticed that although the effect of GLV-1h343 treatment on the primary tumor is similar to GLV-1h108, this effect did not reflect the mice life expectancy with 40% survival 52 days post treatment, which is 6,7% higher than GLV-1h68 (Figure 30).

On the other hand, the anti-PlGF GLV-1h344 showed a significant improvement of MEL1936 tumor-bearing mice survival. When treated with this virus, after 52 days, 70% of MEL1936 tumor-bearing mice survived. This result was very close to the 77% survival after the anti-VEGF GLV-1h108 treatment.

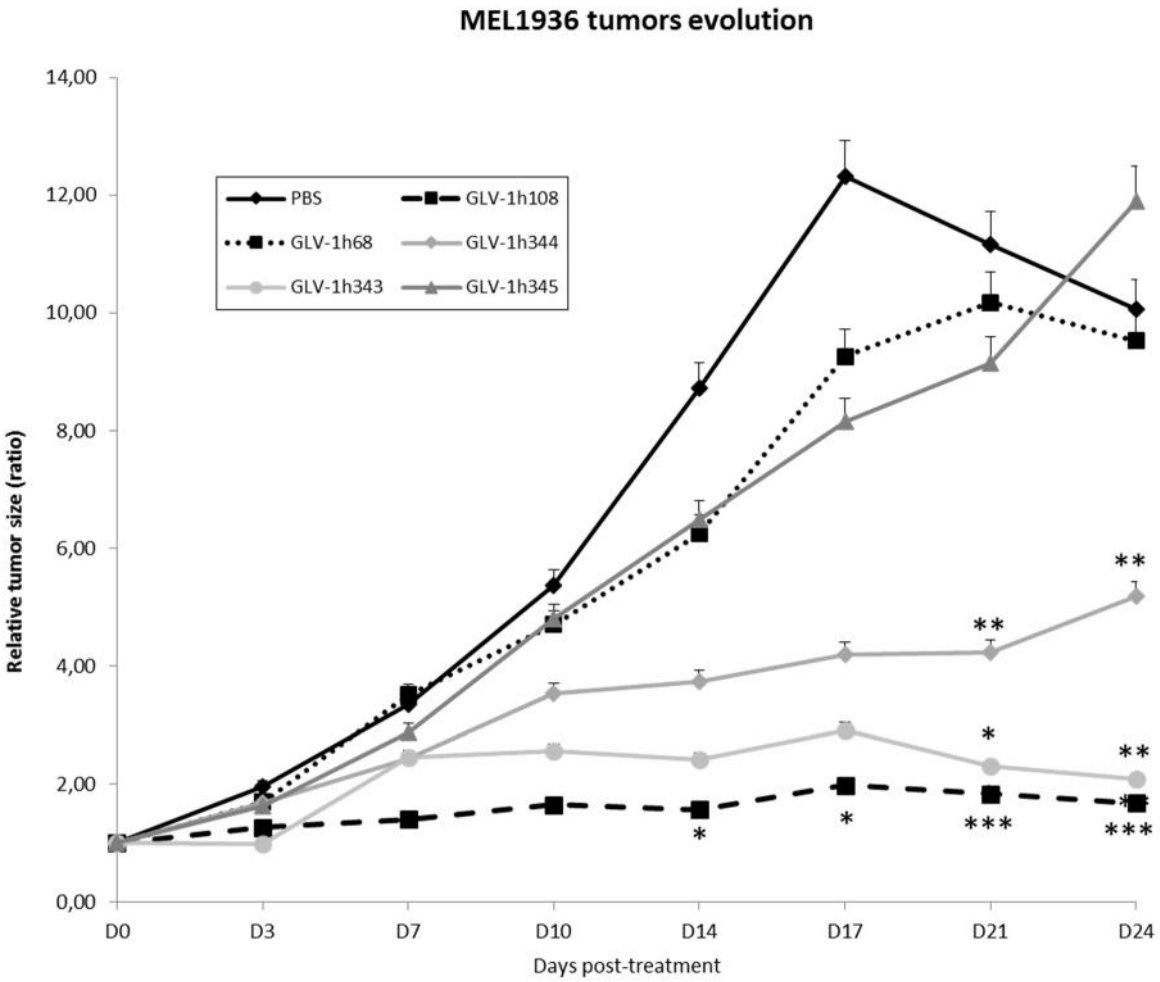

Figure 29: MEL1936 tumor evolution after oncolytic VACV treatment. MEL1936 tumor volumes were measured two times a week. The statistical relevance of the anti-angiogenesis treated groups compared to the GLV-1h68 group have been determined by a One-way ANOVA test and represented by * if $p<0.05$, ** if $p<0.01$ and $p<0.001$.

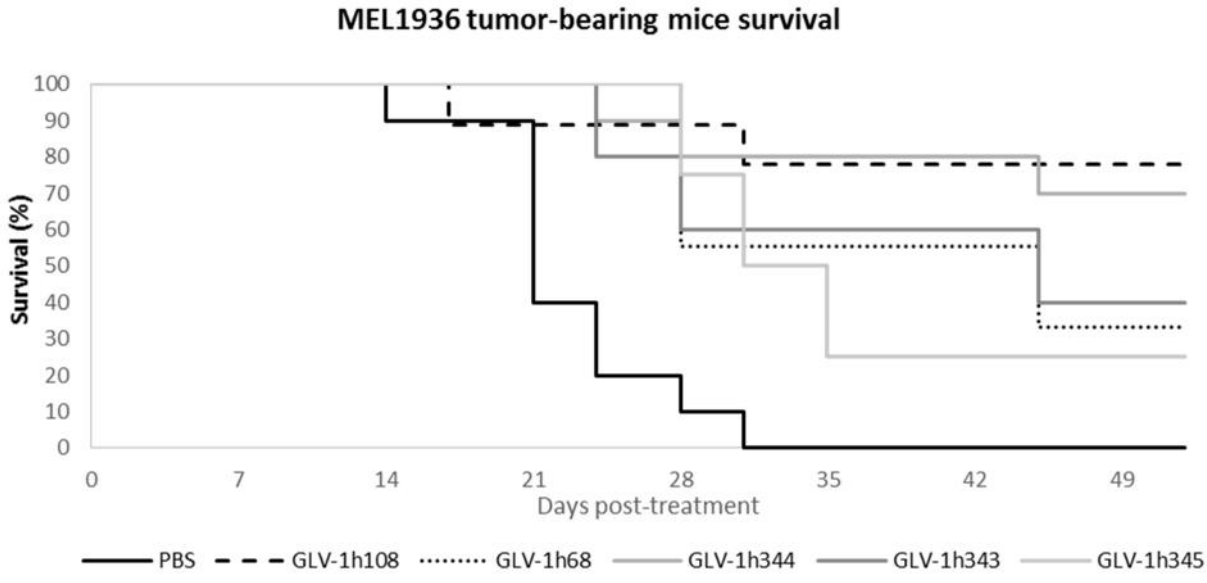

Figure 30: MEL1936 tumor-bearing mice survival after VACV treatment.

4.10.3 Combination therapy to circumvent angiogenesis resistance

We established that angiogenic factors not only had an effect on tumor vasculature, but also on their migration and relation with the immune system (see 4.9). We also established that VEGF blockade improved VACV oncolytic therapy by increasing its infectivity *in vitro* and *in vivo* (see 4.8). However, bevacizumab treatment was shown to have a limited effect on tumor cell homing. The last aim of this thesis was yet to find a suitable way to circumvent resistance to anti-angiogenesis therapies.

4.10.3.1 Anti-Ang-2 and Anti-VEGF combined therapy mediated by VACV

A light blockade of Ang-2 by VACV expressing the anti-Ang-2 scAb was shown to limit the homing of PC14PE6-RFP cells in other words it decreased the amount of PC14PE6-RFP cells able to migrate out of the primary tumor. That is why we tested the hypothesis according to which the combination of Ang-2 and VEGF blockade would improve VACV treatment. Thereby, Colo205 tumor-bearing mice have been treated with GLV-1h495 hoping to see a strong reduction of the tumor vasculature and tumor cells progression.

4.10.3.1.1 Ang-2 combination therapy lead to a faster tumor growth delay

Therefore, 28 nude mice were implanted with 4×10^6 Colo205 cells subcutaneously and treated with GLV-1h108 (anti-VEGF), GLV-1h68, GLV-1h492 (anti-Ang-2) and GLV-1h495 (anti-VEGF and anti-Ang-2), when tumors reached a volume of 150 to 200 mm^3. We observed that the combination of VEGF and Ang-2 blockade led to a significant tumor growth delay starting 3 days post-treatment. The combination therapy did not resulted in a stronger tumor growth delay compared to VEGF and PlGF blockades alone, but it did block Colo205 response to VACV treatment faster than Ang-2 blockade alone, with a tumor growth delay being significant 28 days post-treatment for GLV-1h495 when GLV-1h492 needs 31 days (Figure 31).

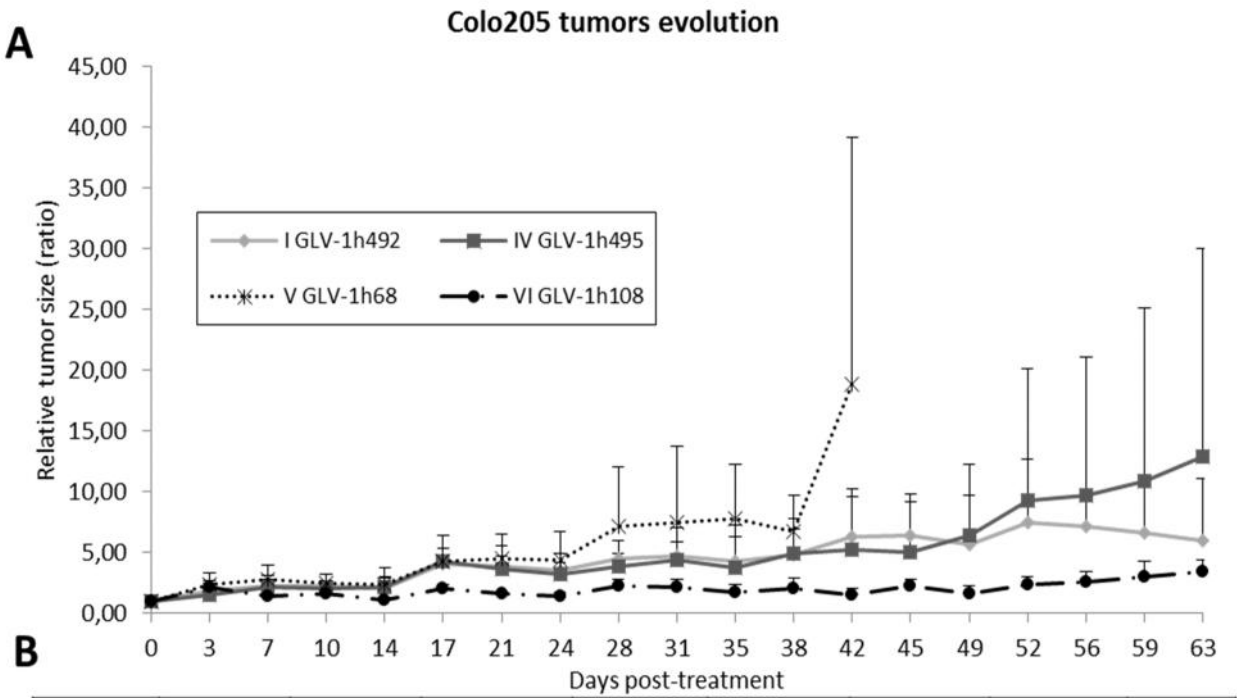

B

	d3	d7	d21	d24	d28	d31	d35	d42
GLV-1h108		p <0.001	p <0.05	p <0.05	p <0.01	p <0.01	p <0.001	p <0.001
GLV-1h492	p<0,05	p <0.05				p <0.05	p <0.05	p <0.05
GLV-1h495	p<0,01	p <0.05			p <0.05	p <0.05	p <0.01	p <0.05

Figure 31: Colo205 tumors evolution after anti-Ang-2 and Anti-VEGF combination therapy. Colo205 tumor volumes were measured bi-weekly for 9 weeks (A), and the statistical relevance has been evaluated by a One-way ANOVA.

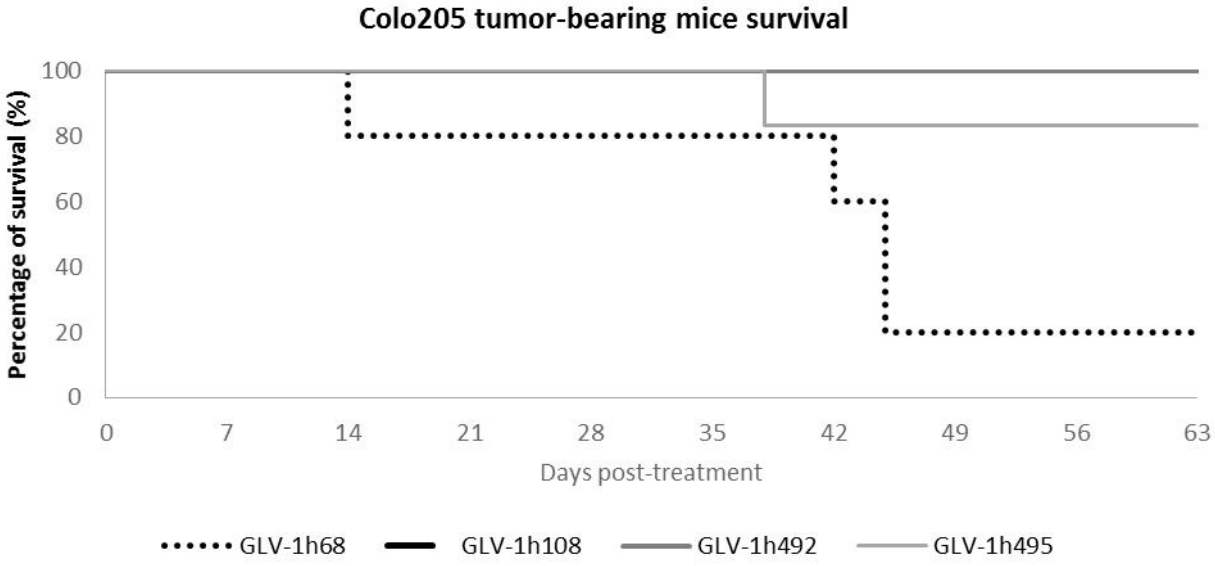

Figure 32: Colo205 tumor-bearing mice survival after anti-Ang-2 and anti-VEGF combination therapy.

All groups treated with viruses harboring anti-angiogenesis scAb showed survival of 100% at termination of the study. Treatment with the control virus GLV-1h68 led to a survival of the mice of 20% (Figure 32).

4.10.3.1.2 Anti-Ang-2 combination therapy modifies Colo205 tumors vasculature.

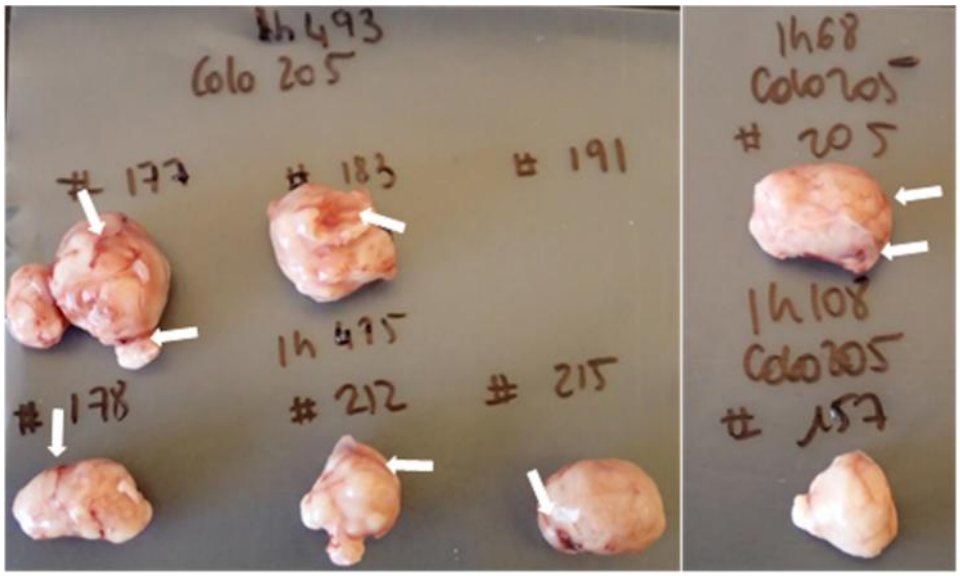

Figure 33.1: Colo205 excised tumors 14 days post-treatment. Tumors were imaged with Olympus TG-1 camera. Blood vessels are shown by white arrows

Ang-2 and VEGF blocking treatments led to different patterns of vasculature visible when observing excised tumors treated either with GLV-1h108, GLV-1h493 or GLV-1h68 (Figure 33.1). On the one hand, GLV-1h493 treated tumors exhibited blood vessels higher in diameters and more structured vasculatures than GLV-1h68 treated tumors that display thinner, deeper and more tortuous blood vessels. On the other hand, GLV-1h108 treated tumors only exhibit very few and thin blood vessels. These patterns are still visible 8 weeks post-treatment (Figure 33.2).

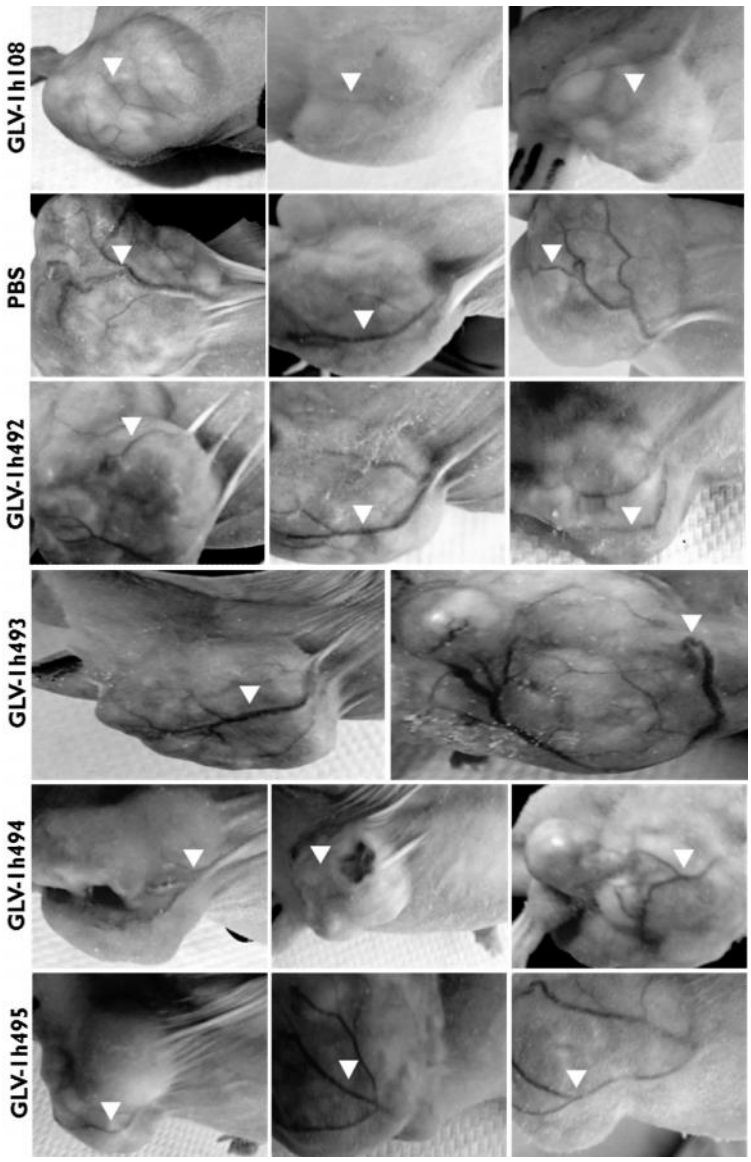

Figure 33.2: Colo205 tumors 8 weeks post-treatment. Nude mice were imaged with an Olympus TG-1 camera. Blood vessels are shown by white arrows.

4.10.3.2 Anti-PlGF and Anti-VEGF combined therapy mediated by VACV.

The combination of PlGF and VEGF blockade was evaluated *in vivo*. Forty-seven nude mice were implanted with 5 × 10^6 MEL1936 cells, and treated with either GLV-1h68, GLV-1h108 (anti-VEGF), GLV-1h344 (anti-PlGF) or GLV-1h471 (anti-PlGF and anti-VEGF).

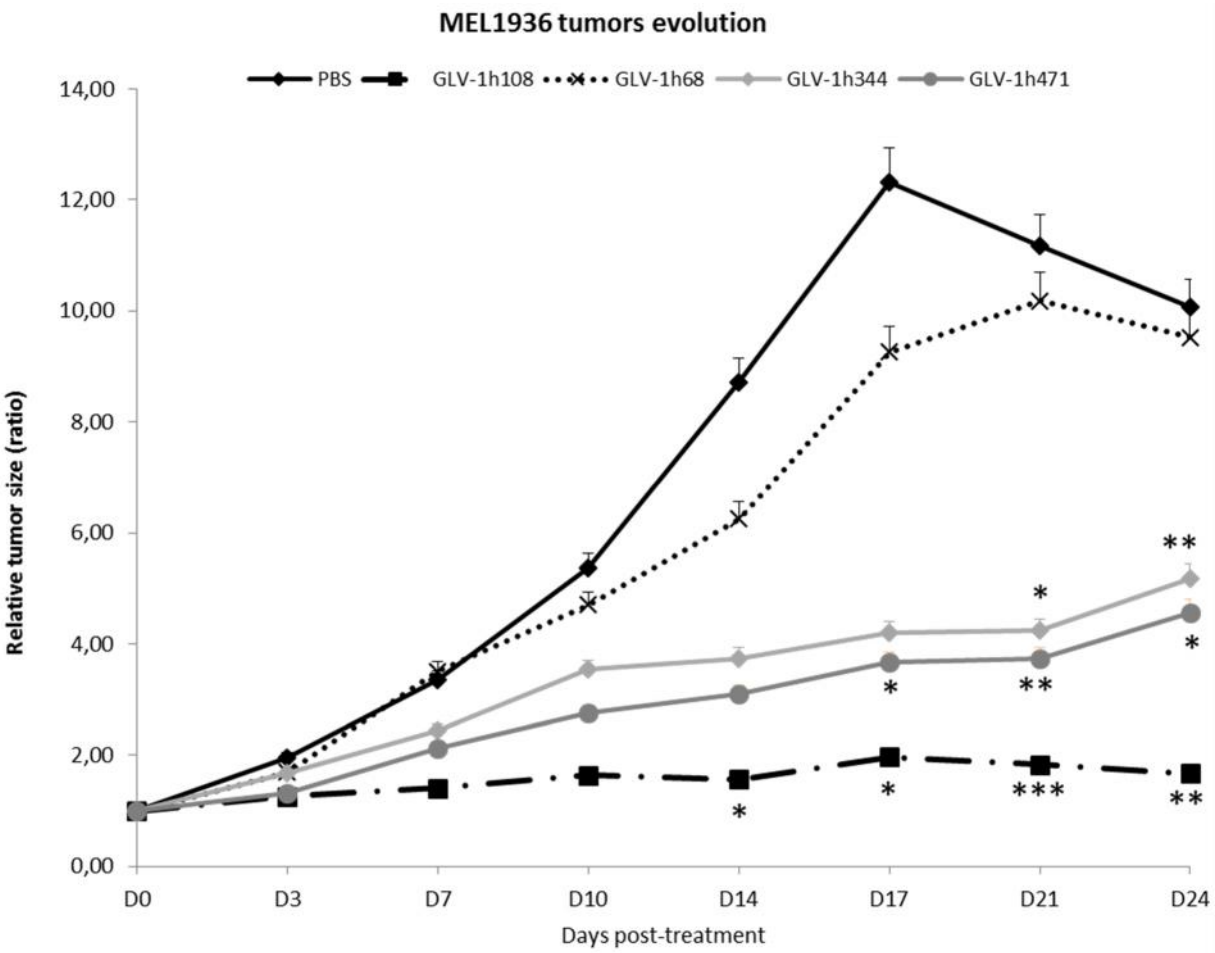

Figure 34: MEL1936 tumors evolution after VACV-mediated PlGF and VEGF blockade. Tumor volumes were measured biweekly. The statistical relevance of the measurements compared to GLV-1h68 were determined using a One-Way ANOVA test.

The data showed that the combination of PlGF and VEGF blockades, as observed previously for Ang-2 (see 4.10.3.1.1), led to a faster tumor growth delay compared to PlGF blockade alone, but not when compared to VEGF blockade only (Figure 34). Nevertheless, the combination treatment did improved the overall survival of MEL1936 tumor-bearing mice when compared to VEGF and PlGF blockades alone (Figure 35).

Blood samples of MEL1936 tumor-bearing mice were 21 days post-infection. The serum was extracted and evaluated for PlGF expression. Even though the number of samples was not sufficient to obtain statistically significant results (p values ranging from 0.06 to 0.09), a trend could be observed, VEGF blockade led to an increased expression of PlGF in MEL1936 tumor-bearing mice.

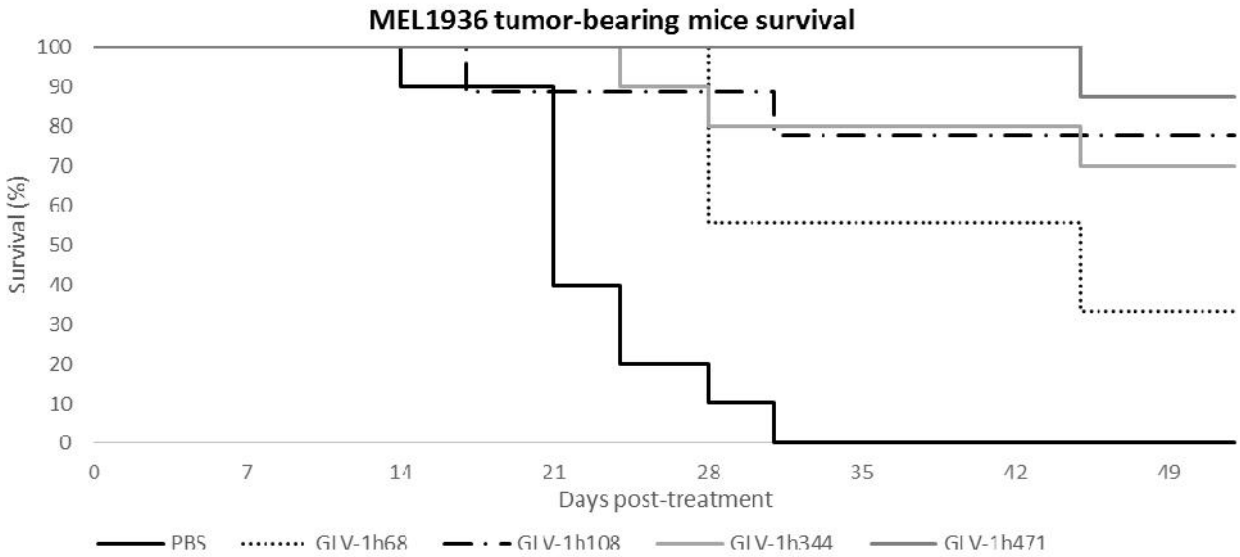

Figure 35: Survival of MEL1936 tumor-bearing mice after PlGF and VEGF blockade by VACV.

VEGF blockade was found to increase PlGF expression in MEL1936 tumor-bearing mice when compared to the GLV-1h68 treated group. These MEL1936 tumors, to circumvent VEGF blockade and sustain their vasculature, over-expressed PlGF (Figure 36).

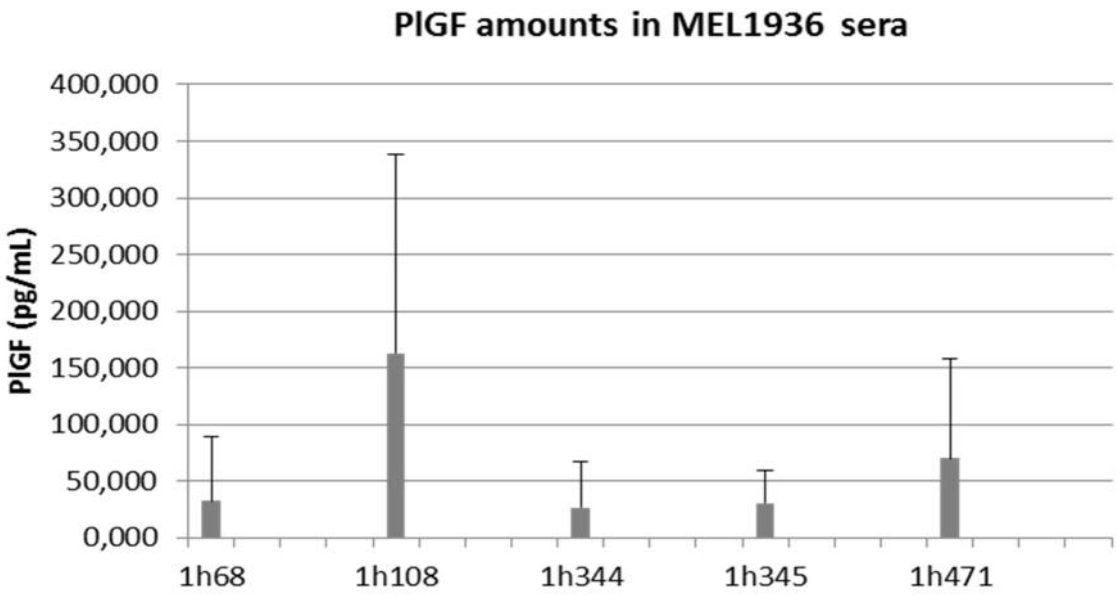

Figure 36: PlGF quantification in mice sera.

The use of the GLV-1h471 for treatment limited the effect of this over-expression by blocking PlGF as well as VEGF.

The second tumor model used to evaluate the anti-PlGF therapy with or without combination with VEGF blockade, was A549. Like previously, 4×10^6 A549 cells were implanted subcutaneously in nude mice, and once tumor volumes reached 450-500 mm^3, mice were treated either with 1×10^7pfu of the viruses described previously, or with a weekly dose of 5 mg/kg of anti-PlGF scAb (aPlGF). This aPlGF antibody was produced using the same DNA sequence used to construct the GLV-1h344 virus, was stably expressed in CV-1 and HEK293 human mammalian cells, to avoid any bacterial contaminations. The functionality of the aPLGF antibody was confirmed in ELISA. Supernatants of HEK293 and CV-1 cells transfected with 5 μg of the aPlGF expression plasmid were harvested, and the flag-tagged aPlGF antibody was purified using the M2 Flag Immunoprecipitation kit. The purified protein has then been used in a DC protein assay and a quantitative ELISA as primary antibody for PlGF quantification (Figure 37).

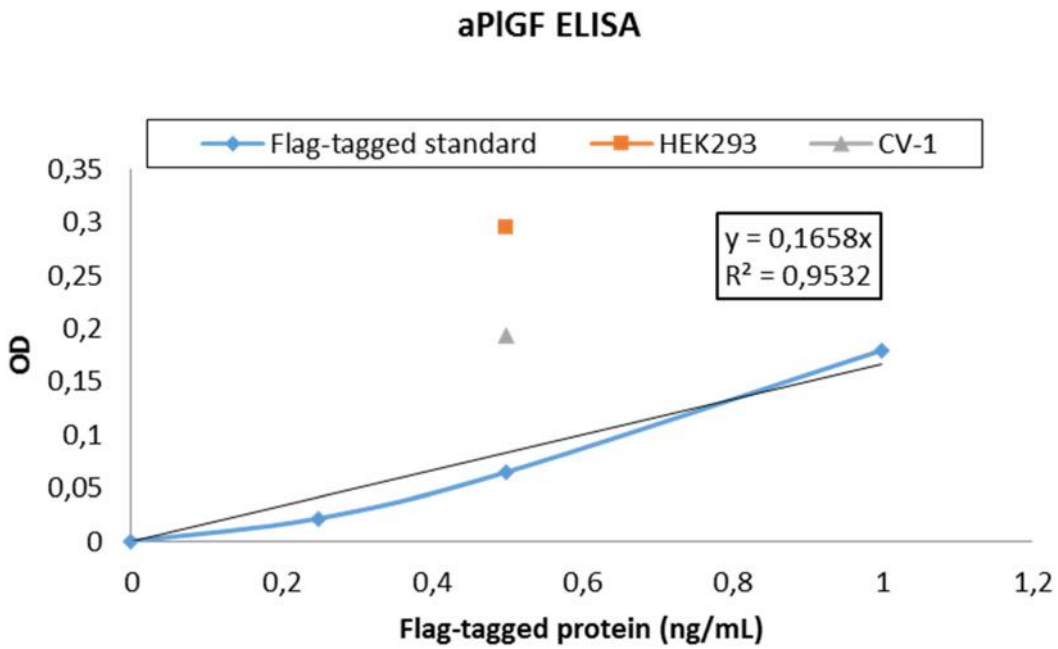

Figure 37: Flag-tag ELISA of aPlGF purified antibody. A two-fold serial dilution of a flag-tagged protein starting at 1 ng/mL and 100 ng of PlGF protein were coated respectively into standard wells and samples of an ELISA plate.

A

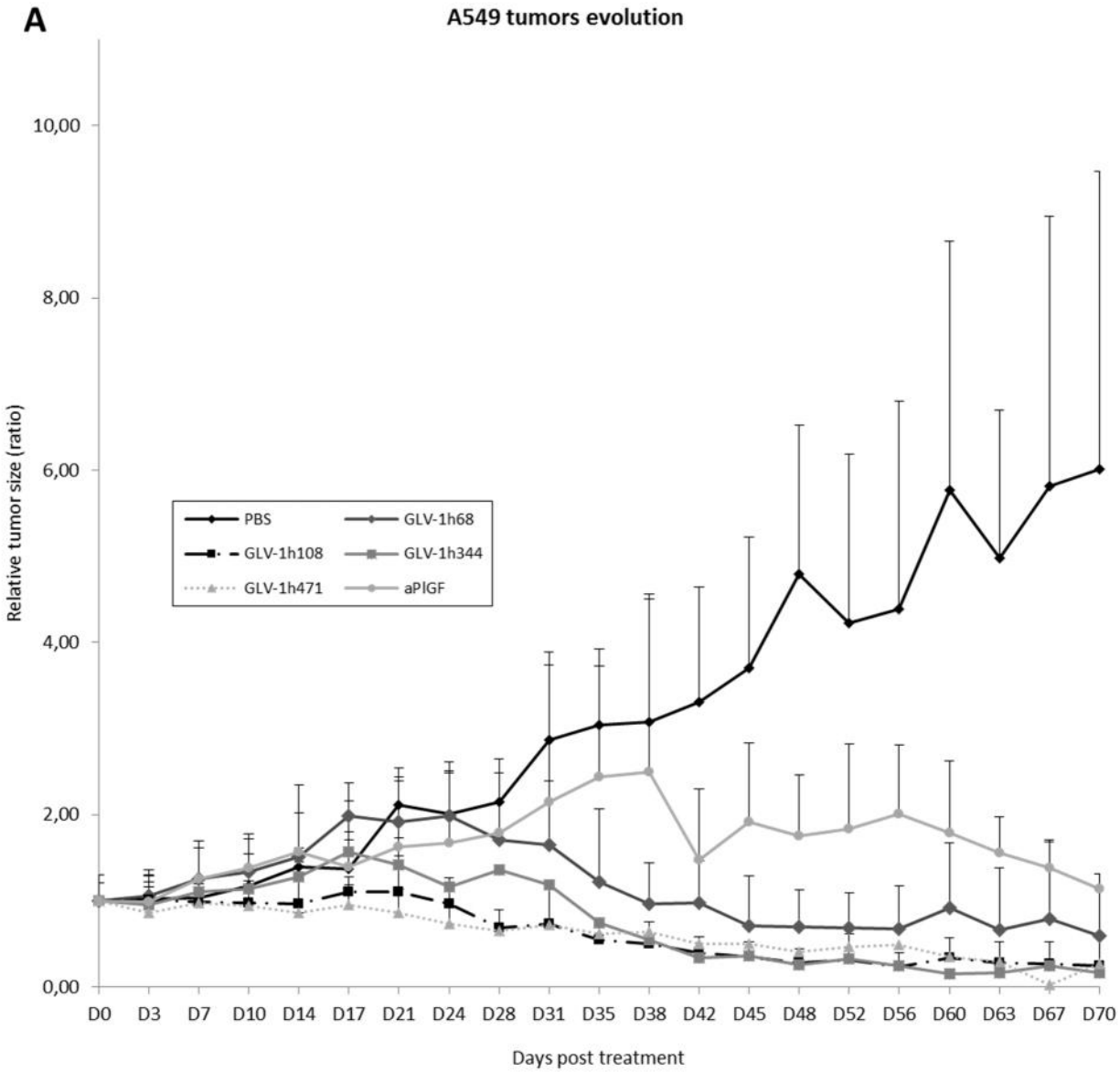

B

	d7	d10	d14	d17	d21	d28
GLV-1h108		p<0.05	p<0.01	p<0.01	p<0.01	p<0.01
GLV-1h471	p<0.05	p<0.01	p<0.01	p<0.001	p<0.001	p<0.01

C

	d10	d14	d17	d28	d31	d35	d42	d45	d48
GLV-1h68			p<0.05						
GLV-1h108				p<0.01	p<0.05	p<0.01	p<0.05		
GLV-1h344						p<0.05	p<0.05	p<0.05	p<0.05
GLV-1h471	p<0.05	p<0.05		p<0.01	p<0.05	p<0.01	p<0.05		

Figure 38: A549 tumors evolution after anti-angiogenesis treatment. (A) A549 tumors were monitored biweekly. The statistical relevance of tumor sizes compared to the GLV-1h68 (B) and the aPlGF (C) treated group was determined by a One-way ANOVA test.

The ELISA proved that aPlGF binds to its target and can be detected by its flag-tag, consequently, aPlGF antibody was used to compare the effect of PlGF blockade by VACV and PlGF blockade alone. HEK293 cells supported the transfection process better than

CV-1 cells, and were used to produce aPlGF antibody in a larger scale (Figure 37). The purity of the purification product was evaluated rudimentary, by comparing the amount of protein detected by the DC protein assay to the amount detected by ELISA.

The observation of the tumor growth showed that all the vaccinia virus based treatments induced a stronger tumor regression compared to the aPlGF treatment alone, and thus underlined the VACV effect (Figure 38). The aPlGF treated tumors did not regressed but only exhibit a growth delay, compared to the vaccinia virus-treated tumors. GLV-1h344 treatment resulted impaired A549 tumor progression more efficiently than the aPlGF treatment. Unfortunately, due to the decreasing number of GLV-1h68 treated-mice the statistical relevance of these results could only be evaluated until 28 days post treatment.

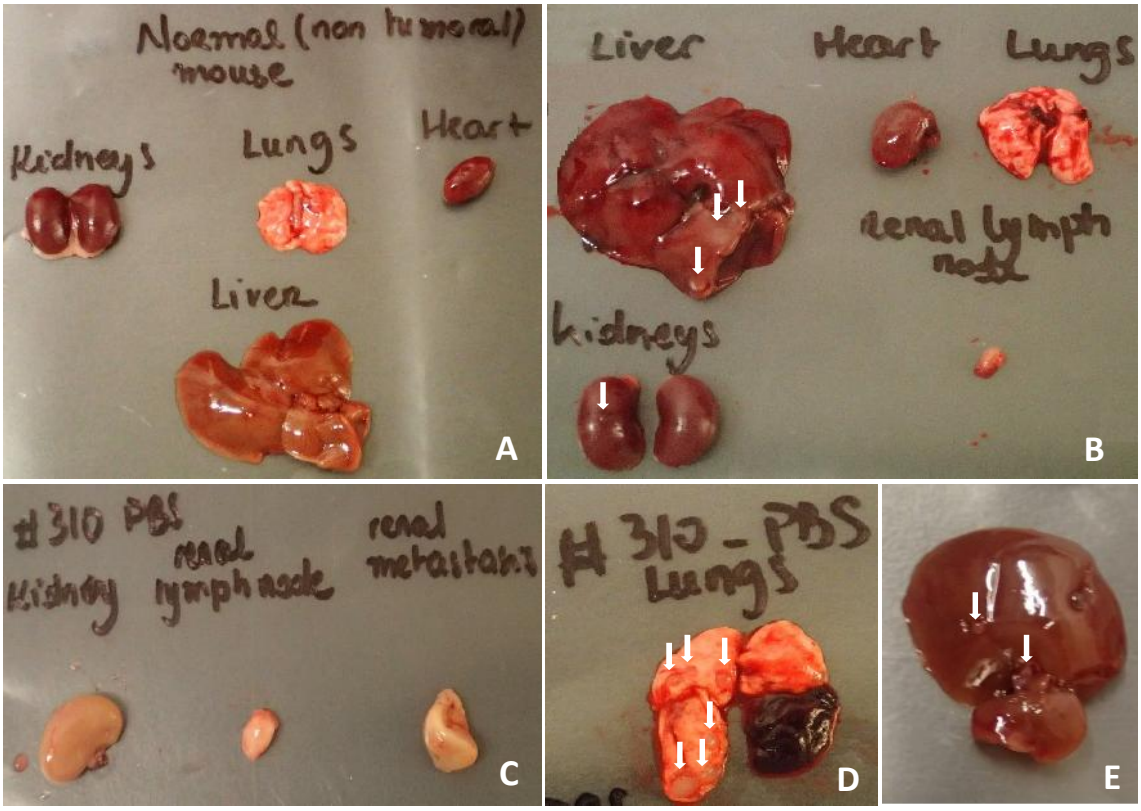

Figure 39.1: Comparison of organs of a healthy nude mouse and A549 tumor-bearing untreated or treated with GLV-1h68, Organs of a healthy nude mouse (A), and A549 tumor-bearing mice treated with GLV-1h68 (B) or PBS (C, D, E) were excised and imaged using Olympus TG-1. Metastases visible to the naked eye are shown by white arrows. Sizes cannot be compared since the scale is unknown.

The combination of VACV with the PlGF blockade lead to an added therapeutic effect. The combination of VEGF and PlGF blockade mediated by the GLV-1h471 VACV strain, resulted in a stable therapeutic effect on tumor bearing mice. At the termination of the

experiment, organs were examined for sign of metastases (Figure 39). We can clearly see that the PlGF blockade and GLV-1h68 treatment alone reduced the incidence of A549 cells migration to metastatic niches.

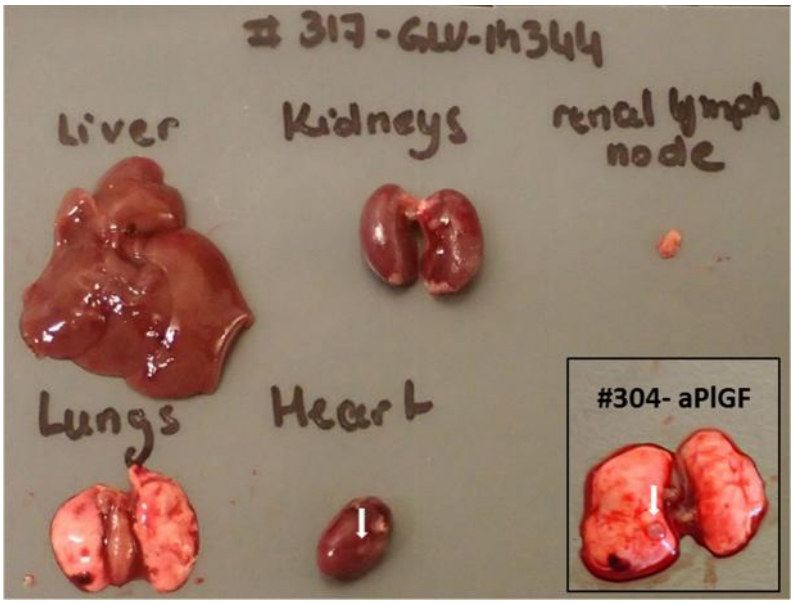

Figure 39.2: Observation of GLV-1h344 and aPlGF treated organs. Organs of were excised and images with Olympus TG-1. Sizes cannot be compared since the scale is unknown. Metastases are indicated by white arrows.

It is challenging to foresee the response of the tumor to the anti-angiogenesis treatment, we cannot predict if tumor cells are going to over-express a specific angiogenic factor, but targeting several of them, especially when they are implicated in other mechanisms like promoting tumor survival and known to be expressed in a wide range of tumor types, could be a good strategy to improve anti-angiogenic monotherapies.

5 Discussion

Tumor-induced angiogenesis has been widely studied. Angiogenesis regulation is often regarded as a balance between angiogenic and anti-angiogenic molecules. When the balance shifts in favor of angiogenesis stimulators, due to their over-expression by tumor cells, an angiogenic switch activates the normally quiescent endothelial cells to form more blood vessels. This phenomenon is one of the hallmarks of tumor pathogenesis and contributes to the progression of cancer from a dormant *in situ* lesion to a life-threatening metastatic disease causing millions of death each year [2-6]. Angiogenic factors are key effectors in the activation of endothelial cells. VEGF, PlGF and Ang-2 are angiogenic factors abnormally expressed by a broad range of tumor types [12, 89, 90-91]. VEGF was identified as a powerful activator of endothelial cells [12-13] and PlGF, which belong to the VEGF family, was shown to influence angiogenic factors as well leukocyte recruitment to tumors [23]. Ang-2, does not directly influence angiogenesis but supports VEGF and PlGF angiogenic effect by triggering the removal of the pericyte coat from endothelial cells [20]. The precise understanding of the mechanisms involved in this process would help improving the current panel of anti-angiogenesis treatments available to cancer patients.

5.1 A549 tumor cells can form blood vessel-like structures

The ability of tumor cells to induce the formation of a new vasculature has been studied extensively over four decades now [92]. However several mechanisms leading to the creation of this vascular system are still poorly understood. The ability of certain tumor types, like melanomas, to physically participate to the structure of the vascular system was confirmed by numerous studies but stays controversial [78-82]. It was shown *in vitro,* and in clinical samples, that melanomas are able to form functional blood vessel-like structures [81]. Blood vessels formed by melanoma cells were shown to be predominantly localized in the most aggressive and invasive areas of the tumors, confirming the functionality and importance of these tumor-cell-based vascular structures, in the tumor progression. During our study we observed for the first time that the lung adenocarcinoma cell line A549 was also able to form similar blood vessel-like structures *in vitro* while HeLa cells cannot. These findings confirm that this phenomenon, known as vasculogenic mimicry, is indeed a physiological phenomenon

possible in certain conditions, in certain tumor cell types, and not only an artefact. This ability to adapt to their environment and change their physiological function to promote tumor progression requires us to reconsider the anti-angiogenesis strategy against cancer. If tumor-induced angiogenesis is not only depending on endothelial cells being recruited to the tumor site by angiogenic factors over-expressed by tumor cells, a reduction of these factors would surely impair tumor progression by reducing the endothelial cells-made blood vessels but not the blood vessels created by tumor cells. The tumor would still be able to meet its need through the tumor cells-made blood vessels. Only blocking angiogenic factors would not solve that issue, however VACV-mediated angiogenesis blockade targets regular blood vessels and tumor-cells-made blood vessels, preventing the tumor to use this mechanism to circumvent treatment.

5.2 PC14PE6-RFP tumor cells binds to the endothelium

The versatility of tumor cells differs from cell line to cell line. While A549 cells can mimic endothelial cells and form blood vessel-like structures, PC14PE6-RFP cells cannot form these kind of structures by themselves but they can mimic pericytes cells and cover endothelial cells. *In vitro*, in presence of PC14PE6-RFP cells, endothelial cells form bi-layered blood vessels-like structures, with the endothelial cells in the inner part [83-84]. This allows a direct interaction between tumor cells and the endothelium. This could explain the strong vascular leakage induced by PC14PE6-RFP tumors. This cell line strongly expresses several angiogenic factors directly on the endothelial cells, making it challenging to block since there is a very small perimeter of intervention for anti-angiogenic factors antibodies to take action. The implementation of anti-VEGF, -PlGF and/or -Ang-2 antibodies in the protein panel of VACV, allows the direct delivery of anti-angiogenesis agents around endothelial cells.

5.3 A personalized treatment is necessary for a successful anti-angiogenesis cancer treatment.

Nevertheless, treating tumors blindly with anti-angiogenesis viruses will not show the results expected if the levels of expression of different angiogenic factors are not verified prior to treatment. Since we saw that not only the expression level of the

angiogenic factor targeted is important, but the whole angiogenic profile has to be known. For instance, in case of an anti-Ang-2 based treatment, the level of Ang-1 and VEGF would help to predict the outcome of the treatment. This could be the reason why Ang-2 blockade for cancer treatment gave controversial results in preclinical studies. When some studies confirms that Ang-2 over-expression stimulates tumor progression in patients with breast or colon carcinomas [77, 78] others discredit this affirmation by describing the inhibitory effect of Ang-2 on tongue carcinomas [79]. The accuracy of these studies is not to question, the different angiogenic profiles of these cell lines most likely explain the discrepancies in the results obtained. Moreover, when evaluating Ang-2 blockade for cancer treatment, the level of blockade should also be considered. We saw that phenomenon in Colo205 tumors, only moderate blockades of Ang-2 led to tumor growth delays, proving that treating cancer by blocking Ang-2 requires a fine balance and knowledge of the angiogenic profile of the tumor-treated.

This also applies to VEGF blockade, in spite of the strong significant tumor growth delays observed in all the tumor cells types tested during our study, the clinical trials results for the anti-VEGF treatment bevacizumab proved that blocking VEGF alone is not sufficient for a long-lasting tumor regression. Different escape mechanisms impairing bevacizumab efficiency were described, including the over-expression of other angiogenic factors that may take over the tumor vasculature stimulation and allow the recurrence of the tumor in patients. Thus, knowing the angiogenic profile of the patient's tumor before the treatment and follow its evolution would help with the choice of the angiogenic factor to block. In this case, a combination therapy mediated by VACV would prevent and address the creation of tumor cell-made blood vessels as well as the expression of other angiogenic factors to stimulate the vasculature. Thus therapeutic VACV targeting several angiogenic factors could help ensuring a long lasting treatment of the tumor, and ultimately the remission of patients.

5.4 Fluid mechanics principles guiding the reduction of PC14PE6-RFP and A549 tumor cells dissemination

The consequences of the over-expression of VEGF, Ang-2 and PlGF by tumor cells are clearly described by fluid mechanics and the Starling forces. Starling forces are described as the addition of the osmotic and hydrostatic forces responsible for the fluid

movements in and out of the capillaries [94, 95] Depending of the balance of these forces, either fluids are displaced from the blood vessel to the tissues or from the tissues to the blood vessel. More specifically, these forces include the blood hydrostatic pressure (BHP) pushing the fluid into the tissue, the interstitial fluid hydrostatic pressure (IFHP) and the blood osmotic pressure (BOP) going from the tissues to the blood vessel, and finally the interstitial fluid osmotic pressure (IFOP) moving the fluids from the blood vessel into the tissues. Several factors, including the blood vessels permeability, have an effect on the balance of Starling forces. It is widely acknowledged that tumors generally exhibit a very high interstitial fluid hydrostatic pressure, with a value of 8-16 mmHg in tumoral tissues, as opposed to a normal range of around 0 mmHg. This phenomenon is due to the irregular fenestrated to discontinuous phenotypes of the tumor blood vessels. There are three types of blood vessels, continuous, with a close connection between adjacent cells, allowing only small molecules (<10 nm) to pass through, fenestrated capillaries, containing windows that offer an easy passage to small and larger molecules (10-100 nm), and finally discontinuous capillaries exhibiting wide gaps between endothelial cells, thus providing an opening large enough for small molecules and cells to cross the endothelial barrier. Continuous capillaries are found surrounding the lungs among other organs, the fenestrated ones are usually found around kidneys and intestines while the discontinuous capillaries surround liver spleen and ovaries. The over-expression of angiogenic factors by tumors widens the gap between endothelial cells, increasing the diffusive permeability of the capillaries and thus the amount of fluid entering the tumor interstitium [3, 96-100]. To release the pressure generated by the fluid accumulation within the tumor, the IFHP pressure increases to transfer the overload of fluid back into the blood circulation [95, 101]. However this is not the only mechanism responsible for the interstitium drainage, this is also the role of the lymphatic vessels. It has been confirmed that lymphatic vessels secrete a wide range of chemokines that attract tumor cells in the lymphatic capillaries. Circulating tumor cells can then reach lymph nodes and metastatic niches for implantation. The Starling forces increase resulting from the over-expression of angiogenic factors by tumor cells would ease metastases formation [102-104]. The A549 tumor model illustrates exactly this phenomenon, since it was shown that the blockade of PlGF and VEGF by GLV-1h344 and GLV-1h108 tend to limit

the scope of the metastatic areas. This anti-metastatic effect was also observed after Ang-2 blockade in PC14PE6-RFP tumors, where the expression of an anti-Ang-2 scAb under the early promoter (SE) led to a strong decrease of the detection of human tumor cells in the thoracic area of mice treated with GLV-1h338, compared to the one treated with the parental GLV-1h68 strain. These findings confirm the important role of several different angiogenic factors, in addition to VEGF in the tumor progression.

5.5 Effect of -angiogenic factors on endothelial and tumor cells adhesion pattern

Due to their importance for the evolution of tumors, angiogenic factors and mostly VEGF have been extensively studied. VEGF was described in numerous publications as the most potent angiogenic factor over-expressed in a broad range of tumor types [12]. The signaling cascade of VEGF in endothelial cells leading to the stimulation of their survival and proliferation for the construction of the tumor blood supply has also been determined [105]. Nevertheless the impact of VEGF on the adhesion pattern of tumor cells is still poorly understood. We saw that VEGF, PlGF and Ang-2 had an effect on the expression of adhesion protein by endothelial cells but also by tumor cells. These data widen the role of angiogenic factors in the tumor progression. More than allowing the tumor to be sustained in nutrients, angiogenic factors have a direct effect on how tumor cells interact with the surroundings cells [106-110]. The over-expression of VEGF, PlGF and/or Ang-2 could thereby help the tumor to control the environment. Since the adhesion proteins modulated by the angiogenic factors, e-selectin, p-selectin, VCAM-1 and ICAM-1 are known to be implicated in the docking and recruitment of immune cells to activated endothelial cells [70, 111], VEGF, PlGF and Ang-2 could affect the immune response against the tumor by influencing the adhesion protein levels and thus the immune cells able to bind and integrate the tumor [112-116]. In other words, controlling the tumor environment would enable the tumor to modulate the immune response by selectively allowing “tumor friendly” immune cells to enter the tumor while keeping the “threatening” ones out.

This could be the reason why VEGF significantly inhibits ICAM-1 expression in PC14PE6-RFP cells, an adhesion protein known to be crucial in the firm docking of leukocytes on the endothelium to allow their transmigration into the inflamed tissue.

The tumor could then avoid or at least decrease lymphocyte killer cell cytotoxicity [117]. The decrease of its expression, would impair the accessibility of the immune system to the tumor [74]. This phenomenon has been described in human endothelial cells cultures *in vitro*. We can see that ICAM-1 expression increases when PC14PE6-RFP tumor cells are cultured in presence of Ang-2. These findings mean that Ang-2 not only has an effect on pericytes, but is also able to modify PC14PE6-RFP adhesion and thus migration potential. It also confirms our findings according to which PC14PE6-RFP can mimic pericyte cell function, since the migration potential of pericytes increases when stimulated with Ang-2.

It might stand to reason that tumor cells only have interest in decreasing the expression of adhesion proteins facilitating the transmigration of immune cells, but we can clearly see that tumor cell lines react differently to VEGF, Ang-2 and PlGF. These tumor models have different strategies to colonize their environment. Some of them may rely on the immune system to stimulate the development of the vasculature and the tumor. It is now commonly accepted that part of the immune system (e.g. M2 macrophages, Th2 lymphocytes or N2 neutrophils) enables tumor progression [111]. When looking at these results, it become obvious that tumor cells react differently to angiogenic factors. It is then difficult if not inaccurate to establish a general pattern describing tumor cell reaction when stimulated with a particular angiogenic factor. The correlation between abnormal expression of e-selectin by tumor cells, and their relative aggressiveness and increased invasiveness, has been described in human colon, pancreatic and non-small cell lung carcinomas in patients [33, 118-119]. In these studies the correlation between e-selectin, p-selectin, ICAM-1 and VCAM-1 expression and the metastatic potential of these tumors has been established, demonstrating the direct role of adhesion proteins in tumor invasiveness and metastases formation .

5.6 VEGF blockade increases vaccinia virus infectivity

As discussed earlier, VEGF plays a key role in tumor progression by inducing the construction of a vasculature but also by stimulating the expression of adhesion proteins for the migration of tumor cells and the control of their micro-environment. When considering a vaccinia virus based treatment involving VEGF blockade, it is important to evaluate the effect of VEGF and VEGF blockade on tumor cells but also on

the ability of vaccinia virus to colonize and lyse these tumor cells. We saw in the second part of this study that VACV-mediated VEGF blockade led to an increased infectivity of VACV, in A549 cells. The amount of RFP expressed by VACV increased by 2 fold when the virus was expressing the anti-VEGF scAb GLAF-1, revealing a protective effect of VEGF against VACV entry or replication. We also observed an increasing amount of cells following the increase of VEGF amounts, even in presence of GLAF-1, demonstrating that VEGF not only stimulates endothelial cells survival but also tumor cells survival. Because VEGF increased the number of cells available for VACV, the more VEGF input we had, the more TurboFP635 signal, and thus VACV, we observed. These data further prove that angiogenic factors, and more specifically VEGF, do not only promote tumor development by stimulating the formation of a vasculature, but also have a direct effect on tumor cells survival or mitosis. We can then suggest that blocking VEGF does not only improves VACV treatment by facilitating vaccinia virus infectivity, but also by decreasing its effect on tumor cells survival.

Moreover, since we observed that when A549 cells are infected with a GLAF-1 expressing virus at an MOI of 0.01, the amount of TurboFP635 measured is still ten fold higher than when infected with a regular VACV. We can also suggest that VEGF blockade by an anti-VEGF VACV allows the use of lower amounts of virus for better results. Not only does VEGF blockade impair tumor cells survival, but it also improves VACV entry and/or replication in vitro. The effect of this improved infectivity has also been observed *in vivo*, PC14PE6-RFP tumors were colonized more efficiently when infected with anti-VEGF VACV leading to a faster regression of tumors. VACV mediated VEGF-blockade would require less virus for the treatment of a cancer patient than a simple VACV. It would be interesting to see if the human VEGF structure resembles the viral VEGF and thus decreases vaccinia virus replication by blocking viral VEGF expression. There is only limited knowledge about the structure or specific function of the viral VEGF, thus answering that question will require a better characterization of VACV proteome.

It is hard to determine if human VEGF intervenes at the replication or entry level. The possibility that VEGF either activate an innate defense mechanism within the tumor cell or decreases the expression of receptors required for vaccinia virus entry is hard to

verify, the receptor of vaccinia virus still being unknown. Moreover the effect of human and viral VEGF on the ability of tumor cells to activate their defense mechanism has not yet been described, it is thus hard to draw conclusions on the mechanism leading to the improved infectivity of anti-VEGF VACV.

5.7 Therapeutic vaccinia viruses can colonize tumor endothelial cells.

VEGF blockade also improved VACV replication in murine tumor endothelial cells *in vitro*. Murine cells were described as poor if not non-responder to GLV-1h68 infection [85]. Nevertheless, murine endothelial cells appeared to be sensitive to vaccinia virus infection, especially to the anti-angiogenesis viruses. The parental VACV strain GLV-1h68 was almost undetectable in 2H-11 cells 24 and 48 hours post-infection, confirming previously published data [85]. In the meantime, the anti-Ang-2 and anti-PlGF viruses, GLV-1h493 and GLV-1h344, displayed higher titers. The combination of VEGF blockade to the inhibition of PlGF or Ang-2 improved VACV even more importantly. GLV-1h471 (anti-PlGF and anti-VEGF) improved VACV at early time points, while GLV-1h495 (anti VEGF and anti-Ang-2) was found at higher titers 72 and 96 hours post-infection. This experiment unveiled the effect of VEGF, PlGF and Ang-2 in VACV replication as well as the interest of a combination therapy.

The effect of VEGF blockade on VACV replication on tumor endothelial cells would be an additional explanation for the strong tumor regression induced by GLV-1h108 in all the tumor models tested, regardless of the amount of VEGF they express, since tumor endothelial cells could act as a reservoir of vaccinia virus. Moreover, even though VACV replication had a limited cytotoxic effect on endothelial cells, it brings GLAF-1 production closer to its target, and eases the access to VEGF. This hypothesis also applies to GLV-1h495 and GLV-1h471, since VEGF blockade combined to Ang-2 or PlGF inhibition were shown to significantly improve VACV replication compared to GLV-1h68. The combination therapies confer a substantial benefit for VACV replication in tumor endothelial cells.

It is also interesting to notice that the therapeutic efficiencies observed throughout the different animal studies, correlates with the ability of VACV to infect tumor endothelial cells. We observed that a small amount of GLV-1h493, in other words a mild blockade of

Ang-2, led to an increased colonization of 2H-11 cells. GLV-1h108, GLV-1h495 and GLV-1h471 also distinguished themselves by replicating in 2H-11 more efficiently than GLV-1h68. Tumor endothelial cells could act as a viral reservoir for tumor infection. Altogether, these data further confirm the importance of the vascular endothelium for the success of cancer treatment by VACV.

6 Conclusions

This study suggests that alternate blood vasculature structures are formed by tumor cells to sustain tumor progression by providing an appropriate blood supply and also by promoting a pro-tumoral immune system. This study also unveiled the direct effect of angiogenic factors on tumor cell adhesion patterns and dissemination. Moreover, we observed that VEGF significantly impairs therapeutic vaccinia virus replication and dissemination within a tumor, demonstrating the benefit of a VACV mediated VEGF blockade for treatment efficacy. The ability of lung adenocarcinoma cell lines A549 and PC14PE6-RFP to mimic endothelial cells and pericytes, respectively, was described and considered for the first time here as a potential way of resistance to currently approved anti-angiogenesis treatments against cancer, like bevacizumab. Vaccinia virus-mediated anti-angiogenesis has been shown to improve oncolytic viral therapy in several tumor models compared to the use of the standard GLV-1h68 therapeutic vaccinia virus and the use of an anti-angiogenic factor antibody. As a conclusion, we can say that tumor-induced angiogenesis influences tumor progression in more ways than only providing an adapted blood supply to the tumor, however angiogenesis blockade mediated by vaccinia virus seems to be able to prevent these process while preventing resistance mechanisms.

7 References

1. Cancer Facts & Figures, American Cancer Society, 2014

2. Hanahan, D., Weinberg, R.A., 2000. The hallmarks of cancer. Cell 100, 57–70.

3. Dudley, A.C., 2012. Tumor Endothelial Cells. Cold Spring Harb Perspect Med 2. doi:10.1101/cshperspect.a006536

4. Folkman, J., 1971. Tumor Angiogenesis: Therapeutic Implications. N Engl J Med 285, 1182–1186. doi:10.1056/NEJM197111182852108

5. Furuya, M., Nishiyama, M., Kasuya, Y., Kimura, S., Ishikura, H., 2005. Pathophysiology of tumor neovascularization. Vascular health and risk management 1, 277.

6. Hanahan, D., Weinberg, R.A., 2011. Hallmarks of Cancer: The Next Generation. Cell 144, 646–674. doi:10.1016/j.cell.2011.02.013

7. Harris, A.L., 2003. Angiogenesis as a new target for cancer control. European Journal of Cancer Supplements 1, 1–12.

8. Rundhaug, J.E., 2003. Matrix Metalloproteinases, Angiogenesis, and Cancer Commentary re: AC Lockhart et al., Reduction of Wound Angiogenesis in Patients Treated with BMS-275291, a Broad Spectrum Matrix Metalloproteinase Inhibitor. Clin. Cancer Res., 9: 00–00, 2003. Clinical cancer research 9, 551–554.

9. Hanahan, D., Folkman, J., 1996. Patterns and Emerging Mechanisms of the Angiogenic Switch during Tumorigenesis. Cell 86, 353–364. doi:10.1016/S0092-8674(00)80108-7

10. Shahi, P.K., Pineda, I.F., 2008. Tumoral Angiogenesis: Review of the Literature. Cancer Investigation 26, 104–108. doi:10.1080/07357900701662509

11. Weis, S.M., Cheresh, D.A., 2011. Tumor angiogenesis: molecular pathways and therapeutic targets. Nature medicine 17, 1359–1370.

12. Ferrara, N., 2009. VEGF-A: a critical regulator of blood vessel growth. Eur Cytokine Netw 20, 158–163.

13. Ferrara, N., Hillan, K.J., Gerber, H.P., Novotny, W., 2004. Discovery and development of bevacizumab, an anti-VEGF antibody for treating cancer. Nature Reviews Drug Discovery 3, 391–400.

14. Byrne, A.M., Bouchier-Hayes, D. j., Harmey, J. h., 2005. Angiogenic and cell survival functions of Vascular Endothelial Growth Factor (VEGF). Journal of

Cellular and Molecular Medicine 9, 777–794. doi:10.1111/j.1582-4934.2005.tb00379.x

15. Witmer, A.N., Blijswijk, B.C. van, Noorden, C.J.F. van, Vrensen, G.F.J.M., Schlingemann, R.O., 2004. In Vivo Angiogenic Phenotype of Endothelial Cells and Pericytes Induced by Vascular Endothelial Growth Factor-A. J Histochem Cytochem 52, 39–52. doi:10.1177/002215540405200105

16. Senger, D.R., Perruzzi, C.A., Feder, J., Dvorak, H.F., 1986. A Highly Conserved Vascular Permeability Factor Secreted by a Variety of Human and Rodent Tumor Cell Lines. Cancer Res 46, 5629–5632.

17. Senger, D.R., Connolly, D.T., Water, L.V.D., Feder, J., Dvorak, H.F., 1990. Purification and NH2-Terminal Amino Acid Sequence of Guinea Pig Tumor-secreted Vascular Permeability Factor. Cancer Res 50, 1774–1778.

18. Ferrara, N., Gerber, H.-P., LeCouter, J., 2003. The biology of VEGF and its receptors. Nat Med 9, 669–676. doi:10.1038/nm0603-669

19. Bach, F., Uddin, F.J., Burke, D., 2007. Angiopoietins in malignancy. European Journal of Surgical Oncology (EJSO) 33, 7–15.

20. Felcht, M., Luck, R., Schering, A., Seidel, P., Srivastava, K., Hu, J., Bartol, A., Kienast, Y., Vettel, C., Loos, E.K., 2012. Angiopoietin-2 differentially regulates angiogenesis through TIE2 and integrin signaling. The Journal of Clinical Investigation 122, 1991.

21. Yuan, H.T., Khankin, E.V., Karumanchi, S.A., Parikh, S.M., 2009. Angiopoietin 2 is a partial agonist/antagonist of Tie2 signaling in the endothelium. Molecular and cellular biology 29, 2011–2022.

22. Ribatti, D., 2008. The discovery of the placental growth factor and its role in angiogenesis: a historical review. Angiogenesis 11, 215–221. doi:10.1007/s10456-008-9114-4

23. Dewerchin, M., Carmeliet, P., 2012. PlGF: A Multitasking Cytokine with Disease-Restricted Activity. Cold Spring Harb Perspect Med 2. doi:10.1101/cshperspect.a011056

24. Broermann, A., Winderlich, M., Block, H., Frye, M., Rossaint, J., Zarbock, A., Cagna, G., Linnepe, R., Schulte, D., Nottebaum, A.F., Vestweber, D., 2011. Dissociation of VE-PTP from VE-cadherin is required for leukocyte extravasation and for VEGF-induced vascular permeability in vivo. J Exp Med 208, 2393–2401. doi:10.1084/jem.20110525

25. Liao, F., Li, Y., O'Connor, W., Zanetta, L., Bassi, R., Santiago, A., Overholser, J., Hooper, A., Mignatti, P., Dejana, E., 2000. Monoclonal antibody to vascular endothelial-cadherin is a potent inhibitor of angiogenesis, tumor growth, and metastasis. Cancer research 60, 6805–6810.

26. Orive, G., Hernández, R.M., Gascón, A.R., Igartua, M., Rojas, A., Pedraz, J.L., 2001. Microencapsulation of an anti-VE–cadherin antibody secreting 1B5 hybridoma cells. Biotechnology and Bioengineering 76, 285–294. doi:10.1002/bit.10050

27. Haidari, M., Zhang, W., Chen, Z., Ganjehei, L., Mortazavi, A., Warier, N., Vanderslice, P., Dixon, R.A.F., 2012. Atorvastatin preserves the integrity of endothelial adherens junctions by inhibiting vascular endothelial cadherin tyrosine phosphorylation. Experimental cell research.

28. Hermant, B., Bibert, S., Concord, E., Dublet, B., Weidenhaupt, M., Vernet, T., Gulino-Debrac, D., 2003. Identification of Proteases Involved in the Proteolysis of Vascular Endothelium Cadherin during Neutrophil Transmigration. J. Biol. Chem. 278, 14002–14012. doi:10.1074/jbc.M300351200

29. Suzuki, Y., Ohtani, H., Mizoi, T., Takeha, S., Shiiba, K., Matsuno, S., Nagura, H., 1995. Cell adhesion molecule expression by vascular endothelial cells as an immune/inflammatory reaction in human colon carcinoma. Jpn. J. Cancer Res. 86, 585–593.

30. Schellerer, V.S., Croner, R.S., Weinländer, K., Hohenberger, W., Stürzl, M., Naschberger, E., 2007. Endothelial cells of human colorectal cancer and healthy colon reveal phenotypic differences in culture. Lab Invest 87, 1159–1170. doi:10.1038/labinvest.3700671

31. Liu, G., Place, A.T., Chen, Z., Brovkovych, V.M., Vogel, S.M., Muller, W.A., Skidgel, R.A., Malik, A.B., Minshall, R.D., 2012. ICAM-1–activated Src and eNOS signaling increase endothelial cell surface PECAM-1 adhesivity and neutrophil transmigration. Blood 120, 1942–1952. doi:10.1182/blood-2011-12-397430

32. Guo, P., Huang, J., Wang, L., Jia, D., Yang, J., Dillon, D.A., Zurakowski, D., Mao, H., Moses, M.A., Auguste, D.T., 2014. ICAM-1 as a molecular target for triple negative breast cancer. PNAS 111, 14710–14715. doi:10.1073/pnas.1408556111

33. Zhou, F., Chen, J., Tao, G., Zhu, M., Xie, W., Cao, X., 2014. Increased levels of exhaled sICAM1, sVCAM1, and sE-selectin in patients with non-small cell lung cancer. Respiratory Medicine , 1670–1676. doi:10.1016/j.rmed.2014.08.003

34. Vestweber, D., Blanks, J.E., 1999. Mechanisms that regulate the function of the selectins and their ligands. Physiological Reviews 79, 181–213.

35. Kamba, T., McDonald, D.M., 2007. Mechanisms of adverse effects of anti-VEGF therapy for cancer. British journal of cancer 96, 1788–1795.

36. Papadopoulos, N., Martin, J., Ruan, Q., Rafique, A., Rosconi, M.P., Shi, E., Pyles, E.A., Yancopoulos, G.D., Stahl, N., Wiegand, S.J., 2012. Binding and neutralization of vascular endothelial growth factor (VEGF) and related ligands by VEGF Trap, ranibizumab and bevacizumab. Angiogenesis 1–15.

37. Shojaei, F., Wu, X., Malik, A.K., Zhong, C., Baldwin, M.E., Schanz, S., Fuh, G., Gerber, H.P., Ferrara, N., 2007. Tumor refractoriness to anti-VEGF treatment is mediated by CD11b+ Gr1+ myeloid cells. Nature biotechnology 25, 911–920.

38. Dudley, A.C., Udagawa, T., Melero-Martin, J.M., Shih, S.-C., Curatolo, A., Moses, M.A., Klagsbrun, M., 2010. Bone marrow is a reservoir for proangiogenic myelomonocytic cells but not endothelial cells in spontaneous tumors. Blood 116, 3367–3371. doi:10.1182/blood-2010-02-271122

39. Lohmann, A.E., Chia, S., 2012. Patients with metastatic breast cancer using bevacizumab as a treatment: is there still a role for it? Current treatment options in oncology 1–14.

40. Taugourdeau-Raymond, S., Rouby, F., Default, A., Jean-Pastor, M.J., 2012. Bevacizumab-induced serious side-effects: a review of the French pharmacovigilance database. European journal of clinical pharmacology 1–5.

41. Mancuso, M.R., Davis, R., Norberg, S.M., O Brien, S., Sennino, B., Nakahara, T., Yao, V.J., Inai, T., Brooks, P., Freimark, B., 2006. Rapid vascular regrowth in tumors after reversal of VEGF inhibition. Journal of Clinical Investigation 116, 2610.

42. Ebos, J.M.L., Lee, C.R., Cruz-Munoz, W., Bjarnason, G.A., Christensen, J.G., Kerbel, R.S., 2009. Accelerated metastasis after short-term treatment with a potent inhibitor of tumor angiogenesis. Cancer cell 15, 232–239.

43. Huang, J., Soffer, S.Z., Kim, E.S., McCrudden, K.W., Huang, J., New, T., Manley, C.A., Middlesworth, W., O'Toole, K., Yamashiro, D.J., 2004. Vascular Remodeling Marks Tumors That Recur During Chronic Suppression of Angiogenesis11NIH U10 CA13539-27, subcontract 6641 (JK), NIH 1 R01 CA08895101-A1 (DY), Pediatric Cancer Foundation, and Sorkin Gift Fund. Note: J. Huang and SZ Soffer contributed equally to this work. Molecular cancer research 2, 36–42.

44. Jacobs, B.L., Langland, J.O., Kibler, K.V., Denzler, K.L., White, S.D., Holechek, S.A., Wong, S., Huynh, T., Baskin, C.R., 2009. Vaccinia virus vaccines: past, present and future. Antiviral research 84, 1–13.

45. Roberts, K.L., Smith, G.L., 2008. Vaccinia virus morphogenesis and dissemination. Trends in microbiology 16, 472–479.

46. Harrison, S.C., Alberts, B., Ehrenfeld, E., Enquist, L., Fineberg, H., McKnight, S.L., Moss, B., O'Donnell, M., Ploegh, H., Schmid, S.L., Walter, K.P., Theriot, J., 2004. Discovery of antivirals against smallpox. PNAS 101, 11178–11192. doi:10.1073/pnas.0403600101

47. Röttger, S., Frischknecht, F., Reckmann, I., Smith, G.L., Way, M., 1999. Interactions between vaccinia virus IEV membrane proteins and their roles in IEV assembly and actin tail formation. Journal of virology 73, 2863–2875.

48. Smith, G.L., Law, M., 2004. The exit of Vaccinia virus from infected cells. Virus Research 106, 189–197. doi:10.1016/j.virusres.2004.08.015

49. Smith, G.L., Murphy, B.J., Law, M., 2003. Vaccinia Virus motility. Annual Review of Microbiology 57, 323–342. doi:10.1146/annurev.micro.57.030502.091037

50. Smith, G.L., Vanderplasschen, A., Law, M., 2002. The formation and function of extracellular enveloped vaccinia virus. J Gen Virol 83, 2915–2931.

51. Vanderplasschen, A., Hollinshead, M., Smith, G.L., 1998. Intracellular and extracellular vaccinia virions enter cells by different mechanisms. Journal of general virology 79, 877–887.

52. Vanderplasschen, A., Smith, G.L., 1999. Using confocal microscopy to study virus binding and entry into cells. Meth. Enzymol. 307, 591–607.

53. Van Vliet, K., Mohamed, M.R., Zhang, L., Villa, N.Y., Werden, S.J., Liu, J., McFadden, G., 2009. Poxvirus Proteomics and Virus-Host Protein Interactions. Microbiology and Molecular Biology Reviews 73, 730–749. doi:10.1128/MMBR.00026-09

54. Paiva, L.R., Martins, M.L., Ferreira, S.C., 2011. Questing for an optimal, universal viral agent for oncolytic virotherapy. Physical Review E 84, 041918.

55. Vacchelli, E., Eggermont, A., Sautès-Fridman, C., Galon, J., Zitvogel, L., Kroemer, G., Galluzzi, L., 2013. Trial watch. OncoImmunology 2, e24612. doi:10.4161/onci.24612

56. Thorne, S.H., 2014. Immunotherapeutic potential of oncolytic vaccinia virus. Front. Oncol. 4, 155. doi:10.3389/fonc.2014.00155

57. McFadden, G., 2005. Poxvirus tropism. Nature Reviews Microbiology 3, 201–213. doi:10.1038/nrmicro1099

58. Rojas, J.J., Thorne, S.H., 2012. Theranostic Potential of Oncolytic Vaccinia Virus. Theranostics 2, 363–373. doi:10.7150/thno.3724

59. Zhang, Q., Yong, A.Y., Wang, E., Chen, N., Danner, R.L., Munson, P.J., Marincola, F.M., Szalay, A.A., 2007. Eradication of solid human breast tumors in nude mice

with an intravenously injected light-emitting oncolytic vaccinia virus. Cancer research 67, 10038–10046.

60. Frentzen, A., Yong, A.Y., Chen, N., Zhang, Q., Weibel, S., Raab, V., Szalay, A.A., 2009. Anti-VEGF single-chain antibody GLAF-1 encoded by oncolytic vaccinia virus significantly enhances antitumor therapy. Proceedings of the National Academy of Sciences 106, 12915–12920.

61. Arnaoutova, I., Kleinman, H.K., 2010. In vitro angiogenesis: endothelial cell tube formation on gelled basement membrane extract. Nature protocols 5, 628–635.

62. Chrobak, K.M., Potter, D.R., Tien, J., 2006. Formation of perfused, functional microvascular tubes in vitro. Microvascular Research 71, 185–196. doi:10.1016/j.mvr.2006.02.005

63. Davis, G.E., Bayless, K.J., Mavila, A., 2002. Molecular basis of endothelial cell morphogenesis in three-dimensional extracellular matrices. The Anatomical Record 268, 252–275. doi:10.1002/ar.10159

64. Davis, G.E., Koh, W., Stratman, A.N., 2007. Mechanisms controlling human endothelial lumen formation and tube assembly in three-dimensional extracellular matrices. Birth Defects Research Part C: Embryo Today: Reviews 81, 270–285. doi:10.1002/bdrc.20107

65. Zhou, Q., Kiosses, W.B., Liu, J., Schimmel, P., 2008. Tumor endothelial cell tube formation model for determining anti-angiogenic activity of a tRNA synthetase cytokine. Methods 44, 190–195.

66. Aricescu, A.R., Lu, W., Jones, E.Y., 2006. A time- and cost-efficient system for high-level protein production in mammalian cells. Acta Crystallographica Section D Biological Crystallography 62, 1243–1250. doi:10.1107/S0907444906029799

67. Donat, U., Weibel, S., Hess, M., Stritzker, J., Härtl, B., Sturm, J.B., Chen, N.G., Gentschev, I., Szalay, A.A., 2012. Preferential Colonization of Metastases by Oncolytic Vaccinia Virus Strain GLV-1h68 in a Human PC-3 Prostate Cancer Model in Nude Mice. PLoS ONE 7, e45942. doi:10.1371/journal.pone.0045942

68. Bais, C., Wu, X., Yao, J., Yang, S., Crawford, Y., McCutcheon, K., Tan, C., Kolumam, G., Vernes, J.-M., Eastham-Anderson, J., Haughney, P., Kowanetz, M., Hagenbeek, T., Kasman, I., Reslan, H.B., Ross, J., Van Bruggen, N., Carano, R.A.D., Meng, Y.-J.G., Hongo, J.-A., Stephan, J.-P., Shibuya, M., Ferrara, N., 2010. PlGF Blockade Does Not Inhibit Angiogenesis during Primary Tumor Growth. Cell 141, 166–177. doi:10.1016/j.cell.2010.01.033

69. Faryammanesh, R., Lange, T., Magbanua, E., Haas, S., Meyer, C., Wicklein, D., Schumacher, U., Hahn, U., 2014. SDA, a DNA Aptamer Inhibiting E- and P-Selectin

Mediated Adhesion of Cancer and Leukemia Cells, the First and Pivotal Step in Transendothelial Migration during Metastasis Formation. PLoS One 9. doi:10.1371/journal.pone.0093173

70. Wittchen, E.S., 2009. Endothelial signaling in paracellular and transcellular leukocyte transmigration. Front Biosci 14, 2522–2545.

71. Bagley, R.G., Weber, W., Rouleau, C., Teicher, B.A., 2005. Pericytes and endothelial precursor cells: cellular interactions and contributions to malignancy. Cancer research 65, 9741–9750.

72. Vitale, G., Dicitore, A., Gentilini, D., Cavagnini, F., 2010. Immunomodulatory effects of VEGF: Clinical implications of VEGF-targeted therapy in human cancer. Cancer biology & therapy 9, 694–698.

73. Qian, B.Z., Pollard, J.W., 2010. Macrophage diversity enhances tumor progression and metastasis. Cell 141, 39–51.

74. Patil, S.S., Gentschev, I., Adelfinger, M., Donat, U., Hess, M., Weibel, S., Nolte, I., Frentzen, A., Szalay, A.A., 2012. Virotherapy of Canine Tumors with Oncolytic Vaccinia Virus GLV-1h109 Expressing an Anti-VEGF Single-Chain Antibody. PLoS One 7. doi:10.1371/journal.pone.0047472

75. Holash, J., Maisonpierre, P.C., Compton, D., Boland, P., Alexander, C.R., Zagzag, D., Yancopoulos, G.D., Wiegand, S.J., 1999. Vessel cooption, regression, and growth in tumors mediated by angiopoietins and VEGF. Science 284, 1994–1998.

76. Yu, Q., Stamenkovic, I., 2001. Angiopoietin-2 Is Implicated in the Regulation of Tumor Angiogenesis. Am J Pathol 158, 563–570.

77. Kirschmann, D.A., Seftor, E.A., Hardy, K.M., Seftor, R.E.B., Hendrix, M.J.C., 2012. Molecular Pathways: Vasculogenic Mimicry in Tumor Cells: Diagnostic and Therapeutic Implications. Clinical Cancer Research 18, 2726–2732. doi:10.1158/1078-0432.CCR-11-3237

78. Misra, R.M., Bajaj, M.S., Kale, V.P., 2012. Vasculogenic Mimicry of HT1080 Tumour Cells In Vivo: Critical Role of HIF-1α-Neuropilin-1 Axis. PLoS ONE 7, e50153. doi:10.1371/journal.pone.0050153

79. Paulis, Y.W.J., Soetekouw, P.M.M.B., Verheul, H.M.W., Tjan-Heijnen, V.C.G., Griffioen, A.W., 2010. Signalling pathways in vasculogenic mimicry. Biochimica et Biophysica Acta (BBA) - Reviews on Cancer 1806, 18–28. doi:10.1016/j.bbcan.2010.01.001

80. Upile, T., Jerjes, W., Radhi, H., Al-Khawalde, M., Kafas, P., Nouraei, S., Sudhoff, H., 2011. Vascular mimicry in cultured head and neck tumour cell lines. Head & neck oncology 3, 1–7.

81. Hendrix, M.J.C., Seftor, E.A., Hess, A.R., Seftor, R.E.B., 2003. Angiogenesis: Vasculogenic mimicry and tumour-cell plasticity: lessons from melanoma. Nature Reviews Cancer 3, 411–421. doi:10.1038/nrc1092

82. Hallani, S.E., Boisselier, B., Peglion, F., Rousseau, A., Colin, C., Idbaih, A., Marie, Y., Mokhtari, K., Thomas, J.-L., Eichmann, A., Delattre, J.-Y., Maniotis, A.J., Sanson, M., 2010. A new alternative mechanism in glioblastoma vascularization: tubular vasculogenic mimicry. Brain 133, 973–982. doi:10.1093/brain/awq044

83. Lugassy, C., Wadehra, M., Li, X., Corselli, M., Akhavan, D., Binder, S.W., Péault, B., Cochran, A.J., Mischel, P.S., Kleinman, H.K., Barnhill, R.L., 2012. Pilot Study on "Pericytic Mimicry" and Potential Embryonic/Stem Cell Properties of Angiotropic Melanoma Cells Interacting with the Abluminal Vascular Surface. Cancer Microenvironment 6, 19–29. doi:10.1007/s12307-012-0128-5

84. Lugassy, C., Péault, B., Wadehra, M., Kleinman, H.K., Barnhill, R.L., 2013. Could pericytic mimicry represent another type of melanoma cell plasticity with embryonic properties? Pigment Cell & Melanoma Research 26, 746–754. doi:10.1111/pcmr.12120

85. Weibel, S., Hofmann, E., Basse-Luesebrink, T.C., Donat, U., Seubert, C., Adelfinger, M., Gnamlin, P., Kober, C., Frentzen, A., Gentschev, I., Jakob, P.M., Szalay, A.A., 2013. Treatment of malignant effusion by oncolytic virotherapy in an experimental subcutaneous xenograft model of lung cancer. J Transl Med 11, 106. doi:10.1186/1479-5876-11-106

86. Weibel, S., Raab, V., Yu, Y.A., Worschech, A., Wang, E., Marincola, F.M., Szalay, A.A., 2011. Viral-mediated oncolysis is the most critical factor in the late-phase of the tumor regression process upon vaccinia virus infection. BMC Cancer 11, 68. doi:10.1186/1471-2407-11-68

87. Cooke, V.G., LeBleu, V.S., Keskin, D., Khan, Z., O'Connell, J.T., Teng, Y., Duncan, M.B., Xie, L., Maeda, G., Vong, S., Sugimoto, H., Rocha, R.M., Damascena, A., Brentani, R.R., Kalluri, R., 2012. Pericyte Depletion Results in Hypoxia-Associated Epithelial-to-Mesenchymal Transition and Metastasis Mediated by Met Signaling Pathway. Cancer Cell 21, 66–81. doi:10.1016/j.ccr.2011.11.024

88. Reinboth, J., Ascierto, M.L., Chen, N.G., Zhang, Q., Yu, Y.A., Aguilar, R.J., Carretero, R., Worschech, A., Zhao, Y., Wang, E., Marincola, F.M., Szalay, A.A., 2012. Correlates Between Host and Viral Transcriptional Program Associated with Different Oncolytic Vaccinia Virus Isolates. Hum Gene Ther Methods 23, 285–296. doi:10.1089/hgtb.2012.057

89. Van de Veire, S., Stalmans, I., Heindryckx, F., Oura, H., Tijeras-Raballand, A., Schmidt, T., Loges, S., Albrecht, I., Jonckx, B., Vinckier, S., Van Steenkiste, C.,

Tugues, S., Rolny, C., De Mol, M., Dettori, D., Hainaud, P., Coenegrachts, L., Contreres, J.-O., Van Bergen, T., Cuervo, H., Xiao, W.-H., Le Henaff, C., Buysschaert, I., Masouleh, B.K., Geerts, A., Schomber, T., Bonnin, P., Lambert, V., Haustraete, J., Zacchigna, S., Rakic, J.-M., Jiménez, W., Noël, A., Giacca, M., Colle, I., Foidart, J.-M., Tobelem, G., Morales-Ruiz, M., Vilar, J., Maxwell, P., Vinores, S.A., Carmeliet, G., Dewerchin, M., Claesson-Welsh, L., Dupuy, E., Van Vlierberghe, H., Christofori, G., Mazzone, M., Detmar, M., Collen, D., Carmeliet, P., 2010. Further Pharmacological and Genetic Evidence for the Efficacy of PlGF Inhibition in Cancer and Eye Disease. Cell 141, 178–190. doi:10.1016/j.cell.2010.02.039

90. Ahmad, S.A., Liu, W., Jung, Y.D., Fan, F., Wilson, M., Reinmuth, N., Shaheen, R.M., Bucana, C.D., Ellis, L.M., 2001. The Effects of Angiopoietin-1 and -2 on Tumor Growth and Angiogenesis in Human Colon Cancer. Cancer Res 61, 1255–1259.

91. Etoh, T., Inoue, H., Tanaka, S., Barnard, G.F., Kitano, S., Mori, M., 2001. Angiopoietin-2 Is Related to Tumor Angiogenesis in Gastric Carcinoma Possible in Vivo Regulation via Induction of Proteases. Cancer Res 61, 2145–2153.

92. Beckner, M.E., 1999. Factors promoting tumor angiogenesis. Cancer investigation 17, 594–623.

93. Chen, H.–., Chai, L., Wang, S.–., Shi, Z.–., Wu, Q.–., 2011. Angiopoietin-2 inhibits the growth of tongue carcinoma without affecting expression of vascular endothelial growth factor. Int J Oral Maxillofac Surg 40, 628–632. doi:10.1016/j.ijom.2010.11.005

94. Meng, M.-B., Zaorsky, N.G., Deng, L., Wang, H.-H., Chao, J., Zhao, L.-J., Yuan, Z.-Y., Ping, W., 2014. Pericytes: a double-edged sword in cancer therapy. Future Oncol 1–11. doi:10.2217/fon.14.123

95. Fine, L.G., 2014. Ernest Henry Starling (1866-1927) on the formation and reabsorption of lymph. Nephron Physiol 126, 9–17. doi:10.1159/000362620

96. Shieh, A.C., Swartz, M.A., 2011. Regulation of tumor invasion by interstitial fluid flow. Physical Biology 8, 015012. doi:10.1088/1478-3975/8/1/015012

97. Hashizume, H., Baluk, P., Morikawa, S., McLean, J.W., Thurston, G., Roberge, S., Jain, R.K., McDonald, D.M., 2000. Openings between defective endothelial cells explain tumor vessel leakiness. The American journal of pathology 156, 1363.

98. Parikh, S.M., Mammoto, T., Schultz, A., Yuan, H.T., Christiani, D., Karumanchi, S.A., Sukhatme, V.P., 2006. Excess circulating angiopoietin-2 may contribute to pulmonary vascular leak in sepsis in humans. PLoS medicine 3, e46.

99. Roviezzo, F., Tsigkos, S., Kotanidou, A., Bucci, M., Brancaleone, V., Cirino, G., Papapetropoulos, A., 2005. Angiopoietin-2 Causes Inflammation in Vivo by Promoting Vascular Leakage. J Pharmacol Exp Ther 314, 738–744. doi:10.1124/jpet.105.086553

100. Kalomenidis, I., Kollintza, A., Sigala, I., Papapetropoulos, A., Papiris, S., Light, R.W., Roussos, C., 2006. Angiopoietin-2 levels are elevated in exudative pleural effusions. CHEST Journal 129, 1259–1266.

101. Martinez-Corral, I., Makinen, T., 2013. Regulation of lymphatic vascular morphogenesis: Implications for pathological (tumor) lymphangiogenesis. Experimental Cell Research. doi:10.1016/j.yexcr.2013.01.016

102. Figueroa-Vega, N., Díaz, Á., Adrados, M., Paniagua, A., Aragonés, J., Martín-Pérez, E., Leskela, S., Moreno-Otero, R., González-Amaro, R., Marazuela, M., 2010. The association of the angiopoietin/Tie-2 system with the development of metastasis and leukocyte migration in neuroendocrine tumors. Endocrine-related cancer 17, 897–908.

103. Holopainen, T., Saharinen, P., D'Amico, G., Lampinen, A., Eklund, L., Sormunen, R., Anisimov, A., Zarkada, G., Lohela, M., Heloterä, H., 2012. Effects of Angiopoietin-2-Blocking Antibody on Endothelial Cell–Cell Junctions and Lung Metastasis. Journal of the National Cancer Institute 104, 461–475.

104. Schulz, P., Fischer, C., Detjen, K.M., Rieke, S., Hilfenhaus, G., von Marschall, Z., Böhmig, M., Koch, I., Kehrberger, J., Hauff, P., 2011. Angiopoietin-2 drives lymphatic metastasis of pancreatic cancer. The FASEB Journal 25, 3325–3335.

105. Pathway Map: Development_VEGF-family signaling | Map Search (FREE!) [WWW Document], n.d. URL http://pathwaymaps.com/maps/445/ (accessed 6.12.13).

106. Griffioen, A.W., Damen, C.A., Martinotti, S., Blijham, G.H., Groenewegen, G., 1996. Endothelial Intercellular Adhesion Molecule-1 Expression Is Suppressed in Human Malignancies: The Role of Angiogenic Factors. Cancer Res 56, 1111–1117.

107. Hermant, B., Bibert, S., Concord, E., Dublet, B., Weidenhaupt, M., Vernet, T., Gulino-Debrac, D., 2003. Identification of Proteases Involved in the Proteolysis of Vascular Endothelium Cadherin during Neutrophil Transmigration. J. Biol. Chem. 278, 14002–14012. doi:10.1074/jbc.M300351200

108. Hossain, M., Qadri, S.M., Liu, L., 2012. Inhibition of nitric oxide synthesis enhances leukocyte rolling and adhesion in human microvasculature. Journal of Inflammation 9, 28.

109. Ishida, T., 2003. Targeted Disruption of Endothelial Cell-selective Adhesion Molecule Inhibits Angiogenic Processes in Vitro and in Vivo. Journal of Biological Chemistry 278, 34598–34604. doi:10.1074/jbc.M304890200

110. Suzuki, Y., Ohtani, H., Mizoi, T., Takeha, S., Shiiba, K., Matsuno, S., Nagura, H., 1995. Cell adhesion molecule expression by vascular endothelial cells as an immune/inflammatory reaction in human colon carcinoma. Jpn. J. Cancer Res. 86, 585–593.

111. Rahman, A., Fazal, F., 2009. Hug Tightly and Say Goodbye: Role of Endothelial ICAM-1 in Leukocyte Transmigration. Antioxid Redox Signal 11, 823–839. doi:10.1089/ars.2008.2204

112. Griffioen, A.W., 2008. Anti-angiogenesis: making the tumor vulnerable to the immune system. Cancer Immunology, Immunotherapy 57, 1553–1558.

113. Franses, J.W., Baker, A.B., Chitalia, V.C., Edelman, E.R., 2011. Stromal Endothelial Cells Directly Influence Cancer Progression. Sci Transl Med 3, 66ra5–66ra5. doi:10.1126/scitranslmed.3001542

114. Danese, S., Dejana, E., Fiocchi, C., 2007. Immune Regulation by Microvascular Endothelial Cells: Directing Innate and Adaptive Immunity, Coagulation, and Inflammation. J Immunol 178, 6017–6022.

115. Bachireddy, P., Rakhra, K., Felsher, D.W., 2012. Immunology in the clinic review series; focus on cancer: multiple roles for the immune system in oncogene addiction. Clinical & Experimental Immunology 167, 188–194.

116. Dirkx, A.E.M., Egbrink, M.G.A. oude, Castermans, K., Schaft, D.W.J. van der, Thijssen, V.L.J.L., Dings, R.P.M., Kwee, L., Mayo, K.H., Wagstaff, J., Steege, J.C.A.B., Griffioen, A.W., 2006. Anti-angiogenesis therapy can overcome endothelial cell anergy and promote leukocyte-endothelium interactions and infiltration in tumors. FASEB J 20, 621–630. doi:10.1096/fj.05-4493com

117. Ohm, J.E., Gabrilovich, D.I., Sempowski, G.D., Kisseleva, E., Parman, K.S., Nadaf, S., Carbone, D.P., 2003. VEGF inhibits T-cell development and may contribute to tumor-induced immune suppression. Blood 101, 4878–4886. doi:10.1182/blood-2002-07-1956

118. Köhler, S., Ullrich, S., Richter, U., Schumacher, U., 2010. E-/P-selectins and colon carcinoma metastasis: first in vivo evidence for their crucial role in a clinically relevant model of spontaneous metastasis formation in the lung. Br J Cancer 102, 602–609. doi:10.1038/sj.bjc.6605492

119. Gebauer, F., Wicklein, D., Stübke, K., Nehmann, N., Schmidt, A., Salamon, J., Peldschus, K., Nentwich, M.F., Adam, G., Tolstonog, G., Bockhorn, M., Izbicki, J.R.,

Wagener, C., Schumacher, U., 2013. Selectin binding is essential for peritoneal carcinomatosis in a xenograft model of human pancreatic adenocarcinoma in pfp−−/rag2−− mice. Gut 62, 741–750. doi:10.1136/gutjnl-2011-300629

8 Appendix

8.1 List of figures

Figure 1 : Cancer new cases and deaths in 2014 in United States 1

Figure 2 : Hallmarks of cancer 3

Figure 3 : : The VEGF family and its receptors..... 6

Figure 4 : : Role of angiopoietins in angiogenesis 8

Figure 5 : PlGF pleiotropic effect..... 9

Figure 6 : Schematic representation of Vaccinia virus replication cycle.....13

Figure 7 : Therapeutic VACV GLV-1h68 37

Figure 8 : Anti-VEGF and anti-Ang-2 VACVs.....37

Figure 9 : Schematic representation of Anti-Ang-2 VACVs.....38

Figure 10 : Schematic representation of Anti-PlGF VACVs.....39

Figure 11 : Angiogenic profiles of human tumor cells.....50-51

Figure 12 : Oncolytic activity of anti-angiogenesis vaccinia viruses in MEL1936 and Colo205 tumor cells 53

Figure 13 : Anti-PlGF and Anti-ang-2 scAb binding.....54

Figure 14 : Blood vessel-like structures formed by murine endothelial cells 55

Figure 15 : PC14PE6-RFP supernatant does not contain cell lysis products.....55

Figure 16 : Quantification of 2H-11 blood vessel-like structures 56

Figure 17 : Effect of VEGF, Ang-2 and PlGF on VCAM-1, ICAM-1, e-selectin and p-selectin expression in tumor cells.....57-59

Figure 18 : Human tumor cells forming blood vessel-like structures 62

Figure 19 : Reduction of a PC14PE6-RFP-tumor-induced hematoma 64-65

Figure 20 : Therapeutic effect of VACV in tumor endothelial cells. 67-68

Figure 21 : VEGF expression by A549 cells.....68

Figure 22 : A549 cells 24 and 72 hours post-infection by GLV-1h189 or GLV-1h413.... 70-71

Figure 23 : Quantification of TurboFP635 in A549 cells infected with GLV-189 and GLV-1h413 (anti-VEGF).... 72-73

Figure 24 : PC14PE6-RFP tumors colonization rate 74

Figure 25 : β-actin expression in lungs of PC14PE6-RFP tumor-bearing mice 10 days post-treatment 75

Figure 26 : Viral distribution of anti-angiogenesis and parental GLV-1h68 vaccinia viruses in PC14PE6-RFP tumor-bearing mice 10 days post-treatment 76

Figure 27 : Colo205 tumors relative tumor size 78

Figure 28 : Colo205 tumor-bearing nude mice survival after VACV oncolytic treatment 79

Figure 29 : MEL1936 tumors evolution after oncolytic VACV treatment 81

Figure 30 : MEL1936 tumor-bearing mice response to VACV treatment 82

Figure 31 : Colo205 tumors evolution after anti-Ang-2 and Anti-VEGF therapy.... 83

Figure 32 : Colo205 tumor-bearing mice survival after anti-Ang-2 and anti-VEGF combination therapy 84

Figure 33 : Colo205 tumors vascularization 84-85

Figure 34 : MEL1936 tumors evolution after VACV-mediated PlGF and VEGF blockade 86

Figure 35 : MEL1936 tumor-bearing mice survival after PlGF and VEGF blockade by oncolytic VACV 87

Figure 36 : PlGF quantification in mice sera.... 87

Figure 37 : Flag-tag ELISA of aPlGF purified antibody 89

Figure 38 : A549 tumors evolution after anti-angiogenesis treatment 90

Figure 39 : Comparison of organs of healthy nude mouse and A549 tumor-bearing untreated or treated with oncolytic VACV 91

8.2 Publications

Weibel, S., Hofmann, E., Basse-Luesebrink, T.C., Donat, U., Seubert, C., Adelfinger, M., **Gnamlin, P**., Kober, C., Frentzen, A., Gentschev, I., Jakob, P.M., Szalay, A.A., 2013. Treatment of malignant effusion by oncolytic virotherapy in an experimental subcutaneous xenograft model of lung cancer. J Transl Med 11, 106. doi:10.1186/1479-5876-11-106

8.3 Eidesttatliche Erklärung

Erklärung gemäß § 4 Absatz 3 Der Promotionsordnung der Fakultät fur Biologie der Bayerische Julius-Maximilians-Universität Würzburg

Hiermit erkläre ich, die vorgelegte Dissertation selbständig angefertigt zu haben une kiné Andersen als die von mir angegebenen Quellen une Hilfsmittel verwendet zu haben.

Des Western erkläre ich, dass die vorliegende Arbeit Weser in gleicher noch in ähnlicher Form bereits in einem anderen Prüfungsverfahren vorgelegt wurde.

Zuvor habe ich neben dem akademischen Grade" Master of Science" keine weiteren akademischen Grade erworben.

Die vorliegende Arbeit wurde von Prof. A. A. Szalay betreut.

Würzburg, den

Prisca Gnamlin

8.4 Acknowledgements

First of all, I would like to thank my supervisor, Prof. Dr. Szalay, for giving me the opportunity to work on this very interesting and challenging project, and carry out my work from the University of Würzburg to Genelux Corporation, San Diego. I am grateful for his constant support and mentorship.

I would also like to thank Dr. Alexa Frentzen who designed all the anti-angiogenesis VACVs used in this study. She took the time to guide me through my first experiments in San Diego where I gain respect for her as a scientist and as a person.

I acknowledge Dr. Weibel who introduced me to this interesting project.

I do not forget to thank Dr. Nanhai Chen and Dr. Qian Zhang who took time to answer my questions and help me at numerous occasions. As well as Prof. Dr. Grummt who corrected my dissertation.

Next, I want to thank former and current Genelux and AG Szalay group members who welcomed me. I would like to thank specifically Alexa, Qian, Anu, Uma, Robin, Joe, Jason, Rohit and my teeny tiny Elli for their immovable good mood, enthusiasm and care.

Last but not least I would like to thank my fellow PhD students, past and present. Desi, Sandeep, Lorenz, Klaas, Ivan, Jenny, Duong, Simon, and Christina thank you for your help, care and the good times we shared over the past three years!